Active Stirling Engine

A thesis submitted in partial fulfilment of the

requirements for the Degree

of Doctor of Philosophy in Electrical Engineering

in the University of Canterbury

by Vinod Kumar Gopal

University of Canterbury

2012

Table of Contents

Table of figures and tables

Acknowledgments

I wish to express my sincere appreciation to Late Associate Professor Richard Duke for supervising me and making me stay focused throughout this research. I wish to thank Dr. Don Clucas whose idea sowed the seed and helped shape the outcome of this research. I express my sincere gratitude to Dave Fanner, Josh Baker, Lincoln Frost and Michael Gschwendtner for assisting me in this project. I wish to thank Dr. Paul Gaynor for editing this thesis.

This thesis is dedicated to my Late Mother Mrs. Meenakshi Kunjamma (my Paaru). She spent all her life to bring me up to be a responsible and educated person. I would not even be in engineering school without her love, hard work and unconditional support.

All of it happened due to the divine grace flowing through my Guru and mentor Sri Mata Amritanandamayi, my beloved Amma. I submit this humble work at her lotus feet.

“To my Amma, for everything, that will ever be me, for teaching me what unconditional love is”

Abstract

Micro Combined Heat and Power systems or microCHP systems generate heat and electricity for a home. Stirling engines are widely used as prime movers in microCHP applications. Stirling engine is an external combustion engine having an enclosed working fluid (as helium) that is alternately compressed and expanded to operate a piston. The displacer shuttles the working fluid between the hot and cold ends. The piston is coupled to a transmission and to an electrical machine to generate power. Conventional Stirling engines are not controllable to a great degree. The piston and displacer are connected to the same crank and they maintain the same phase difference throughout the cycle. Also the piston and displacer are normally constructed to move in a sinusoidal fashion.

The Active Stirling Engine is a new concept introduced in this thesis which has a free displacer. The displacer is driven separately compared to a coupled drive in conventional Stirling engines. The displacer motion can be non-linear with dwell at each ends of the stroke, opening up the possibilities to increase the pressure volume diagram which indicates the work done by the engine. A separately driven displacer also allows introducing phase control and stroke control to improve the controllability of a Stirling engine.

This thesis examines the effect of non-linear displacer motion and phase control of the displacer on Stirling engine performance. Simulations are performed in Sage, the leading Stirling engine simulation software, to understand the effect of displacer phase control. A test rig is constructed with the actively controlled displacer connected to a linear machine controlled by a programmable servo. Heat is applied to the test rig though an electric heating coil. The test rig is charged with nitrogen at 20Bar pressure. The power piston is connected to a rotating electrical machine via the transmission. The rotating electrical machine is used to start the engine and to act as the generator.

The test rig is instrumented to determine the linear position of the displacer and piston, angular position of the rotating electrical machine shaft, temperatures, pressures and flow. A LabVIEW™ based data acquisition system is set up to capture data from the test rig. Data is collected at various test cases. The simulation result is compared against post processed data.

An efficiency improvement of 15% is achieved using this method and is demonstrated experimentally. Applications in micro combined heat and power systems utilising the improved efficiency due to non linear motion and controllability due to phase control are explored in this thesis.

Glossary

ASE. Actively Controlled Stirling engine or Active Stirling Engine. In this type of Stirling engine, the displacer will be disconnected from the main crank and will be driven separately. The engine will have the capability to change phase and dwell, on the fly.

Burner. A device, as in a furnace, stove, or gas lamp that is lighted to produce a flame.

Cycle. A thermodynamic cycle consists of a series of thermodynamic processes transferring heat and work, while varying pressure, temperature, and other state variables, eventually returning a system to its initial state. In the process of going through this cycle, the system may perform work on its surroundings, thereby acting as a heat engine.

Data Acquisition System. Data acquisition is the process of sampling signals that measure real world physical conditions and converting the resulting samples into digital numeric values that can be manipulated by a computer. Data acquisition systems (abbreviated with the acronym **DAS** or **DAQ**) typically convert analog waveforms into digital values for processing.

Displacer. A displacer shuttles the working fluid between the cold and hot ends in a Stirling engine.

Encoder. An encoder is a device that converts information from one format to another. A linear encoder similarly converts linear position to an electronic signal. Such encoders can be either absolute or incremental. The signal from an absolute encoder gives an unambiguous position within the travel range without requiring knowledge of any previous position. The signal from an incremental encoder is cyclical, thus ambiguous, and requires counting of cycles to maintain absolute position within the travel range. Both can provide the same accuracy, but the absolute encoder is more robust to interruptions in transducer signal.

Generator. In electricity generation, an **electric generator** is a device that converts mechanical energy to electrical energy. A generator forces electrons in the windings to flow through the external electrical circuit. It is somewhat analogous to a water pump, which creates a flow of water but does not create the water inside.

Heat engine. A heat engine is a system that performs the conversion of heat or thermal energy to mechanical work. It does this by bringing a working substance from a high temperature state to a lower temperature state.

Heat exchanger. A heat exchanger is a piece of equipment built for efficient heat transfer from one medium to another. The media may be separated by a solid wall, so that they never mix, or they may be in direct contact.

Linear Motor. A motor which works in the linear direction and reverses at the end of travel.

microCHP. Micro Combined Heat and Power system. A home appliance replacing conventional boilers used to heat a home or dwelling. MicroCHP systems generate heat and electricity for a home.

Numerical integration. In numerical analysis, numerical integration constitutes a broad family of algorithms for calculating the numerical value of a definite integral, and by extension, the term is also sometimes used to describe the numerical solution of differential equations.

Open and closed cycle. A closed cycle reuses the working fluid while an open cycle exhausts it.

Piston. A piston is a component of reciprocating engines, reciprocating pumps, gas compressors and pneumatic cylinders, among other similar mechanisms. It is the moving component that is contained by a cylinder

and is made gas-tight by piston rings. In an engine, its purpose is to transfer force from expanding gas in the cylinder to the crankshaft via a piston rod and/or connecting rod. In a pump, the function is reversed and force is transferred from the crankshaft to the piston for the purpose of compressing or ejecting the fluid in the cylinder. Piston is housed in a cylinder.

Primary coolant. Primary coolant collects the heat from the cylinder and transfers it to the secondary coolant through a heat exchanger

PV Diagram. A pressure volume diagram is used to describe a thermal cycle involving the following two variables; Volume (on the X axis) and Pressure (on the Y axis). The diagrams are useful when one wants to calculate the work done by the system, the integral of the pressure with respect to volume. One can often quickly calculate this using the PV diagram as it is simply the area enclosed by the cycle.

Regenerator. In a Stirling engine, the regenerator is an internal heat exchanger and temporary heat store placed between the hot and cold spaces such that the working fluid passes through it first in one direction then the other. Its function is to retain within the system that heat which would otherwise be exchanged with the environment at temperatures intermediate to the maximum and minimum cycle temperatures, thus enabling the

thermal efficiency of the cycle to approach the limiting Carnot efficiency defined by those maxima and minima.

Servo. Servomechanism or servo is a device used to provide control of a desired operation through the use of feedback. The term correctly applies only to systems where the feedback or error-correction signals help control mechanical position, speed or other parameters.

Stirling engine. An external combustion engine used as a prime mover.

Thermocouple. A thermocouple is a device consisting of two different conductors (usually metal alloys) that produce a voltage proportional to a temperature difference between either ends of the pair of conductors.

Transmission. A mechanism to convert linear motion into rotary motion. A transmission transmits the power generated by the piston to the load.

Quasistatic process. A quasistatic process is a thermodynamic process that happens infinitely slowly. However, it is very important to note that no real process is quasistatic. Therefore in practice, such processes can only be approximated by performing them infinitesimally slowly. A quasistatic process ensures that the system will go through a sequence of states that are infinitesimally close to equilibrium (so the system remains in quasistatic equilibrium), in which case the process is typically

reversible. The word "reversible" applies to processes, not systems. The reversibility of the Carnot cycle is not the fact that it is a cycle which gets back to its starting point, it is the point that you can run it in reverse and use it as a heat pump rather than a heat engine. Any reversible process is necessarily a quasistatic one. However, some quasisatic processes are irreversible, if there is heat flowing (in or out of the system) or if entropy is being created in some other way. For example, an infinitesimal compression of a gas in a cylinder where there exists friction between the piston and the cylinder is a quasistatic, but not reversible process. Although the system has been driven from its equilibrium state by only an infinitesimal amount, heat has been irreversibly lost due to friction, and cannot be recovered by simply moving the piston infinitesimally in the opposite direction.

1. Introduction and History of Stirling engine Development

Stirling machines are a form of heat engine using expansion and compression at different temperatures of a gaseous working fluid for their operation. They incorporate a novel component, a thermal regenerator [1]; a form of heat exchanger [2] acting as a thermodynamic sponge alternately accepting and rejecting heat to and from the working fluid. This helps in recycling a major fraction of the energy flow from one cycle [3] to the next. Stirling engines exhibit high thermal efficiencies between given temperature limits because of the regenerator. Stirling machines may be used as a prime mover [4], accepting heat from a high temperature source, converting some of the heat to work and rejecting heat at a lower temperature. They may also be used as a refrigerator or heat pump, lifting heat from a low temperature source and rejecting it at a higher temperature with an input of work.

Kinematic Stirling engines are explored in this thesis as a candidate for a micro combined heat and power application. IC engines are noisy, have vibrations and need a service every 200 to 300 hours of operation. Fuel cells, another candidate, are at least 10 years out in the future when this research was done and free piston Stirling engine, another type of Stirling

engine is not controllable and difficult to balance. Due to these reasons, kinematic Stirling engines are considered for the application.

1.1 Reverend Robert Stirling and his engine

The Stirling engine was invented in 1816 by Reverend Robert Stirling a Minister in the Church of Scotland. Robert Stirling and his brother James, one of the leading engineers of the time, worked on regenerative systems for many years [5]. The Stirling brothers made a number of engines some of which were used in practical applications. In those days similar machines were called air engines or hot-air engines or caloric engines with the name of the inventor prefixed.

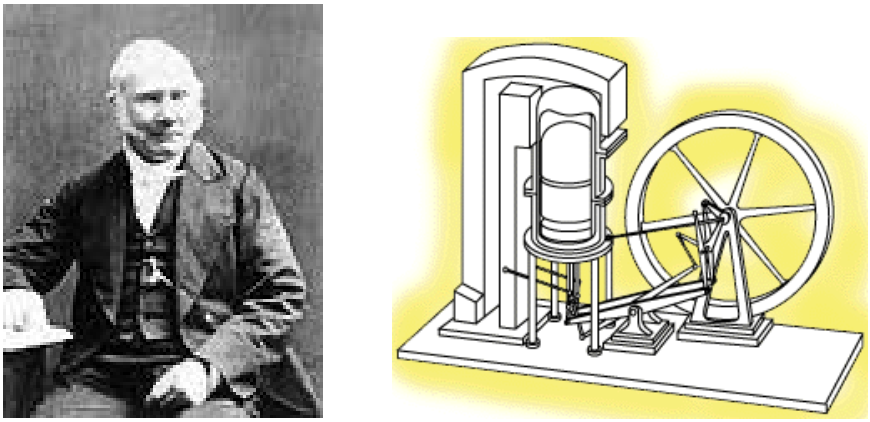

Figure 1-1 Reverend Robert Stirling and his engine [6]

The name ‘Stirling Engines’ was coined to embrace all types of closed cycle regenerative gas engines regardless of the identity of the working fluid. The generic title ‘Ericsson Engines’ [7] was used to embrace all types of open cycle valve regenerative gas engines. Throughout the 19th century hot air engines were made and used in relatively large numbers. The early air engines were used in a variety of applications, mainly generation of power and pumping water [8]. The history of these early air engines has been well surveyed by Finkelstein [9] and by Sier [10].

Stirling engines enjoyed substantial commercial success around 1900. The lack of suitable materials hampered its further development and the improvements in internal combustion engines and electrical machines led to its eventual demise [5].

1.2 Philips Stirling engine development

Philips Electric Company in Eindhoven, Netherlands was interested in developing kerosene fuelled electric power generators to replace heavy lead acid batteries used in valve radios of the time. The valve radios were power hungry and the batteries used for them were bulky. Philips started working on Stirling machines in the late 1930’s which laid the foundation of all the present interest in Stirling machines. Philips developed a Stirling engine which was an order or magnitude better in terms of efficiency,

speed and power density to any other previous generation Stirling engines. However, improvements in thermionic valve design and the invention of electronic transistors and subsequent development of dry battery powered transistor radios eliminated the need for the market for which the engine was intended. The history and technology of the Philips Stirling developments has been written in detail in an interesting book by Hargreaves [11].

Philips recognized the importance of their work and proceeded with the development of larger Stirling engines. They switched to lighter working fluids like hydrogen and helium to permit high speeds and high power densities. The term “air engine” thus became redundant. By 1948, Philips had a V4 engine on test and Major automakers including Henry Ford II had visited their laboratories. Because of its quiet operation and favorable torque characteristics, the Stirling engine is particularly well suited for ship and submarine propulsion. This is the application Philips chose to pursue. General Motors of Detroit, Michigan licensed the Stirling engine from Philips and it continued from 1958 to 1970. The GM programme was very extensive with a wide range of engines from 10hp to 800hp. Later, Ford motor company picked up the GM license with Philips and worked principally on a 135kW engine for the Ford Torino sedan. The Torino engine which started life in the GM programme as a torpedo motor was

developed at the Philips laboratories while Ford concentrated on the vehicle installation, drive train and other aspects [12].

In 1978, US Department of Energy, Philips and Ford had a co-operative programme to develop a 67kW engine with $160 million funding. This programme was cancelled in the early 1980's. Philips management shortly decided that power system development was outside their corporate game plan and they disbanded the research and development team at Philips. The long-term leader of the Philips Stirling research team, Dr. Rolf Meijer was in the US to assist the Ford Company in their Stirling engine development. Rather than returning home for early retirement, he remained in the USA and founded Stirling Thermal Motors. Stirling Thermal Motors was renamed STM Power Inc. in 1990. STM Power Inc. was a developer of on-site, electricity and cogeneration systems or "Power units". The Company believes that electricity and heat produced by its "Power Units" are expected to be more economical than other energy conversion technologies (fuel cells, micro turbines and photovoltaic systems) competing in the distributed generation (DG) market. A 25 kW Power Unit, began testing in December 1999. A renewable DG product, the Sun Dish Solar system, has been installed in five test facilities. Another product is the 10 kW PowerUnit, based on the STM 4-70 Stirling engine, which is being developed as an adaptation of the engine that was built in conjunction with

General Motors Corporation for use in GM's hybrid electric car. Re-configured as a Power Unit, it was designed to deliver a rated capacity of 10 kW of electricity and 20kW of heat. The 10 kW Power Unit will measure approximately 3ft * 3ft * 2ft (about the size of a small residential air conditioning unit).

Around 1968 Philips gained two other licensees, United Stirling AG of Sweden and the German combine MAN-MWM. United Stirling became wholly owned by the Swedish government. United Stirling manufactured Stirling engines for replacing bus engines. The aim was to build quiet, efficient and low polluting bus engines for public transport. The engines cost three times that of an equivalent diesel engine and hence were not commercially successful. Then United Stirling produced many models of four cylinder engines from 25 to 75kW. These were intended for automotive and marine propulsion, solar power generation and for battery charging units on non nuclear submarines. In the early 1980's united Stirling invested in solar power generation in co-operation with McDonnell Douglas Corporation building several installations for major utility companies in the US. The MAN-MWM combine concentrated on developing engines for heavy vehicles and underwater propulsion. Around 1977, the German Ministry of Defense got interested and the programme was promptly classified as secret. In 1990, United Stirling

(then Kockums) announced a licensing agreement with MAN-MWM to produce a 600kW V12 engine. This was probably to be used as the main propulsion unit for non nuclear, air independent submarines. As the former USSR broke up and the threat to Scandinavian countries was removed, the programme was abandoned [8].

1.3 Other notable Stirling engine developments

There were notable contributions made by others acting independently of Philips. Most notable is the work of William Beale. In the early 1960's Beale became interested in the Philips work. He studied the Stirling engine and concluded that the kinematic linkage coupling the crankshaft and reciprocating pistons and displacer was unnecessary. Thus the free piston Stirling engine [13] was born. Beale became successful in developing the free piston system and started the company Sunpower Inc. of Athens, Ohio. Over the last 50 years they have worked on the free piston Stirling engine and are unparalleled in their field. Another highly competent team of technologists is Stirling Technology Inc. of Richland, Washington. They started working under the direction of William Martini, a noted pioneer in the Donald Douglas Laboratories, LA, California (part of McDonnell Douglas Astronautic Company) on the development of the artificial heart [14].

1.4 Stirling engine development in Japan

In the late 1970's the Japanese entered the Stirling engine field in a substantial way. The Japanese Government Ministry of International Trade funded the R&D work on four engines from 3kW to 30kW. They were natural gas fired and were intended to be used as cogeneration systems and drivers for heat pumps. In 1977, a consortium of British universities and industries including BP Plc, embarked on an ambitious project to produce six 2 cylinder 20kW Stirling engines. Novel features like ceramic pistons and a heat pipe system were experimented with [8].

1.5 Stirling engine development in US

In 1978, engineers at Ford Motor Company began developing designs of a solar-powered Stirling engine. Through the years, companies like McDonnell-Douglas, Lockheed Martin and Boeing all worked to improve on the technology and design. In 1996, Stirling Energy Systems, based in Scottsdale, Arizona USA, was formed to develop this technology and has worked in a cooperative public-private partnership relationship with Sandia National Laboratories and US Department of Energy, to bring the SunCatcher™ [15] to market. The SunCatcher™ is a proprietary solar-to-grid-quality electricity generation technology. It is a 25-kilowatt solar dish Stirling system that is designed to automatically track the sun so as to

collect and focus solar energy on to a power conversion unit (PCU), which generates electricity. The system consists of a solar concentrator in a dish structure that supports an array of curved glass mirror facets. These mirrors collect and concentrate solar energy into grid-quality electricity. The conversion process in the PCU involves a closed-loop, high-efficiency four-cylinder reciprocating Stirling Engine.. A total of 60 SunCatcher™ Power Systems have been operating since January 2010. Prototypes of the system have been running for over two decades which provided the learning to design the current systems.

1.6 Development in Stirling engine refrigeration and cryocooling

The possibilities of using the Stirling engine for refrigeration has a history of almost as long as its use as a power system. In a letter to the British periodical 'The Athenaeum' in 1834, John Herschel discussed the Stirling system as a possible refrigerator [8]. This is the earliest known reference. The first widespread commercial application of Stirling refrigerators came from the Philips research and development program on power systems in the 1950's. Any Stirling engine that produces power when supplied with heat will also work effectively as a refrigerator. All that is necessary to achieve this is to terminate the source of heat supply and to drive the shaft to keep the machine working. Philips found their Stirling power systems

were very effective refrigerators when motored. The commercial prospect was identified as a very low temperature refrigerator to achieve cryogenic temperatures (Below 110K). Cryocoolers [16] are used in spacecraft for a variety of purposes. Principal applications are for cooling infrared detectors and high temperature superconductor research. Cryocoolers are also used to prevent evaporation in cryogenic fuel tanks. Cryogenic engineering is a specialist field involved with the separation and purification of gases [17] . This technology has lot of applications in medical, education, commercial, Industrial, food preservation and metallurgy. The book by Graham Walker (1983) summarises the technology of cryogenic refrigerators [18].

Philips recognized the commercial possibilities of the Stirling cryocooler. A separate team was established to develop it as a commercial product under the leadership of Dr. Kohler. He is recognized as the father of the cryocooler.

In 1956, Philips introduced a single piston/displacer unit of about 1kW (at 80K) cooling capacity capable of producing about 8 litres of liquid air per hour. The unit was unchallenged and only required electric power and cooling water to achieve cryogenic temperatures. Soon auxiliary equipment became available including a device to separate liquid nitrogen from liquid air. A four cylinder version of the liquefier provided the capacity for

substantial liquid air production. It is estimated that Philips sold around 15000 of these cryogenic units and recovered most of their investment in the Stirling engine programme. The principle field of application of Stirling cryocoolers turned out to be a very miniature form and not the large systems as Philips envisaged. These miniature cryocoolers are used to cool the infrared detectors of night vision equipment and missile guidance systems. The surfaces of the infrared detectors are responsive to particular wavelengths at very low temperatures [19]. The infrared chips needed electrically driven closed cycle cryocoolers in the field and a market for these kind of cryocoolers emerged by late 1950's/early 1960's. As electronics technology advanced, the infrared chips became smaller and the refrigeration requirements diminished. [8]

In the 1970's US military services established the production of common module cryocoolers of ¼ to 1W (at 80K) capacity. With the ready availability of these relatively low cost cryocoolers, it became the practice to match the electronic detector system to the available cooler rather than to design and custom make a cooler for the application. The large scale production of common module coolers continued in the United States throughout the 1980's and an estimated 40,000 units were manufactured annually. In the late 80's continuing miniaturization of the detector assemblies prompted development of a new generation of super miniature

Stirling cryocoolers. One of the most successful of these new generation Stirling cryocoolers was made by Ricor of Israel. Over the past 50 years, a substantial amount has been invested in efforts to produce a spacecraft cryocooler able to meet the stringent demands of reliability, low mass, low volume, low vibration, low EMI [3], able to operate in any orientation in zero gravity environment, able to withstand launch vibration and a life time of ten years [8].

2. Combined Heat and Power or CHP systems

2.1 Introduction to CHP systems

In some energy applications, energy is required in multiple forms. These energy forms typically include some combination of heating, ventilation, and air conditioning, mechanical energy and electric power. Often, these additional forms of energy are produced by a heat engine, running on a source of high-temperature heat [20]. A heat engine can never have perfect efficiency, according to the second law of thermodynamics [21], therefore a heat engine will always produce a surplus of low-temperature heat or waste heat. This heat is useful for heating applications even though it is not practical to transport heat energy over long distances, unlike electricity or fuel energy.

An energy efficient system must generate electricity near locations where the waste heat can be put to good use. This is known as a combined heat and power (CHP) system, or "cogeneration" [22].

In a central power plant, the supply of surplus heat may well exceed the local heat demand. In such cases, if it is not desirable to reduce the power production, the excess waste heat must be disposed in cooling towers without being used.

A CHP system works mainly from the heat demand. Fuel input to the CHP plant is restricted, reducing both the heat and power output to balance the heat demand. In doing this, the power production is limited by the heat demand.

CHP systems are able to increase the total energy utilization of primary energy sources, such as fuel and concentrated solar thermal energy. Thus CHP has been steadily gaining popularity in all sectors of the energy economy, due to the increased costs of fuels, particularly oil-based fuels, and due to environmental concerns, particularly climate change.

In a traditional power plant delivering electricity to consumers, about 30% of the heat content of the primary heat energy source, such as biomass, coal, solar thermal, natural gas, petroleum or uranium, reaches the consumer, although the efficiency can be 20% for very old plants and 45% for newer gas plants. In contrast, a CHP system converts 10%–25% of the primary heat to electricity, and most of the remaining heat is captured for hot water or space heating. In total, as much as up to 93% of the heat from the primary energy source goes to useful purposes when heat production does not exceed the demand.

A microCHP system utilises the same principles, but uses a small single home scale generating unit that is installed as an alternative to a standard

domestic boiler [23]. When operating, the microCHP system generates both electricity and hot water. The electricity produced is available for use in the house or exported to the national grid and the hot water is used for both central heating and domestic hot water. The electrical efficiency of microCHP systems in development is 10 to 25% and overall energy recovery efficiency is above 90%. The use of a microCHP system can play an important role in the effort to reduce atmospheric pollution and carbon dioxide emissions, a leading contributor to climate change. Better efficiency will also allow better utilisation of natural resources.

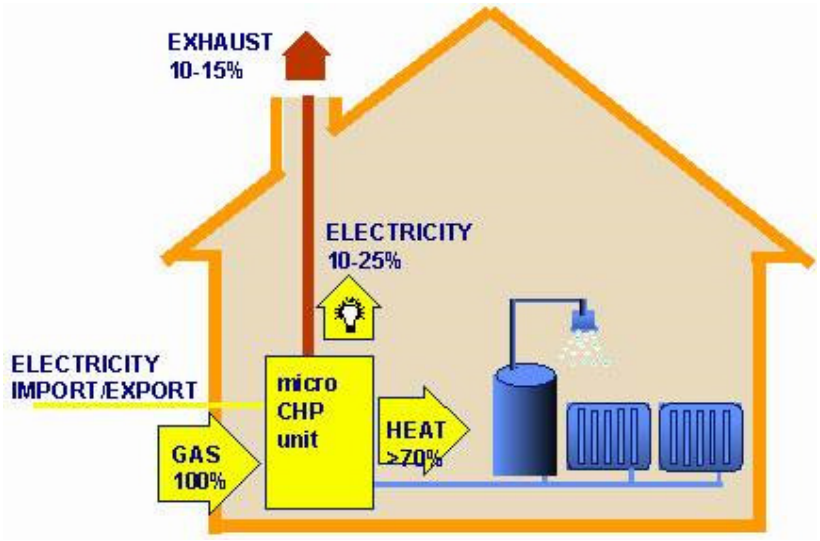

Figure 2-1 MicroCHP system illustration [8]

The development of microCHP systems has also been facilitated by recent technological developments of small heat engines, gas turbines [24], fuel

cells [25] and internal combustion engines [26]. MicroCHP is not economically viable in many markets around the world. MicroCHP systems need to be efficient to generate more electricity and provide a better payback. This thesis explores the potential of improving the efficiency and manufacturing cost of microCHP systems.

To date, microCHP systems achieve much of their savings, and thus attractiveness to consumers, through a net metering model [27] wherein home-generated power exceeding the instantaneous in-home needs is sold back to the electrical utility. This system is efficient because the electricity generated is distributed and used instantaneously over the electrical grid. The main losses are in the transmission from the source to the consumer, which will typically be less than losses incurred by storing energy locally or generating power at less than the peak efficiency of the microCHP system. Therefore from a purely technical standpoint dynamic demand management [28] and net-metering are very efficient.

Another positive to net-metering is the fact that it is fairly easy to configure. The user's electrical meter is simply able to record electrical power exiting as well as entering the home or business. As such, it records the net amount of power entering the home. For a grid with relatively few microCHP users, no design changes to the electrical grid need be made.

2.2 WhisperGen® microCHP systems

There are various technologies used for the prime mover in the microCHP space. The leading ones are kinematic Stirling engines, free piston Stirling engines and fuel cells. Internal combustion engines are not generally preferred due to the noise levels and service requirements. During the time of this research, only one microCHP system was commercially available. This was the WhisperGen® microCHP manufactured in Christchurch, New Zealand and deployed in Europe. All other microCHP systems were undergoing early trials or in experimental stage of development. Due to this reason, the WhisperGen system is analysed in detail.

Whisper Tech Ltd. is a leading manufacturer of the kinematic Stirling engine based WhisperGen® microCHP systems and supporting this research programme. WhisperGen® microCHP systems consume compressed natural gas as its fuel and generate 1kW electricity and 7.5kW heat. WhisperGen® microCHP systems are the size of a domestic dishwasher. They produce heat and power at the point of demand. The system avoids distribution losses and maximises utilisation of primary energy and offers significant contribution to CO_2 mitigation targets. The WhisperGen® microCHP system offers significant improvement over condensing boilers [29] used for space and water heating. Stirling engines

operate on a principle that heated gas expands and the cooled gas compresses. For the WhisperGen® system, a mixture of air and fuel is burned in an external combustion burner, which heats up the finned heater heads of the Stirling engine. Heat is transferred through the finned heater heads to heat nitrogen gas within four cylinders. The heated nitrogen gas expands in the top hot heat exchanger and is then moved to the lower water cooled cylinder where it contracts. Cooling water removes heat from the cold cylinder and is used for domestic water heating. Central heating water returns through the exhaust heat exchanger, where it is pre-heated by the hot gases from the engine exhaust. Water then passes to a water jacket in the engine, where it is heated further and in the process provides cooling for the "cold end" of the engine. Resulting hot water is then piped out to the heating system. At times of high heat demand an auxiliary burner provides additional heating.

The Stirling engine has no valve gear. No fuel or air is taken into or out of the cylinder. It is a completely closed cycle of operation. This allows the system to operate in a clean and quiet manner. Rapid heating and cooling creates pressure changes in the nitrogen gas. The rapid pressure changes of the gas force the pistons to move. The up and down motion of the pistons are connected to a rotary generator through a transmission [30]. A single

phase squirrel cage induction machine [31] is used as the electrical generator in the WhisperGen® .

2.3 Control of existing microCHP systems

In microCHP systems, electric power is generated when the system is running. Primary control of microCHP systems is the heat demand signal, which starts and stops the engine. MicroCHP systems are sized to handle the average thermal load of a house. An auxiliary burner (also called the boost burner) is used in the system to increase the thermal output as and when required. The auxiliary burner is coupled to the main exhaust heat exchanger and is turned on to increase the heat output.

In normal operation, the auxiliary burner is switched on and off to achieve the control aspect (outer control loop) for the heating. The disadvantage of using an auxiliary burner is that the energy going into the auxiliary burner is not generating electricity. This part of the system works like a conventional boiler.

The proposed system in this thesis uses phase control of the displacer, to achieve power modulation instead of using on off control.

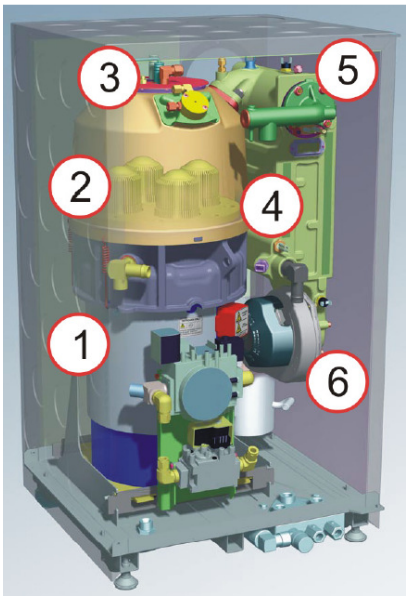

Figure 2-2 Inside the WhisperGen® microCHP system

A drawing of the WhisperGen® microCHP system is shown in Figure 2.2. The primary set point for the system is the heat demand signal provided by the central heating controller.

1. An electrical generator that provides 230V AC power

2. A Stirling engine that provides motive power for the generator

3. A gas burner assembly, which provides heat necessary for the operation of the Stirling engine

4. A heat exchanger that recovers heat from the hot gases produced by the burner

5. An auxiliary burner that provides additional heat at times of high heat demand

6. An exhaust fan connected to a balanced flue [32]. This provides the combustion air for the burner and passes the hot gases from the combustion process through the heat exchanger to the atmosphere

On receiving the heat demand signal from the central heating controller, the primary burner is started. Once the heater head achieves a certain temperature, the engine is started by motoring the electrical machine. Starting the induction machine is achieved through power electronics. The main and auxiliary winding of the Induction machine is connected across two H Bridges and they are driven in quadrature [33]. An algorithm considers the ramping up time and the instant of changeover to the grid to calculate the instant of starting on the mains AC cycle. The utility AC input is monitored and the cranking is started at the predetermined instant on the mains AC cycle. Once the engine has cranked up to speed, the electrical machine is connected to the grid and it exports the power generated. The main winding is connected directly across the grid and the auxiliary winding is connected through a suitable capacitor. The machine works as

an induction generator with a positive slip and exports the power generated to the utility grid. Once the system is exporting electricity, a control system regulates the fuel burning rate to set the operating point to 1kW electricity generation.

Once the primary coolant reaches a set temperature, the heat demand signal is withdrawn by the central heating controller and the engine stops. The central heating controller waits for the coolant temperature to drop to a predefined set point before triggering the heat demand signal to repeat the cycle.

3. Fundamentals of Stirling Engines

3.1 Introduction to Stirling engine technology

Heat engines are generally described in terms of cyclic processes in which a gas absorbs heat at a high temperature, releases heat at a lower temperature and performs an amount of work. Carnot [34] showed in the 1820s that the maximum theoretical efficiency available from a reversible heat engine depends only on the temperature change in the cycle [35].

$$\eta = \frac{W}{Q_e} = 1 - \frac{T_c}{T_e} \qquad (3.1)$$

Where η is the efficiency, W (Joules) is the work done by the engine, Q_e (Joules) is the heat fed to the engine, T_c (Kelvin) is the temperature at which heat is rejected and T_e (Kelvin) is the temperature at which heat is absorbed.

The processes which occur in even the simplest physically implemented thermal machine are complicated, as such it is not possible to calculate precisely what is happening from moment to moment. Instead a theoretical model is assumed in which the various events are idealized to the extent necessary to make analysis of their approximate operation possible. To

facilitate the analysis of operation, a repeated sequence of the thermodynamic process called the cycle is assumed.

3.2 Thermodynamic cycles

A thermodynamic cycle consists of a series of thermodynamic processes transferring heat and work, while varying pressure, temperature, and other state variables, eventually returning a system to its initial state [36]. In the process of going through this cycle, the system may perform work on its surroundings, thereby acting as a heat engine.

State quantities depend only on the thermodynamic state, and cumulative variation of such properties adds up to zero during a cycle. Process quantities (or path quantities), such as heat and work are process dependent, and cumulative heat and work are non-zero. The first law of thermodynamics dictates that the net heat input is equal to the net work output over any cycle. The repeating nature of the process path allows for continuous operation, making the cycle an important concept in thermodynamics. Thermodynamic cycles often use quasistatic processes [37] to model the workings of actual devices.

Thermodynamic power cycles are the basis for the operation of heat engines, which supply most of the world's electric power and run almost all

motor vehicles. Power cycles can be divided according to the type of heat engine they seek to model. The Otto cycle [38] models gasoline engines and the diesel cycle [39] models diesel engines, both of which are internal combustion engines. Brayton cycle [40] models gas turbines and jet engines. Rankine cycle [41] models steam turbines. Brayton and Rankine cycles model external combustion engines.

Two primary classes of thermodynamic cycles are power cycles and heat pump cycles [3]. Power cycles are cycles which convert some heat input into a mechanical work output, while heat pump cycles transfer heat from low to high temperatures using mechanical work input. Cycles composed entirely of quasistatic processes can operate as power or heat pump cycles by controlling the process direction. On a pressure volume diagram [36] the clockwise and counterclockwise directions indicate power and heat pump cycles, respectively.

In a thermodynamic cycle, the indicated PV diagram provides the work done, which is a plot of the Pressure vs. Volume in a cycle. This is in fact enough information to fully describe a simple system from a thermodynamic standpoint. The diagrams are useful when one wants to calculate the net work done by the system, the integral of the pressure with respect to volume. One can often quickly calculate this using the PV

diagram as it is simply the area enclosed by the cycle. For an ideal system the net variation in state properties during a thermodynamic cycle is zero, it forms a closed loop on a PV diagram. A PV diagram's Y axis shows pressure (P) and X axis shows volume (V) as shown in Figure 3-1.

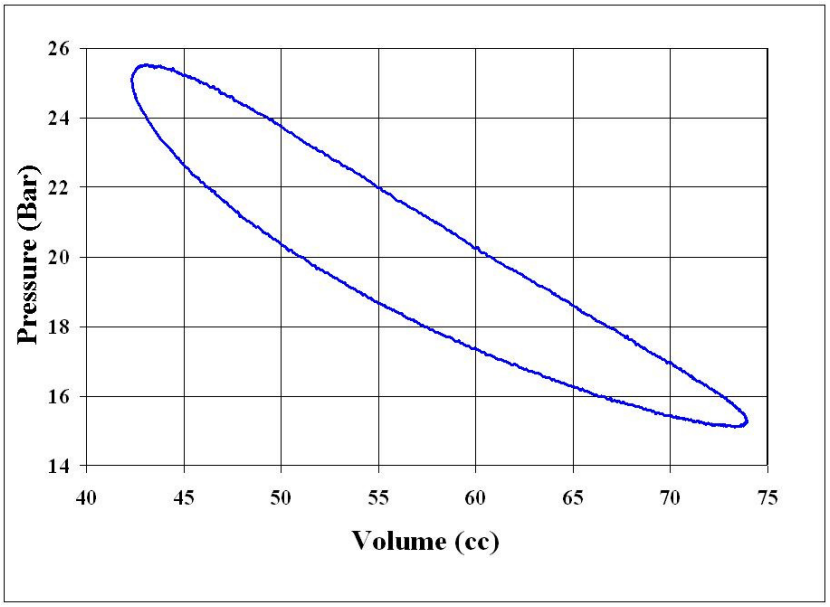

Figure 3-1 PV Diagram of a Stirling engine

The area enclosed by the loop is the net work (W) done by the process:

$$W = \oint P dV \tag{3.2}$$

This work is equal to the balance of heat (Q) transferred into the system:

$$W = Q = Q_{in} - Q_{out} \tag{3.3}$$

Equation (3.3) makes a cyclic process similar to an isothermal (infinite heat transfer) process: even though the internal energy changes during the course of the cyclic process, when the cyclic process finishes the system's energy is the same as the energy it had when the process began. If the cyclic process moves clockwise around the loop, then W will be positive, and it represents a heat engine. If it moves counterclockwise, then W will be negative, and it represents a heat pump.

A Stirling machine is a device which operates on a closed regenerative thermodynamic cycle [3] with cyclic compression and expansion of the working fluid at different temperature levels, and where the flow is controlled by volume changes so that there is a net conversion of heat to work and vice versa. Stirling machines are capable of operating as prime movers, heat pumps, refrigerating engines or pressure generators.

3.3 The Stirling cycle

The ideal Stirling cycle, conceptually illustrated in Figures (3.2) and (3.3), is a highly idealised thermodynamic cycle, comprising of four thermodynamic processes, including two isothermal and two isochoric processes. The theoretical efficiency of a Stirling cycle operating between high temperature T_e and low temperature T_c is the same as that of the Carnot cycle. Heat is supplied to the cycle at T_e. Part of the heat is

converted to work and part of it is rejected as heat at a lower temperature T_c. The displacer is used to transfer the gas between hot and cold ends and should not be confused with the power piston.

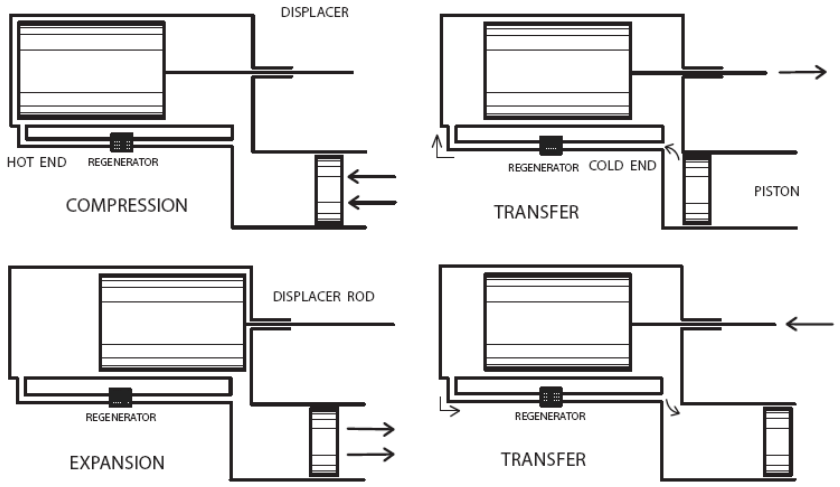

Figure 3-2 Sequence (compression-transfer-expansion-transfer) of ideal piston and displacer motions of a Stirling engine

A matrix of fine wire mesh called the regenerator is used in the path between hot and cold ends (not shown in Figure 3-2) and the gas flows from hot end to cold end and vice versa through this regenerator. The effect of regeneration in a Stirling engine is to increase the efficiency greatly by 'recycling' internal heat which would otherwise pass through the engine irreversibly. The design challenge for a Stirling engine regenerator is to provide good heat transfer capacity without introducing too much additional internal dead volume or flow resistance. Dead

volume is the unswept internal volume. A typical design is a stack of fine metal wire meshes, with low porosity to reduce dead space, and with the wire axes perpendicular to the gas flow to reduce conduction in that direction and to maximize convective heat transfer.

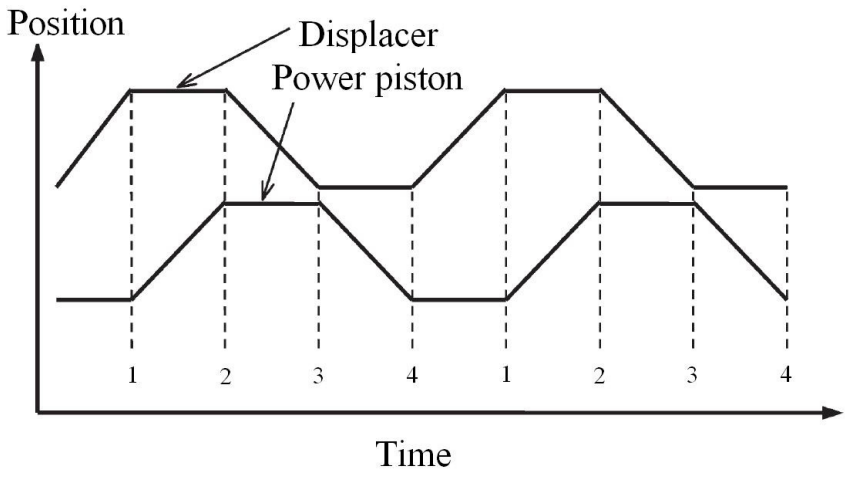

Figure 3-3 Motion profile of an ideal Stirling engine [42]

Figure 3-3 shows the motion profile of an ideal Stirling engine. Process 1-2 is isothermal compression. Heat is transferred from the working fluid at temperature T_c to the external dump

Process 2-3 is isochoric transfer of gas from the cold section to the hot section of the engine. Heat transfer takes place from the regenerator to the working fluid

Process 3-4 is isothermal expansion. Heat is transferred to the working fluid at temperature T_h from an external source

Process 4-1 is the constant volume transfer of gas from the hot section to the cold section. Heat transfer takes place to the regenerator from the working fluid

If the heat transferred in process 2-3 has the same magnitude as in process 4-1, then the only heat transfers between the engine and its surroundings are heat supply at T_h and heat rejection at T_c. This heat supply and heat rejection at constant temperature satisfies the requirement of the second law of thermodynamics for maximum thermal efficiency, so that the efficiency of the Stirling cycle is same as that of the Carnot cycle. The principal advantage of the Stirling cycle over the Carnot cycle lies in the replacement of two isentropic processes by two isochoric processes, which increases the area of the PV diagram. Therefore to obtain a reasonable amount of work from the Stirling cycle, it is not necessary to resort to very high pressures and swept volumes as in a Carnot cycle.

3.4 Ideal and conventional Stirling engines

In the above discussion, it was assumed that all processes were

thermodynamically reversible and that the process of compression and expansion are isothermal, thereby implying infinite rates of heat transfer between the cylinder walls and the working fluid. It is also assumed that all the working fluid is either taking part in the expansion or compression process so that effects of any voids in the regenerator matrix, clearance spaces and pockets contributing to dead volume were neglected. Regeneration is assumed to be perfect with an infinite rate of heat transfer between the regenerator matrix and the working fluid. Also the piston and the displacer were assumed to move in some discontinuous fashion to achieve the working fluid distribution. All fluid dynamic and mechanical friction and leakage effects were neglected. In any practical engine, all these factors contribute towards achieving a thermal efficiency well below the Carnot value of the ideal Stirling cycle. The actual thermal efficiency may be quoted as a fraction of the theoretical Carnot efficiency. A value in excess of 0.3 is evidence of a well designed Stirling engine [12].

The ideal piston and displacer motions cannot be attained in practice largely due to the continuous velocity profiles of real devices used for regulating, storing and transmitting energy such as linkages, springs and flywheels. Mechanisms can be made to have stepped velocity profiles by using cams, for example. But the physical realization will have

limitations due to inertial forces and elasticity.

In a conventional engine, the piston and the displacer will be moving in a nearly sinusoidal manner. The piston and displacer motion profiles of a conventional Stirling engine are shown in Figure (3-4). In the operation of this engine, a significant departure from the ideal arises as a consequence of the near sinusoidal motion of the pistons. The compression and expansion do not take place wholly in one or other of the two spaces.

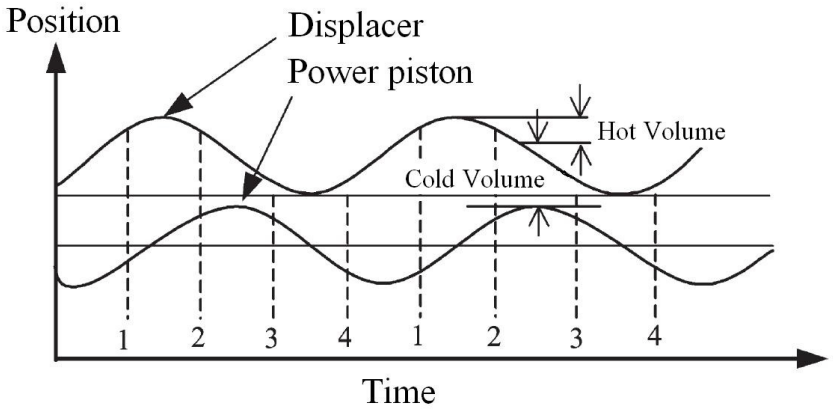

Figure 3-4 Motion profile of a conventional Stirling engine [42]

Sinusoidal piston and displacer motion leads to a pressure volume diagram similar to that shown in Figure 3-1 for a kinematic Stirling engine. The work done by the engine is represented by the area enclosed by the pressure volume diagram. At reasonable operating speeds (500 to

1500 RPM) it is likely that the compression and expansion processes are becoming adiabatic (no heat transfer) and not isothermal. To improve the heat transfer, special heat exchangers are required at the hot and cold ends. These heat exchangers increase flow losses and dead volume which affects the system efficiency.

The mechanical arrangements of Stirling engines are generally divided into three groups known as Alpha, Beta and Gamma arrangements [43]. Alpha engines have a pair of sealed pistons in separate cylinders, which are connected in series by a heater, a regenerator and a cooler. Both Beta and Gamma arrangements are defined by the use of a classic piston-displacer arrangement, the Beta type having them both in the same cylinder and the Gamma type in separate cylinders [44]

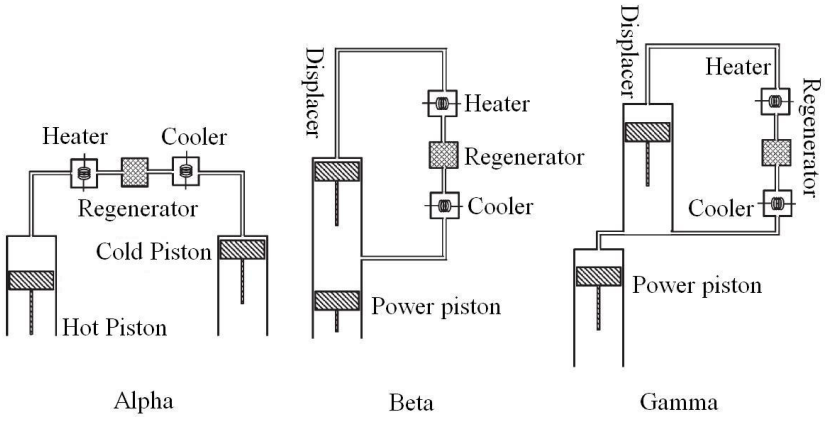

Figure 3-5 Alpha, Beta and Gamma Stirling engine[42]

3.5 Stirling engine control

The power output of a Stirling engine depends on a variety of factors including the temperature of the hot and cold ends, the swept volume to total unswept working gas volume ratio, the phase angle by which the volume variations in the expansion space lead those in the compression space, the mean cycle pressure of the working fluid, the speed of the engine and the dynamic characteristics of the load coupled to the engine. Ideally speaking, all the above mentioned parameters can be used to control and regulate the power output or operating speed of the engine.

3.6 Temperature control of Stirling engines

Conventional microCHP systems use temperature control of the heater heads. The control system regulates the fuel supplied to the burner system to control the hot end temperature to effectively output the power produced at steady state. As the thermal inertia in the system is high, the response is sluggish, often taking many minutes to reach steady state.

3.7 Pressure control of Stirling engines

Earlier automotive designs attempted with Stirling engines used pressure control. A reservoir of high pressure gas that can be admitted to the

working space through a control valve was used. A temporary decrease happens in the engine output when fluid is admitted as the cold fluid needs to come up to the working temperature. However, after this initial transient, the increased pressure increases the power output. A decrease in power output is accomplished by release of the working fluid from the working space. The released fluid is compressed and stored back in the reservoir.

3.8 Stroke control of Stirling engines

Varying the stroke length of one or both the piston and the displacer is an effective method of controlling the power output of a Stirling engine. A reduced stroke has a lower swept volume and consequentially a lower pressure ratio decreasing the output power of the engine. Power reduction is caused by the reduced pressure ratio and swept volume. However, the volume of the fluid not taking part in the process increases or the efficiency drops. This volume is termed the dead volume and a Stirling engine designer always looks for ways to reduce this volume to increase the engine efficiency. Some of the earlier designs of automotive engines used dead volume control as a means to achieve quick acceleration and deceleration.

3.9 Phase control in Stirling engines

In a Stirling engine the volume variations in the expansion space leads the volume variations in the compression space by a phase angle α. This ensures that heat is absorbed by the expansion space and rejected from the compression space. When the phase angle is zero, the pistons move synchronously but in anti-phase. The volume and pressure ratios are very high, but no useful work is done. The PV diagram is a single vertical line and the area enclosed is nil. As the phase angle increases, the power output increases approaching a maximum value at about 90° and decreasing thereafter with further increase in the phase angle. When the phase angle approaches 180° the pistons move synchronously and sympathetically pushing the working fluid from the compression space to the expansion and vice versa. The total volume of the working space remains constant and there is only a slight change in pressure. This is due to the change in the temperature of the working fluid from a minimum value when the compression space volume is a maximum to a maximum value when the expansion space volume is a maximum. No work is done however for there is no change in the total working space volume. PV diagram is again a vertical line with the area enclosed being nil.

An increase in the phase angle beyond 180° will cause a reversal in the

roles of two spaces. The expansion space absorbing heat becomes the compression space and vice versa. The power output is negative indicating that an input of power is required to drive the unit. If input power is available to drive the engine, it will continue to run in the forward direction acting as a heat pump or refrigerator, absorbing heat at low temperature and rejecting heat at high temperature. Phase control is instantaneous. Conventional engines have not explored this control scheme and the Active Stirling Engine attempts to explore this control mechanism for kinematic Stirling engines.

3.10 Dead volume control

Variation of the dead space within the total working space volume can be achieved by connecting different size reservoirs in the crank case of the engine. Valves can be used to cut in and out specific dead volumes as a control scheme even though it is not efficient or easy to perform.

3.11 Speed control

The speed at which a Stirling engine operates will depend on the load applied. Stand alone systems (non grid connected and have a frequency independence) in stationary applications are normally regulated to operate at a constant speed. Direct drive automotive systems need to

operate over a wide range of speed and power levels.

The power output of a Stirling engine is proportional to the speed and the output power can be regulated with adjustments of speed. Speed control is common in Stirling refrigerators particularly in miniature cryocoolers used for infrared night vision equipment. During startup, cryocoolers are operated at maximum speed for a rapid cool down. When the machine achieves the desired cryogenic temperature of the cold tip, a feedback control system reduces the speed of the system to control the cold tip temperature.

4. The problem to be solved

4.1 Effect of phase angle on Stirling engine performance

Stirling engines have a hot end and a cold end. Heat is supplied to the hot end and heat is rejected at the cold end. The displacer shuttles the working gas from the hot end to the cold end and vice versa. The expanding gas pushes the power piston to generate work. In conventional engines, the displacer and piston are connected to the same crank. The displacer leads the piston by a phase angle of approximately 90°. Some engines operate on a phase angle as high as 120°. Even though it can be set to any phase angle, published literature suggests highest power output to be around 90°. One main investigation in this thesis is the effect of phase angle between displacer and the power piston on the performance of a Stirling engine. The variables of interest are indicated power, efficiency, heater head temperature, rejected heat and the pressure variation inside the engine. This thesis investigates the relationship of these variables with respect to the phase angle.

This thesis also investigates the effect of dwell of the displacer along with the phase angle to understand more about improvement in efficiency and controllability. Dwell is the duration for which the piston or displacer stays motionless at either of the dead centers. Dwell is usually expressed as a

percentage of the total duration of a cycle. For example if an engine is operating at 600 Hz, its cycle time is 100 milliseconds. If the dwell of the displacer is 50%, the displacer stays at the dead centers for a total of 50 milliseconds and travels from one dead center to the other and back in 50 milliseconds to complete a cycle. Hence the transition time from one dead center to the other will be 25 milliseconds and the rest time at each dead center will be 25 milliseconds.

When the displacer motion is sinusoidal, the expansion and compression does not take place completely in the respective cylinder. When the motion profile is changed from sinusoidal to the one with dwell, the working gas gets more time during the cycle to expand in the expansion cylinder and to get compressed in the compression cylinder. This property of utilizing the motion profile with dwell will improve the thermodynamics and the total work done by the system. As the work done is the same for the same input power, the efficiency increases due to the dwell. This thesis investigates to confirm this property by practical experimentation and to find out the quantum of efficiency increase.

4.2 Controllability of current microCHP systems

Current microCHP systems do not have a good degree of 'controllability' over the proportions of heat and electrical power produced. MicroCHP

systems employ ON-OFF control for the auxiliary burner and primary burner. The system turns off when the primary coolant reaches the set temperature and turns on when the coolant temperature hits the lower level. Table 4-1 shows the hours of operation of main burner and auxiliary burners on a sample of 62 WhisperGen® microCHP systems running for a total of 92,730 hours. These engines were part of a customer trial conducted in United Kingdom by Whisper Tech Ltd.

# of engines	Hours	# of starts	KWH generated	Boost burner running hours
62	92730	124067	79317	10662
Average	1496	2001	1279	172

Table: 4-1. Data showing operation of 62 WhisperGen® systems

On Average, the engines have started once every 45 minutes. It clearly shows how the auxiliary or boost burner and the engine itself are cycled through on off control to achieve an acceptable operation around a set point. Starting and stopping of a Stirling engine is complicated. While

starting, the engine has to be brought up to the working temperature, cranking has to be set, coolant flow has to be monitored and the burner has to be brought up to the right amount of fuel flow and temperature. The seals and guides will experience a higher wear when the engine starts from rest. Similarly while stopping an engine, the burner is switched off or modulated down, the engine winds down in power until the energy export becomes zero, the engine is motored from that instant to operate like a refrigerator to bring the heater head temperatures down to avoid temperature damage to the seals. Head temperatures are monitored and the engines shut down at an appropriate instant. The seals and guides experience a higher wear and tear while the engine is started or stopped compared to while running.

During startup and run down, the electrical output is reduced. Also when the engine is off, electrical energy is not produced. These factors affect the economics of the system. Startup and run down cost is high when the run time is short. This is another issue this project attempts to solve. Using the ASE, the engine is de-powered (instead of turning off) for controlling the coolant temperature and effectively the total electrical energy generated is improved.

4.3 Making use of phase control

Heat management algorithms may be able to make use of phase control to reduce start and stops, which will improve the life of the engine. Also intelligent central heating controllers provide a PWM signal, which may be made use of by a phase control mechanism to adjust the amount of heat and electricity generated. This is also a subject of investigation in this thesis.

Phase angle control has been investigated previously as a method of power control for Stirling engines. As the power output of the Stirling engine is related to the sine of phase angle between the piston and displacer, changing the phase angle has a direct impact on the power output of the engine. Changing the phase angle from the optimum value actually detunes the engine. Prior art and previous research on the effect of phase angle on Stirling engine performance is discussed in detail in Chapter 5.

4.4 Sinusoidal vs. non linear motion of reciprocating parts

In a conventional Stirling engine, the motion of the displacer and piston are near sinusoidal, resulting in an elliptical PV cycle as seen in Figure 3-1. An ideal cycle will have non-linear motion for the piston and displacer resulting in a larger PV cycle enclosed area. This thesis also explores

whether a non linear displacer motion with dwell at both ends of the stroke can increase the work done and/or efficiency of the engine compared to sinusoidal displacer motion.

In an ideal Stirling engine, most of the expansion has to take place in the hot end or the expansion cylinder and the compression or contraction should take place in the cold cylinder or compression space. In a practical Stirling engine, due to the sinusoidal motion of the piston and displacer, expansion and compression happens in both the cylinders. A move towards ideality will require non linear motion of the piston and the displacer. In this research, the displacer motion is made non linear (with dwell at both the ends of the stroke) to explore the impact of departure from sinusoidal motion. It is assumed that the enclosed area of the PV diagram will enlarge and the indicated power and efficiency of an engine will increase due to the non linear displacer motion and better thermodynamic response.

Equation 4-1 shows the relationship between the work done and the area enclosed by the PV diagram in an ideal Stirling engine.

$$W = Q_e - Q_c = \oint p \, dV_e - \oint p \, dV_c \qquad (4.1)$$

In an ideal engine, the net work done is the difference between the heat absorbed Qe and the heat rejected, Qc. The expansion space pressure

volume diagram and the compression space pressure volume diagram reveal the net work done by a Stirling cycle engine. The proposed scheme allows the closed integral to be larger due to the non linear motion and hence relates to an increase in the power produced by the Stirling engine.

4.5 Achieving phase control and non linear control

To achieve phase control and non linear motion of the displacer, the displacer is disconnected from the crank and driven separately by a linear electrical machine and its servo drive. The term "Active Stirling Engine" [45] is coined to describe systems where the displacer is actively controlled with respect to the piston. Actively controlled Stirling engine or the Active Stirling engine (ASE) is capable to control the displacer motion trajectory based on an external command signal.

The ASE can control the speed, stroke, phase, and motion profile of the displacer to achieve different results from the same engine. The automobile industry is moving towards a similar concept with variable valve timing and active injection systems to improve the performance of IC engines. In an ASE, the displacer is disconnected from the crank and is driven separately to explore the impact of phase and dwell of displacer on engine performance. This system concept is depicted in Figure 4-1.

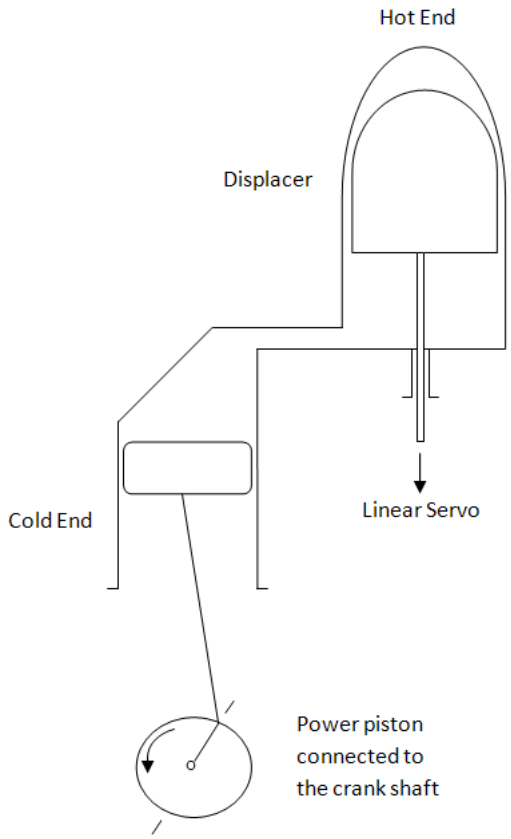

Figure 4-1 Proposed Active Stirling Engine concept

The linear electrical machine is driven by its own servo drive, which facilitates non-linear operation of the displacer. Low temperature differential slow speed Stirling engines have used the non linear piston motion to operate. Kongtragool et al. has conducted a good review of existing solar powered and low temperature differential Stirling engines [42].

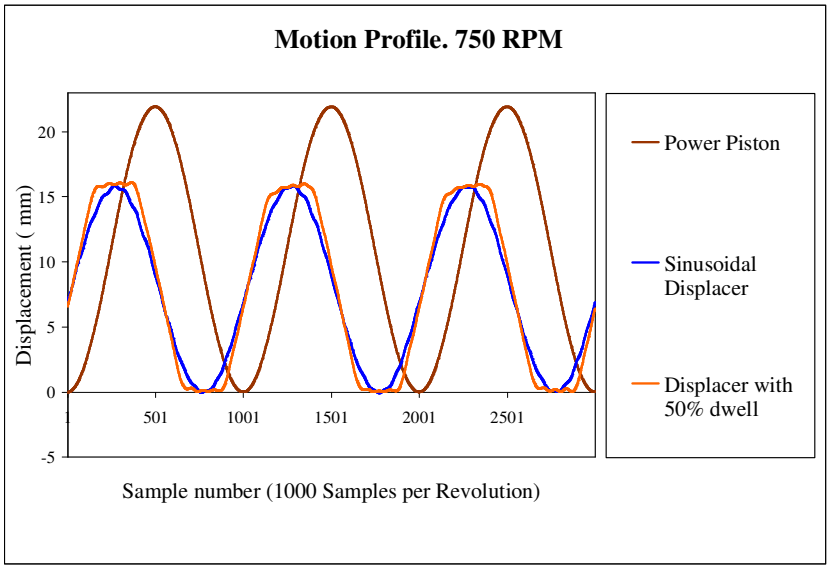

Figure 4-2 Non linear displacer motion for ASE test rig

This project investigates whether it is beneficial in high temperature high speed machines. Figure 4-2 shows the sinusoidal motion of displacer and piston in a conventional Stirling engine along with the proposed non linear motion of displacer with dwell at both ends of stroke. In addition to non linear motion, the displacer will have the ability to employ phase control so that its effects also can be investigated as explained earlier. Data represented in Figure 4-2 is collected from one of the experiments when a Stirling engine is run at 750 RPM with sinusoidal and nonlinear displacer motion.

5. Literature survey

Free displacer engines with a kinematic piston are called Ringbom Stirling engines [46]. In Ringbom engines, displacer control is not possible as it has a free displacer, which works only under gas pressures. Free piston engines with a kinematic displacer drive are termed Martini Stirling engines [44]. The Martini displacer is the name given to machines in which the displacer is driven by a motor that is independent of the power piston movements and the pressure changes. Martini patented such a system to provide power for blood pumping in an artificial heart. This was like a thermo mechanical amplifier in which a small effort expended in moving the displacer causes substantial pressure changes which acting upon the power piston can produce a much greater effect.

A gamma engine with a motor driven Martini displacer and with the power piston linked to a shaft to provide rotating power was operated by Clarke and Horsted [44]. As this motor driven displacer uses a rotary motor with a mechanical arrangement for reversal of the displacer, it could achieve only phase control. C. D. West suggests that "If the displacer is electrically driven by a linear electric motor contained within the pressure vessel, no mechanical connection is required, which greatly eases the seal problem"[44]. The ASE is similar to what C. D. West has suggested,

except the displacer shaft is brought out of the pressure vessel and the linear machine resides outside the pressure vessel.

Brian P. Nuel and Samuel P. Weaver disclose methods for displacer control using electrical machines [47]. Methods incorporating a solenoid, a rotary motor and a linear stepper motor are explained. Moloney discloses a mechanical arrangement to achieve dwell at end of strokes for both displacer and piston [48]. This technique needs physical control of the parameters and therefore electronic control is difficult to implement. Also phase control is not implemented. The mechanical system is complicated and making the bearings survive for the expected service life of a microCHP application is difficult. Walsh discloses a resonant free piston Stirling engine with a virtual rod displacer and linear electrodynamic machine control of displacer drive and damping [49]. The displacer stroke and phase angle is controlled in this scheme. This technique cannot implement dwell. Also as the engine is free piston, the resonant operation can be achieved only over a small speed range. The machine is not balanced and will have unacceptable vibrations while operating.

A phase and stroke control system for a cryocooler is disclosed by Beggs [50]. The displacer drive motor is comprised of two annular magnets embedded in the inner body portion of the displacer adjacent to respective

cylindrical motor coils. A position control system is used to control the displacer. This kind of arrangement is suitable for a cryocooler and not for a microCHP application. In a cryo cooler, the displacer end is cold and for a microCHP application it is on the hot side. The electrical windings and magnets cannot survive in the displacer enclosure without affecting performance. Walsh discloses a free piston Stirling engine with displacer control [51]. The control is used for starting up the system and to modulate power output. This method effectively uses the controlled displacer as a starting aid and is employing stroke control of the linear displacer. Dwell and phase control which is the investigation carried out in this thesis is not examined.

John Otters discloses a Stirling engine with independently movable piston and displacer to optimize the work output of the engine [52]. This attempt is made to make the piston and displacer motion as per an ideal cycle. This concept is mechanically complicated and difficult to implement in a commercial solution. The experimental results with such a mechanism is not published or included. Beremand discloses a free piston Stirling engine constructed for a hydraulic system and includes a driven displacer to circulate the working fluid [53]. The displacer can be moved pneumatically and electrically between the cold and hot ends. Stroke or phase control is not offered. William Beale discloses a method to adjust the displacer stroke

as a means to achieve power control [54]. This is relevant only for free piston engines and is not exploring to increase efficiency. William Beale discloses a variable spring between the piston and displacers to control the phase angle of a free piston to achieve power control and stroke limiting [55]. This method is only relevant for free piston engines and does not use dwell control as a means to improve efficiency. During control of a free piston Stirling engine, the moment of inertia changes from the design value and the vibrations will be higher than acceptable for a microCHP application. This issue may be eliminated or reduced in a dual opposed configuration or a multi cylinder free piston engine. Yasushi Yamamoto discloses a displacer actuator with solenoids used to control displacer stroke [56]. This method is suitable for a very low power application and not suitable for microCHP control. Hyrum T Jarvis discloses a mechanical arrangement to provide dwell at the top and bottom of the stroke of a displacer [57]. The system also uses movable mechanical linkages to adjust dwell, phase and stroke of the displacer. This system is not controllable electronically and involves numerous bearings and complicated mechanical arrangements. Robert Frosh discloses a mechanical arrangement for phase control [58]. Another embodiment discloses a hydraulic coupler for the same purpose. Both the embodiments are not suitable for high speed Stirling engines used for microCHP applications. Also non linear displacer motion or dwell is not offered which will

improve the efficiency. James R. Senft discloses a drive mechanism which can control the phase angle and stroke of piston and displacer in free piston engines [59]. William Beale discloses a free piston Stirling machine having a controllably switchable work transmitting linkage between displacer and piston for stroke control [60]. Free pistons have an issue in that the piston amplitude exceeds maximum design values when the load is removed suddenly. This invention can control the power delivered down the power piston to limit the stroke to avoid system damage. It can control the stroke amplitude, thermal pumping rate and power output. Thomas David McWaters discloses an improved Stirling engine by utilizing transmission trains which includes non circular gears to control the motions of the displacer and power piston in a relationship more ideally suited to obtain dwells [61]. This system also uses counter rotating systems to maintain dynamic balancing. These transmission and mechanical systems are not suitable for Stirling engines for microCHP applications which need to operate thousands of hours without a service. These systems are suitable for engines with smaller loads and which have a low duty cycle of operation. W. G. Livezey discloses a variable power and variable direction Stirling engine using a compound planetary gear system to change phase angle [62]. Rolland B Wallis of General Motors discloses another variable power and variable direction Stirling engine using a simple planetary gear system to change phase angle for automotive applications [63]. David M.

Berchowitz discloses a double acting Stirling engine phase control mechanism for power control of Stirling machines [64]. The aforementioned three references are designed for automotive systems and not suitable for a microCHP application. They only use phase control as a means to control power and not efficiency. Also non liner motion of the displacer is not considered. Kenneth D. Price discloses a three stage electromechanical damper for a Stirling refrigerator displacer [65]. This is used as a phase control method. Bamberg and O'Neil discloses a variable stroke control for the piston of a cryocooler for temperature control [66]. The two references mentioned above are suitable for cryocoolers and refrigerators. Attempt is made to control the stroke of the displacer.

Chien and Liou discloses a stroke control method for power control [67]. This is achieved by altering the contact position between the piston connecting rod and a swash plate. This technique is mechanically complex and is costly to manufacture. Additionally, wear and tear levels of the mechanism during normal use are not acceptable for a microCHP application. Karl Kocsisek discloses a variable displacer pivot point to achieve power control of the Stirling engine without substantial loss of efficiency [68]. This is a good concept, but difficult to implement and manufacture. Jaspers discloses a power control system for a Stirling engine in which the inlet pressure of the hot fluid is controlled via an annular

control element which opens or closes the inlet depending on the differential pressure present [69]. This is very complex in construction and the efficiency is affected. Biermann discloses a stroke control mechanism using the assistance of a circular arc shaped lever arm [70]. This is a mechanical arrangement which offers only stroke control.

Hakansson discloses a system for power control by varying the volume of one of the working cylinders by using a movable cylinder wall [71]. Power control is achieved by this technique at the cost of efficiency. Young discloses a Stirling refrigeration system where a small linear trimming motor is used to control the phase and stroke of the displacer mainly to prevent overstroking in free piston engines [72]. Young discloses a linear motor drive phase control system for the displacer in a cryogenic refrigerator [73]. Both the techniques above are suitable for Stirling refrigerators and not for Stirling engines in microCHP applications. The displacer position is sensed from the back EMF in the displacer drive coil which is a good concept. Alan Chertok discloses a displacer stroke control system for a free piston Stirling engine [74]. This control also allows the FPSE operating characteristics in an acceptable range. Chagnot discloses an apparatus and method for the speed or power control of Stirling machines [75]. This uses positioning a valve arrangement to control the working gas flow within a gas flow passage connecting the hot

and cold sides. The valve can be controlled by the feedback from speed, stroke or power of the engine. But the dwell cannot be used or controlled. This is mainly designed for an automotive application and not for a microCHP. Holliday [76] discloses a stroke control system for a hybrid power system employing a free piston Stirling engine. Nommensen discloses a Stirling engine with two chambers and rotatable rotor disks coupled to a common output shaft [77]. One-way valves or adjustable nozzle valves are used for regulating flow of working fluid to achieve power control. Horn discloses a displacer drive with dwell for a cryogenic cooler to improve the cooling efficiency [78]. The displacer drive is controlled by two solenoids, which fire the displacer to hot and cold end while holding at either of the stops to increase dwell time. This technique is suitable for cryocoolers and not for Stirling engines operating at high temperature for a microCHP application

Phase control was used on an 800 horse power eight cylinder engine made by Electro Motive Division of General Motors at La Grange, Illinois in the 1960's [8]. The eight pistons were all coupled to the crankshaft and the eight displacers were all coupled to a separate displacer shaft. The two shafts were connected by a sun and planet wheel arrangement located at the front of the engine. Adjustment of the interconnecting gear changed the phase angle of the piston and displacer shafts.

In a series of studies of large engines intended for use as locomotives and large off-highway rubber tyred vehicle propulsion engines, Walker [8]. proposed the use of phase control as the means to achieve regenerative braking when stopping or descending a grade. By advancing the phase angle beyond 180° the engine was converted to operate as a heat pump, so that heat was absorbed at ambient temperature and rejected at high temperature to a high temperature thermal store of lithium fluoride for subsequent use in driving the engine. The energy required to drive the propulsion motor as a heat pump was provided by the kinetic energy of the train or truck when braking to a stop or by the potential energy when descending a grade. Walker showed that even with conservative assumptions, loaded mine trucks descending a grade could extract and store enough energy to drive the empty truck halfway back to the load site before new fuel was required.

Dehelean et al. [79] describes a new dwell mechanism for the power piston to increase the area under the PV diagram and the efficiency of the engine. This system is mechanically complex and not one that can be controlled by electronic systems. Nasser et al. [80] describes the simulation of a Martini displacer free piston Stirling engine with sinusoidal and non linear displacer motion for a Gamma type Stirling engine. Phase angle control is explored for a free piston Martini type Gamma engine. In this key

reference publication, the global efficiency and the power of the engine are plotted vs. phase angle. Surprisingly the efficiency is lower for a discontinuous displacer motion compared to sinusoidal motion, which is not what is found during this research. Lloyd [81] is using a driven displacer for a low temperature differential Stirling engine for power production. A stepper motor is used to drive the displacer with dwell at low speeds. This technique is similar to what is used in this thesis for a microCHP application. A linear motor is used instead of a stepper motor, the heat source is at high temperature and the engine speed is twice than that mentioned.

Non linear displacer motion is widely used in low temperature differential Stirling engines [82] and low speed Ringbom Stirling engines. In these types of engines, the amount of non linearity and the phase angle depends on the design parameters and speed of operation. An earlier attempt to control the displacer was developed by Olbermann & Anderson at Unique mobility Inc. [83]. This was a 10kW engine operated at 1800rpm with helium as the working fluid at a mean pressure of 7MPa. A linear motor for assisting, retarding, and controlling displacer motion was the original intent, but a completely pneumatic drive system was later chosen [84]. This system controlled the displacer stroke to modulate the engine power. Another example of a Martini displacer engine is provided by the MTI heat

pump drive [44] by Moynihan and Ackermann, 1984 with a linear motor drive for displacer. The power piston is a metal diaphragm and is used to pump hydraulic fluid which in turn is used to operate the compressor of a less conventional heat pump. Chen et al. explores the phase shift characteristics for cryocoolers [85].

Of all these available literature, very little material is available in public domain which provides the relationships of phase and dwell to the flow of power and overall energy balance in a Stirling engine. Also the controllability of a Stirling engine for a microCHP application is not yet investigated.

6. Modeling and Simulation of Stirling engines

6.1 Introduction

Theoretical aspects of Stirling engines have been developed with varying degrees of sophistication. These are generally classified as orders of analysis, i.e., zeroeth order is the most simple, then first order and second order and the highest level is third order analysis. Third order analysis is an attempt to map exactly the process occurring in a Stirling machine. This classification was done by William Martini [14]

6.2 Zero order analysis and Beale equation

Zero order analysis is based on experience. William Beale [54] of Sunpower, Inc. was the first to note in the 1960's the actual performance of many Stirling engines could be expressed in terms of an equation

$$W = 0.015\ p\ f\ V_0 \qquad (6.1)$$

Where W is power output in watts, p is mean cycle pressure in bar, f is the operating frequency in hertz and V_0 is the swept volume in the compression space in cm^3. The equation is in mixed units and hence the constant 0.015 is not dimensionless. The constant 0.015 was empirically determined and not a theoretical number. The Beale equation is very useful

for quick calculations to determine the size or output or variability of a new Stirling engine. Beale's equation was specifically concerned with the customary temperature regimes for Stirling engines of about 700°C for the hot side and about 30°C for the cold side. A fundamental justification of the Beale equation was later developed by James Senft and by Colin West [44].

6.3 Modified Beale equation

Changes introduced by Senft and West modified the equations to include the effects of hot and cold temperatures. These are particularly helpful in applications using low temperature differential and for heat pump applications. The Zeroeth order recommendation by West [44] is

$$W = 0.025\ p\ f\ V_0\ (T_h - T_c) / (T_h + T_c) \qquad (6.2)$$

where W is the work output in watts, p is the mean cylinder pressure in pascal, f is the operating frequency in hertz, V_0 is the swept volume of the compression space in m^3, T_h is the hot space temperature in Kelvin, and T_c is the cold space temperature in Kelvin.

Stirling refrigerators are rated in terms of the Coefficient of Performance or COP. This is defined as the ratio

$$COP_{Refrigerator} = \text{Heat lifted / Work done} \qquad (6.3)$$

It is customary to refer this in terms of the Carnot value

$$COP_{Carnot} = T_{cold\ space} / (T_{ambient} - T_{cold\ space}) \qquad (6.4)$$

Relative efficiency of a refrigerator can be expressed as

$$COP_{Relative} = COP / COP_{Carnot} \qquad (6.5)$$

COP of a heat pump is the ratio of heat rejected to the work done

$$COP_{HP} = \text{Heat rejected / Work done} \qquad (6.6)$$

This is by definition a factor of unity larger than the equivalent ratio used for refrigerators.

$$COP_{HP} = (\text{Heat lifted} + \text{Work done}) / \text{Work done} \qquad (6.7)$$

$$COP_{HP} = COP_{Refrigerator} + 1 \qquad (6.8)$$

The term refrigerators should be used for machines where the useful product of operation is the amount of heat lifted from the lower temperature and the term heat pump should be used for machines where

the useful product of its operation is the quantity of heat expelled at higher temperature [8]

6.4 First order analysis

Gustav Schmidt, a German mechanical engineering professor in 1860 developed what has now become the classical analysis of the Stirling machine. Schmidt theory [86] provides for the harmonic sinusoidal motion of the pistons or other reciprocating elements, the swept volumes of the expansion and compression spaces to be different, the phase angle can be varied over a wide range and accounts for dead volume. The Schmidt theory is a much closer approximation to the way a real Stirling engine operates even though it is highly idealized. It predicts the thermal efficiency to be equal to the Carnot value of the ideal Stirling cycle, but is normally off by a factor of two compared to a practical Stirling engine. The optimistic projections of the Schmidt theory stem from the fact that isothermal compression and expansion are assumed. This implied infinite rates of heat transfer to and from the working fluid and the cylinder walls. With isothermal processes, there is no need for special heat exchangers provided to facilitate the heat transfer. The Schmidt theory also assumes that the regenerative process is perfect and neglects aerodynamic friction effects by assuming the pressure is same throughout the system. An ideal

gas is assumed, perfect mixing of the gas in cylinders is assumed and leakage past the seals is neglected. These sweeping assumptions make the results predicted very optimistic. Despite the disadvantages, it is fairly easy to analyse and provides closed form solutions.

Following Schmidt's derivation of the isothermal model, the next significant advance in Stirling theory was forwarded by Theodore Finkelstein in 1960 and is known as the "limited heat transfer theory" [86]. This theory allows for heat transfer between the working fluid and cylinder walls to take any prescribed value between the two extremes of isothermal (infinite heat transfer) and adiabatic (zero heat transfer). The Finkelstein theory does not have a closed form solution and involves solving various simultaneous partial differential equations which are tedious to resolve.

6.5 Second order analysis

In the mid 1960's Joseph Smith, a professor of mechanical engineering at MIT, and his co workers Rios and Qvale developed the technique of "decoupled second order analysis" [8]. In this process, the results calculated by first order analyses are corrected to allow for the various parasitic losses that arise in actual Stirling engines. The losses are classified as frictional and thermal effects and further classified as static and dynamic effects. In this technique, all the losses are calculated

separately and are assumed to occur independently of the other losses in the machine. Isothermal-based decoupled analysis tends to be optimistic and adiabatic based decoupled analysis tends to be pessimistic compared to actual performance values of experimental engines.

6.6 Simulation programs for Stirling engine analysis

There have been several simulation programs for Stirling engine analysis. West [44] has provided a listing and critique on 20 different programs. William Martini, in a study commissioned by NASA incorporated the second order decoupled analysis [14] in a computer program for personal computers. His reports are the most extensive exposition of the second order analysis technique including a discussion of the various thermal and frictional parasitic losses and the equations for their estimation. Following the death of William Martini, Marvin Weiss and his colleagues rewrote the program. Separate versions were devised for power systems (MARWEISS) and cryocoolers (CRYOWEISS. [8] [44].

Stirling Numerical Analysis Program (SNAP) is a second order Stirling Engine thermodynamic design and analysis program for the serious researcher and knowledgeable hobbyist written by Alan Altman [87]. It offers many improvements and enhancements over previously available programs plus MAC and PC compatibility, viewable source code and it is

user modifiable. Prof. Thomas of Germany has developed a program for second order analysis (PROSA) which is used for sinusoidal Stirling engine analysis [88]. It was used in the initial stages of analyzing the Active Stirling Engine test rig and to understand its characteristics. The program has a provision for optimizing up-to ten variables at a time.

6.7 Third order analysis

Third order analysis is a term used for an attempt at a realistic and complete understanding of the thermo fluid process occurring in Stirling machines. The first successful third order simulation and analysis was devised by Finkelstein [86]. Subsequently Israel Urieli and David M Berchowitz [89] developed the "quasi steady flow model" which is the current theoretical basis for analyzing Stirling engines. The solution consists of 40 equations of which 13 are differential equations in a range of variables. A consistent set of initial conditions is chosen for the system variables and the set of equations is subsequently integrated through several complete cycles until cyclic steady state has been attained. The numerical solution of so complex a system is prone to various effects of numerical instability, which are often difficult to locate or identify, and various techniques are developed through trial and error to negotiate numerical implementation issues. Urieli and Berchowitz in their book

Stirling Cycle Analysis [89] have provided the complete listing of the digital simulation of Stirling machines including program listings of first, second and third order analysis. Chen and Grifin [90] provide a detailed critique of the mathematical models used for Stirling engine analysis.

David Gedeon has developed a powerful and sophisticated third order simulation program (GLIMPS) and a related optimization program (GLOP) [88]. This has evolved to a more comprehensive successor named "Sage". Sage is a graphical interface that supports simulation and optimization of an underlying class of engineering models. The underlying model class [91] represents, for example, a spring-mass-damper resonant system, a Stirling-cycle machine, or anything else that has been properly coded to work with Sage. Sage version 7 was used for the simulation and analysis of the Active Stirling Engine test rig.

The third order models referenced above all use discretisations in space, where gas is transported by flow relative to the nodes or control volumes in the discretisation in space. These methods appear to be the most widely used but alternative approaches to solving the governing equations for mass, energy, and momentum do exist.

6.8 CFD Modelling

A survey of CFD modeling done on Stirling engines is reported by Anderson [88]. Mahkamov and Ingham reports on implementation of a two-dimensional CFD model for the description of the working process of the Stirling Engine with a complex geometry for its heat exchangers [92]. Mahkamov also reports successful application of 3D CFD modeling for the analysis of Stirling engines [93].

Thermodynamic modeling and simulation is a complex science. Multiple approximations are done to linearise the parameters to run closed form solutions. Laminar flow is assumed almost always and lot of intricate properties like gas elasticity and variation of gas properties with pressure, temperature and flow is not mapped one to one in most software. The sheer volume of computational simulation load and the software complexity prohibits using a simulator.

Even if such a tool were available, this would be proprietary and would not be available with universities or in the open market. Design efforts should be directed to develop an open 4D CFD analysis, which will look into states over time and reflects it in the results.

Sage was used and evaluated as a software tool to provide simulations for the experimental test rig. The non-linear simulation in sage had error due to the harmonics in the displacer motion and was unacceptable. The linear simulations agreed well after providing the heater head temperature to the Sage simulator.

7. Sage Simulation model for the ASE

Sage software package is a one dimensional, time-dependent Stirling cycle modeling tool based on theoretical and empirical equations [91]. The equations to be solved are built up of modular components, allowing each component to be configured to the actual geometry of the engine simulated. The components make up a series of linked gas compartments. The system that is solved then becomes a series of nodes connected by thermal resistances, subject to certain boundary conditions, and can be solved in matrix form.

The Stirling model class in Sage allows modeling of a wide variety of Stirling-cycle coolers and engines within the Sage modeling framework. A Stirling machine is built up from component parts of the designer's choosing representing thermal solids, gas domains, canisters, heat exchangers, piston-cylinder pairs, and so forth. The parts function as a whole by virtue of their interconnections — heat and gas flows through appropriate boundaries, forces acting on appropriate attachment points and pressures on appropriate area faces. Add to this the possibility for user-defined variables and custom optimization specifications and one can see that the possible combinations are endless.

Thermodynamic simulation using Sage has allowed the gas dynamics to be assessed to identify the governing parameters of engine pressures, power, load, gas flow and efficiency. The physical geometry of the engine is translated into the model. Measurements of the ASE test rig parts were taken from the tooling drawings and then converted to the different components in Sage. The physical properties of the materials used were also mapped to the component properties in Sage to build a realistic model.

Gas pressure is governed largely by the ideal gas equation. Pressure variation is therefore governed by mean operating pressure and changes in total gas volume and spatial-mean gas temperature. The mean operating pressure and variation in total gas volume govern the amplitude of gas pressure, while the variation in gas temperature due to heat transfer governs the phasing of the pressure. Engine efficiency and power are largely determined by this pressure phasing.

7.1 Spaces and boundary connections in Sage

Compression spaces or expansion spaces are examples of variable-volume spaces. From a modeling point of view both are essentially identical. Stirling machine rotating mechanisms are broken down into separate components representing the flywheel, kinematic linkage and reciprocating piston or displacer. The component palette of Sage has various types of all

the necessary components like regenerators, heat exchangers, pistons, displacers, bus bars, ducts, seals, cylinders etc. Stirling engine model components communicate with each other using the following boundary connections.

7.2 Force connections in Sage

Force Connections represent either phasor or time ring forces acting on points of attachment. The points of attachment will share the same motion when connected together. Force connections are used primarily for connecting springs and dampers to moving parts.

7.3 Pressure connections in Sage

Pressure Connections represent either phasor or time ring pressure variations acting on area faces. The area faces share the same volume displacement when connected together. They are used primarily for connecting pistons and the like to gas domains.

7.4 Heat flow connections in Sage

Heat Flow Connections represent either steady, spatial grid, or space-time grid heat flows acting on thermal boundaries. Boundaries share the same temperature when connected together. Steady heat flows are useful for

time-averaged parasitic conduction losses. Spatial grid heat flows are useful for steady but distributed heat flows, such as occurs in two dimensional fins. Space-time heat flows are for connecting thermal solids to gas domains.

7.5 Gas flow connections in Sage

Gas Flow Connections represent the flow of gas from one gas domain inlet into another. Two inlets conserve mass flow rate, energy and momentum when connected together.

7.6 Density connections in Sage

Density Connections represents the common mass density between a gas domain and a pressure reservoir. The two share the same mean pressure when connected together. Density connections are used to connect the Stirling working gas to a fixed pressure source in order to establish charge pressure.

The model as it appears in the Sage software is given in Figure 7-1, where a separate icon represents each compartment. Within each compartment lie additional modeling components such as walls, a gas domain, fins, or regenerator mesh. The complete Sage model therefore has a tree-like

structure. Horizontal connections are in axial direction (gas flow), vertical connections represent the radial direction. Heat flow connections are in red, black lines without arrowheads represent mass flow between adjacent compartments, and black lines with arrowheads indicate volumetric changes. While Sage is mainly a one-dimensional model, it does model heat flows perpendicular to the oscillating gas flow. For example, the cooler is connected to the adjacent regenerator and a port in axial direction via mass flow connectors, while the convective heat transfer between the working gas and the heat exchanger fin is modeled in radial direction. It follows the conductive heat transfer between the heat exchanger fin and the adjacent regenerator matrix and the wall of the connecting port in axial direction, as well as the conductive heat transfer to the surrounding heat exchanger wall in radial direction. The outer heat exchanger wall assumes its temperature from axial heat flow connectors to the cooling water, which also affects the negative end of the regenerator housing as it is thermally connected to the outer heat exchanger wall.

7.7 The Sage model of ASE

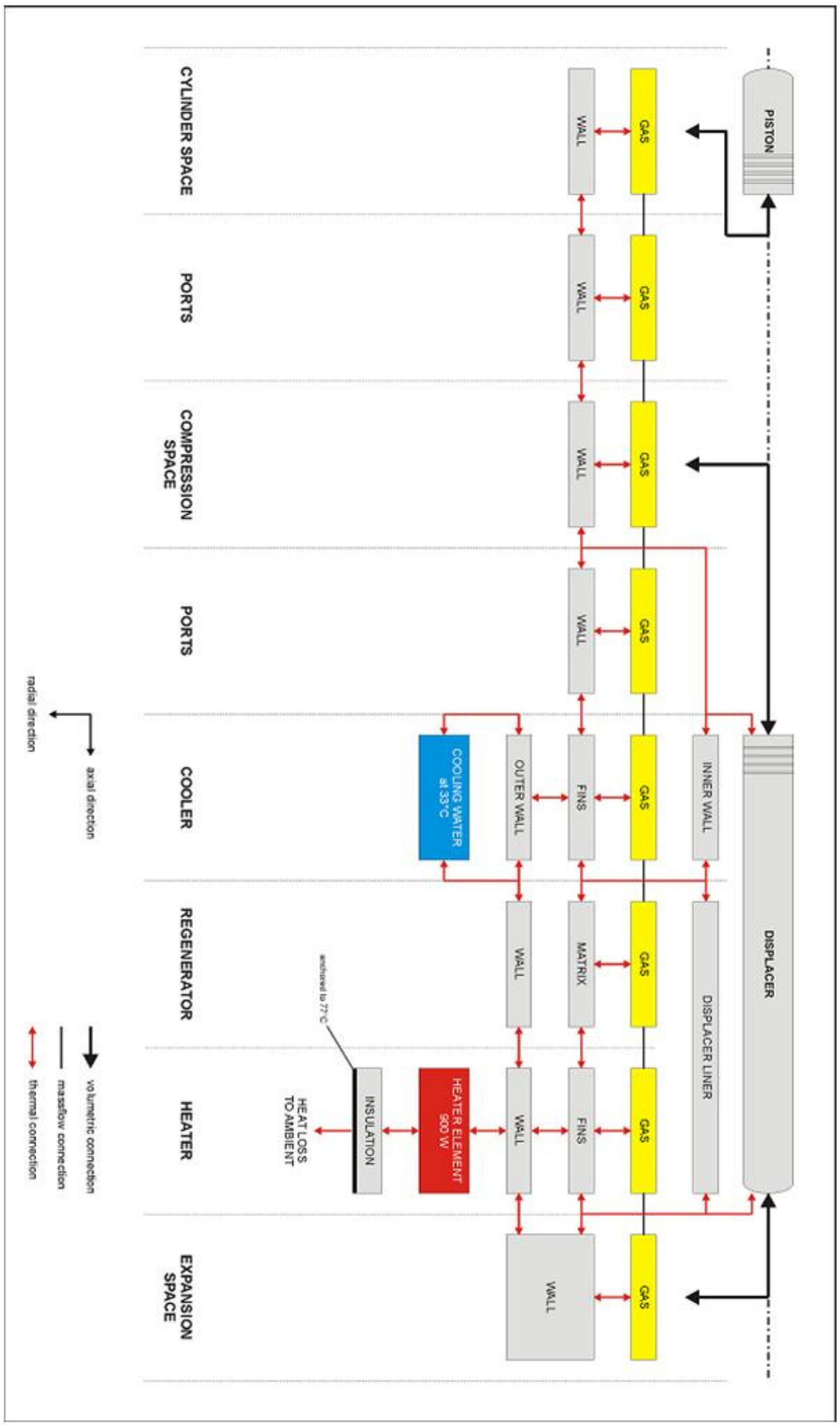

Figure 7-1 Sage simulation model of the ASE.

In a Sage model, the adjacent compartments are connected via directed heat-flow paths. In the case of gas-filled compartments, these also have gas-flow connections. Red lines represent heat connections to components. The walls of all gas-filled components can transfer heat to and from the gas travelling through them.

The walls of the hot and cold sinks (heater and cooler) are set at fixed temperatures, which can have some profile along the length of the compartment. Heat can be conducted to connected components via end-connections only, while convection can occur along the length of the compartment.

7.8 Geometry

The model has been designed to correlate as much as possible with physical parameters. The physical geometry of the engine is largely replicated in the one-dimensional model using minimal approximations. However, some of the two-dimensional heat flows in the actual engine cannot be accurately represented in Sage. In these cases, conduction that occurs perpendicular to the gas flow direction is channeled through the ends of the compartments.

The most critical model variables are the mean operating pressure, gas volumes, hot and cold temperatures, wetted surface areas, and gas flows; which all match the real engine. The convective modeling in Sage is based on many empirical equations. All coefficients related to these equations have been left at their nominal values.

7.9 Validation

An instrumented ASE test rig has provided the majority of data which has been compared to simulation results. Data available from this instrumented engine includes instantaneous pressure in compression and expansion spaces, heater head temperature, power input, swept volume and rejected heat. The heater head temperature was the only quantity of the experimental data that was used to calibrate the Sage model. This had to be done since a high-temperature insulation material whose exact thermal properties were not known surrounded the heater head. By adjusting the thermal properties of the insulation material in order to match the heater head temperature these assumptions could be verified. When key parameters are measured in an engine and input into Sage, the simulated power output is usually within a few percent of the experimental measurements over a range of operating conditions. Simulated instantaneous pressures agree well with experiment, especially in phasing,

which is the primary determinant of output power. However, comparison to experimental results suggests the model also provides an accurate means of assessing trends in performance with changes in operating temperatures, pressures, and engine geometry. Efforts have not been spent to optimize the Sage model as the intention is not to design a prototype, but to test the principle of the Active Stirling Engine under different conditions. Sage was being tested as a possible tool for predicting performance when it comes to the design of a production machine or for scaling. In agreeing well with the experimental quantities, Sage could also be used to quantify and analyse thermal heat flows between components that were difficult to measure. In this method, the thermal loss mechanisms could be easily identified.

Sage is complex and needs expertise in using it to get good results. An experimental setup is needed to fine-tune the Sage software. Using the simulator and then designing around it without a deep understanding of Stirling machines will not yield working engines with usable energy conversion efficiencies. The accuracy of the software should be gauged along with the application at hand. Sage will be a good tool for optimizing an engine rather than designing one from scratch. The experimental values from the test rig will enrich the Sage environment and help the user to develop a deeper understanding of Stirling cycle machines.

8. The ASE Test Rig

8.1 ASE test rig details

The test rig [94] to conduct experimental verification of phase and dwell (non linear motion) control of the displacer was designed around an existing 4 cylinder WhisperGen® engine block. A 4 cylinder WhisperGen® engine block and lower housing is modified to make the test rig. Three of the cylinder ports are closed in the engine block and one of the cold ends and a power piston is used to work as a Gamma configuration [43] engine.

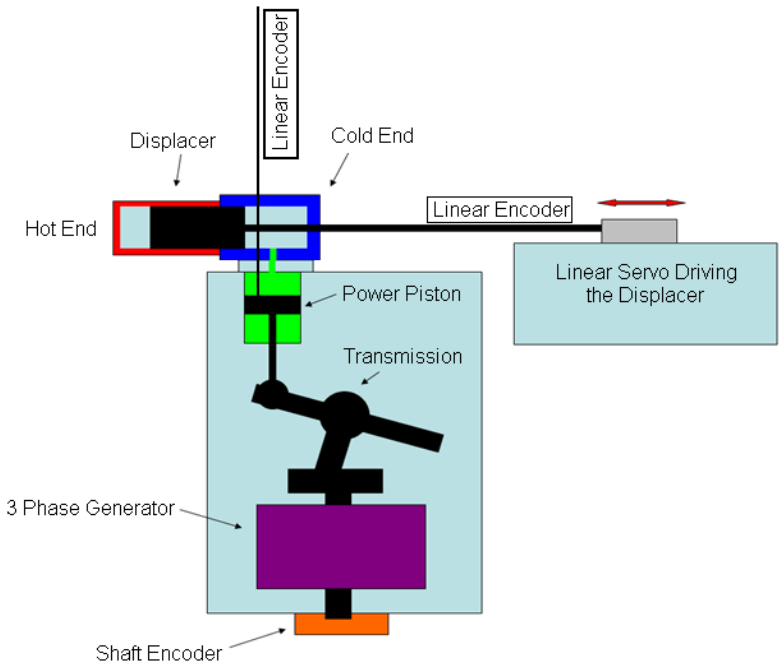

Figure 8-1 Block diagram of the ASE test rig

The power piston is connected to a linear encoder, which measures the power piston position. A smooth cylindrical rod connected to the power piston is brought out through a seal and an optical encoder scale is attached to it. A read head appropriately mounted on a mechanism is placed in close proximity with the scale. When the power piston moves up and down, the scale moves correspondingly and the power piston position can be mapped to an accuracy of 5 microns.

The power piston is connected to a 3phase induction machine through a wobble yoke [95] transmission. The 3phase machine starts the engine operating as a motor. The motor then acts as a generator when the engine is generating power. The 3phase machine is driven by its own electrical drive so that speed control of the engine can be achieved. The drive has a facility to connect a brake resistor to absorb the generated power while the ASE is generating, working as an engine or a prime mover. A rotary encoder connected to the generator shaft provides the shaft position at any point in time. A block diagram of the test rig is shown in Fig. 8-1.

The hot end heater head with the displacer is mounted in transverse direction on top of the engine block. Electric heating coils are clamped on to the heater head to provide the necessary heat input. The heater coil is

powered from a 1kW laboratory power supply, which controls the power input to the hot end.

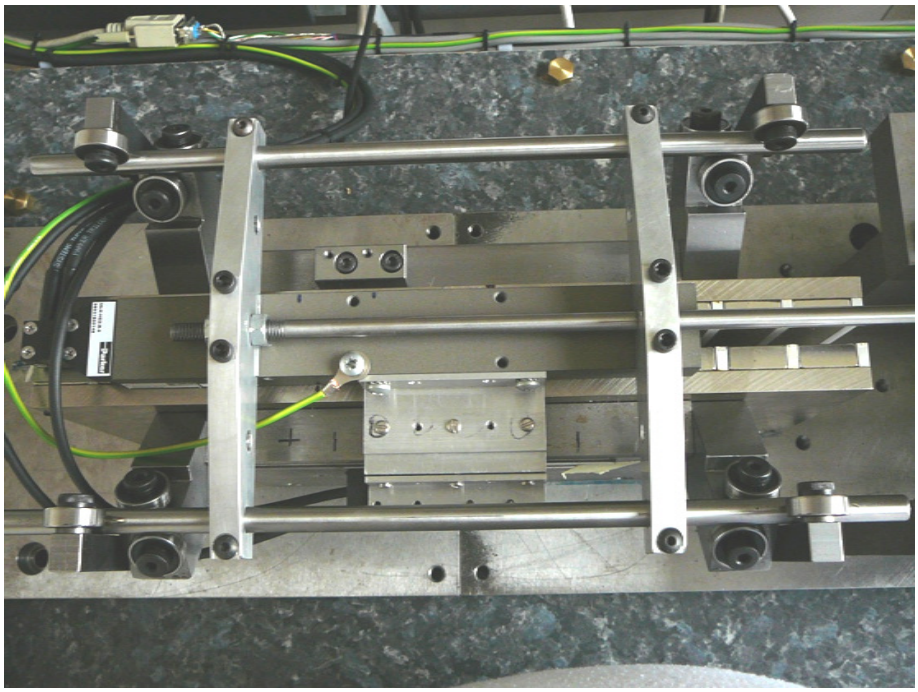

Figure 8-2 Linear machine top view.

A linear electrical servo system is used for controlling the displacer motion profile as shown in Figure 8-2. The forcer (moving part, similar to rotor in rotary machines) is suspended on a carriage supported with 12 custom bearings as shown in Figure 8-2.

The system consists of a Parker Hannifin ML-50 ironless linear servo motor [53], its Aries-13 drive, ACR 9000 servo controller and ACR View

software. The displacer can operate from 0.1mm to 20mm stroke, 5 to 1500 RPM engine shaft speed and 0° to 360° phase displacement from the power piston. The displacer can dwell up to 25% of the time at each end of stroke to create a total of 50% dwell during non linear motion. A magnetic linear encoder read head is mounted on the forcer and a magnetic scale is mounted on the side as shown in Figure 8-3. The linear bearings proved to be a challenge. Simple techniques for mounting the forcer were not working due to unacceptable errors in reading the encoder. Vibration induced position error became unacceptable for conventional mounting systems. Special guides were developed for proper functioning of the linear drive. This is seen in Figures 8-2 and 8-3.

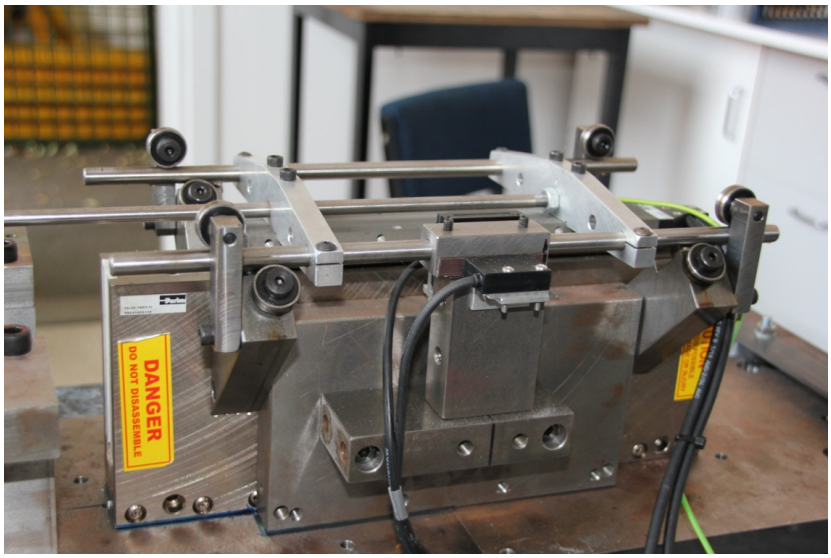

Figure 8-3 Linear machine side view.

The read head moves corresponding to the displacer and the encoder feeds back the displacer position to the servo controller to control the displacer position in closed loop.

Another optical encoder read head is mounted on the forcer with an optical scale mounted to the side of the magnetic head. This optical encoder feeds back the displacer position to the data acquisition system and also provides redundancy in reading displacer position. This was very helpful during initial setup and tuning the displacer servo controller.

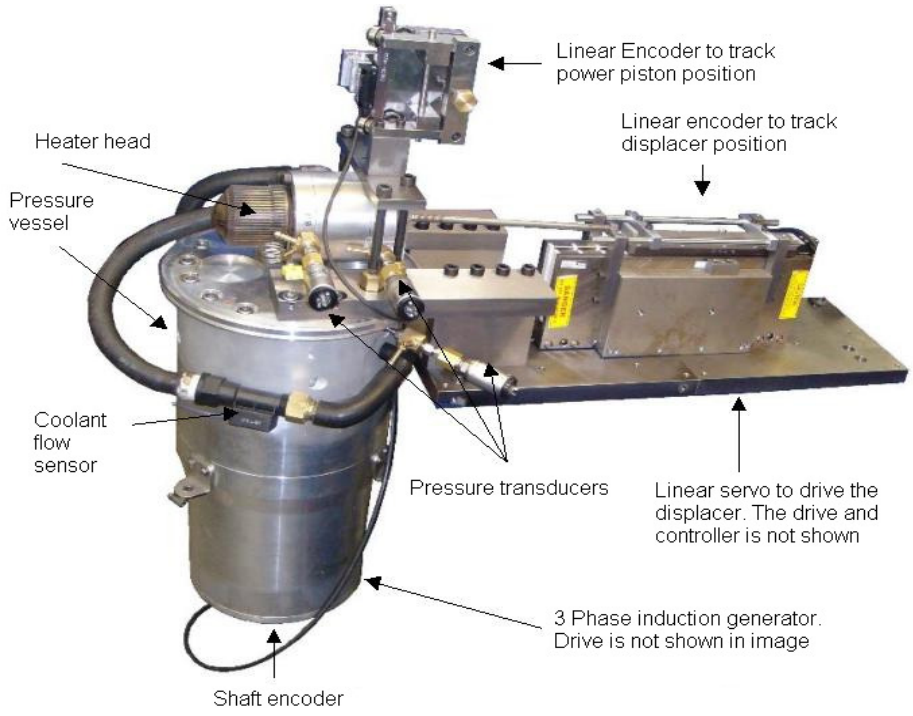

Figure 8-4 The ASE test rig

The ASE test rig (Figure 8-4) is pressurized to 20bar with nitrogen as the working fluid. The rotating shaft from the 3phase AC induction generator is brought out of the pressure vessel through a rotary seal before coupling to the rotary shaft encoder. The shaft encoder provides 1000 pulses per revolution to trigger the data acquisition system. The displacer rod is also brought out through a seal before coupling to the forcer of the linear machine.

The linear servo motor is connected to its own drive. A servo controller controls the linear motor drive. The servo controller is programmed and commanded from the PC. The servo controller has two connections to the PC. One a USB connection to download program parameters during each test and a serial connection to enable a user interface. An application program running on Microsoft Windows is the user interface used to command the servo controller.

The three phase induction machine is connected to a three phase drive. This drive sets the speed of operation of the system. A brake resistor is connected to this drive to absorb any generated power when the test rig runs as an engine. The speed of the three phase induction machine is measured by the data acquisition system and displayed on the PC monitor.

During each of the tests, the speed of the drive is fine tuned to maintain the set speed.

9. Linear Machine in Detail

9.1 Fundamentals of linear electrical machines

The linear motor [96] became more common in the past decade through a dramatic increase in practical and beneficial industrial applications. The linear motor is often described simply as a rotary motor that has been rolled out flat, and the principles of operation are the same. The forcer (the part of the linear machine which moves in the ASE test rig) is made up of coils of winding encapsulated in epoxy, and the track is constructed by placing magnets (usually high power "rare earth" magnets) on steel. The forcer of the motor contains the windings, Hall-effect board, thermistor (to monitor temperature) and the electrical connections. In rotary motors, the rotor and stator require rotary bearings to support the rotor and maintain the air gap between the moving parts. In the same way, linear motors require linear guide rails to maintain the position of the forcer in the magnetic field of the magnet track. Just as rotary servomotors have encoders mounted to them to give positional feedback of the shaft, linear motors require positional feedback in the linear direction. By using a linear encoder, position of the displacer is directly measured for increased accuracy of the displacer position.

The control for linear motors is identical to rotary motors. Like a brushless rotary motor, the forcer and track have no mechanical connection (no brushes). Unlike rotary motors, where the rotor spins and the stator is held fixed, a linear motor system can have either the forcer or the magnet track move (most positioning system applications use a moving forcer and static track). With a moving forcer motor, the forcer weight is small compared to the load. However, a cable management system with high-flex cable is required. With a moving track arrangement, the motor must move the load plus the mass of the magnet track, but no cable management system is required.

Similar electromechanical principles apply whether the motor is rotary or linear. The same electromagnetic force that creates torque in a rotary motor creates a force in its linear counterpart. Hence, the linear motor uses the same controls and programmable positioning as a rotary motor.

A linear motor can be tubular, flat or U-channel shape. The configuration that is most appropriate for a particular application depends on the specifications and operating environment.

9.2 Cylindrical moving magnet linear motors

In the cylindrical moving-magnet design, the forcer is cylindrical in construction and moves along a cylindrical bar that houses the magnets. These motors were among the first to find commercial applications.

9.3 Flat linear motors

There are three types of flat linear motors (all brushless): slotless ironless, slotless iron and slotted iron. Choosing between these types of motors will depend on the specific application

9.4 U-Channel linear motors

U-channel linear motors have two parallel magnet tracks facing each other with the forcer between the plates. The forcer is supported in the magnet track by a bearing system. The forcers are ironless, which means that there is no attractive force and no disturbance forces generated between the forcer and magnet track.

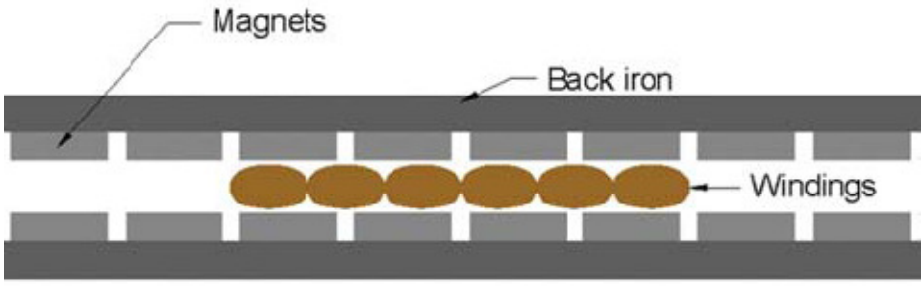

Figure 9-1 U channel ironless linear motor [53]

The ironless coil assembly has low mass, allowing for very high acceleration. Typically, the coil winding is three-phase, with brushless commutation. Increased performance can be achieved by adding air-cooling to the motor, and there are even water-cooled versions available. This design is better suited to reduce magnetic flux leakage because the magnets face each other, housed in a U-shaped channel. The design also minimizes the risk of injury from the powerful magnetic attraction.

The design of the magnet tracks allows them to be combined to increase the length of travel, with the only limit to operating length being the length of the cable management system; encoder length available; and the ability to machine large, flat structures.

Figure 9-2 Overlapping windings and non overlapping windings [53]

The forcer design normally uses overlapping windings which results in shorter overall forcer length. Non-overlapped windings which are less efficient result in longer package length, and are not preferred.

9.5 Linear machine for the ASE test rig

The linear motor chosen for the application is an ironless motor with a U-magnet track. It is model ML-50 from Parker Hannifin. It has an I-beam shape and an overlapping winding design providing very high forces in a compact package.

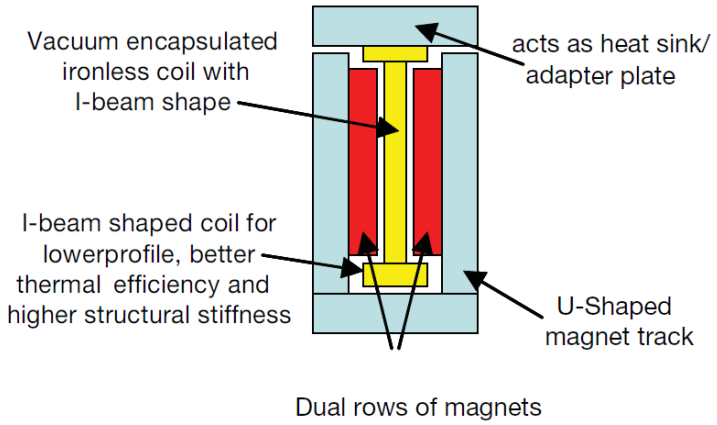

Figure 9-3 Linear motor cross section. The section is perpendicular to the travel. [53]

By overlapping the windings instead of arranging them side-by side, the motor has a very high power density. The I-beam shape is created by flaring out the end turns of the motor at a 90-degree angle. The end turns of a linear motor coil do not contribute to the horizontal force component of the motor. Instead of producing force, the end turns simply produce heat. The I-beam shaped design allows for better heat transfer between the motor coils and the heat sink by increasing the contacting surface area between components. The combination of overlapped windings and the I-Beam shape creates a more thermally efficient motor than most traditional ironless motors. As a result, the payload will experience less thermal expansion due to heat from the motor. In applications like displacer

positioning for Active Stirling Engine, thermal expansion can adversely affect the overall system accuracy.

9.6 Home sensing

The connector module of the forcer has three reflective optical sensors that are looking at the side of the magnets. The nickel-plated magnets and the plastic spacers between the magnets are reflective so black tape can be placed on the face of the magnets to trigger the sensors. Three pieces of tape are placed to trigger home, negative limit and positive limit. The sensors can be configured to be either sinking or sourcing and active high or active low.

9.7 Advantages of ML50 linear motor

The selected motor has several advantages over other comparable machines. It has no attractive force and has a balanced dual magnet track. Hence it is safe and easy to handle and install. There are no forces to deal with during assembly. It does not have cogging. It has a low weight forcer. As there is no iron in the forcer, the weight is lower and hence can achieve a higher acceleration and deceleration and hence a higher mechanical bandwidth.

ML50 provided the maximum available thrust enabling the displacer to achieve maximum speed and stroke for the tests. The system was tested at up to 1500RPM before the error became unacceptable. To preserve the accuracy of measurements, tests were carried out at 750RPM.

9.8 Commutation of a linear motor

In traditional rotary servo systems, it is important for the amplifier to know the position of the rotor. This way it can properly switch current through the motor phases in order to achieve the desired rotation of the shaft. Many times, three digital Hall effect sensors (spaced 60 degrees or 120 degrees apart) are used in order to provide positional information of the shaft within 6 states. The same principle applies to linear motors. The amplifier must know the position of the forcer in relationship to the magnet rail in order to properly switch the windings. Rather than aligning the Hall effect sensors within one complete revolution of the shaft, the Hall effect sensors are matched to the magnetic pole pitch of the motor. The "pole pitch" is the linear distance traveled within one electrical cycle of the motor and is analogous to one revolution of a rotary motor. Once the amplifier establishes the position of the forcer within the electrical cycle, it will then switch the motor phases whenever a transition occurs in the Hall effect sensor states. This is known as trapezoidal commutation [97].

In most modern servo amplifiers, the position of the forcer need only be determined upon power up and enabling of the drive. Once the initial position is recognized, the drive can commutate off the position sensor (normally a linear encoder), which provides significantly higher resolution feedback than the digital HEDs. This allows the motor to be sinusoidally commutated [98]. Sinusoidal commutation provides a smoother switching sequence resulting in fewer disturbances and less heat.

Another method of sinusoidal commutation is through the use of analog Hall effect devices. Analog Hall effect sensors produce a sinusoidal signal as they pass over the magnetic poles of the magnet track. Analog Hall effect sensors have also been used as an inexpensive method of providing positional feedback as well as commutation feedback. However, these devices are susceptible to picking up noise which can affect commutation – which in turn, affects smoothness of travel. In some applications, HEDs are not desired – either from a cost savings standpoint, reduced wiring / component count, or other application specific standpoint. However, the servo drive must still be able to recognize the position of the motor forcer. In this case, automatic commutation can be achieved with a properly equipped servo drive.

9.9 Position feedback and encoder types

There are a variety of methods to provide linear positional feedback to the motion controller. There are analog transducers, rack-and-pinion style potentiometers, and laser interferometers, to name a few. Each has its own level of accuracy and cost. The most popular feedback device for linear motor positioning systems is the linear encoder. Most linear encoders provide an incremental pulse train that provides discrete "counts" back to the motion controller as the encoder "read head" moves along a "linear scale." Typically, the read head is mounted close to the load and the linear scale is applied to the positioner base. There are two popular styles of linear encoders – optical and magnetic. Optical encoders use reflected light scanning techniques to provide feedback with extremely high resolution and accuracy. Optical encoders are capable of providing feedback in the nanometer resolutions. Magnetic encoders use inductive scanning techniques to offer significantly more economical feedback, but have considerably lower accuracy and resolution. Magnetic encoders can typically offer resolutions down between the 1 to 5 micron ranges.

A third variation of linear encoder is the Sine encoder. The Sine encoder produces analog sine and cosine signals instead of discrete pulses. Many modern motion controllers have the ability to interpolate these analog

signals into extremely fine resolutions. For example, the servo controller used can interpolate a 1 Volt peak to peak signal into 14 bits, i.e., the sine/cosine signal period is divided into 16,384 counts. A typical pitch period of a Sine encoder is 1mm, thus the resolution can be interpolated down to 62 nm in the controller.

All of these encoders provide incremental positioning information. Hence, it is necessary to establish a home position any time positional information is lost by the controller, i.e., power down. In some applications it is necessary to have absolute feedback where the actual position of the motor is known immediately and no homing sequence is required. Some encoder manufacturers are now making absolute linear encoders that transfer data using a synchronous serial interface (SSI). An SSI encoder is used as the shaft encoder in the test rig.

9.10 Encoder mounting

When using linear encoders it is critically important to have proper mounting of the scanner (read) head. Inadequate mounting may cause mechanical resonance effects and errors in the measured position caused by vibration of the sensor head. In this case, the achievable bandwidth of the control loop – and hence, the maximum positioning stiffness – is

reduced considerably. In some cases, large gaps of positional information are lost entirely, rendering the system totally inaccurate.

If the linear scale is not aligned straight with the guide bearings, accuracy can be affected in the form of "cosine errors". Fig. 9-4 shows a representation of how linear encoder scale misalignment can cause cosine errors.

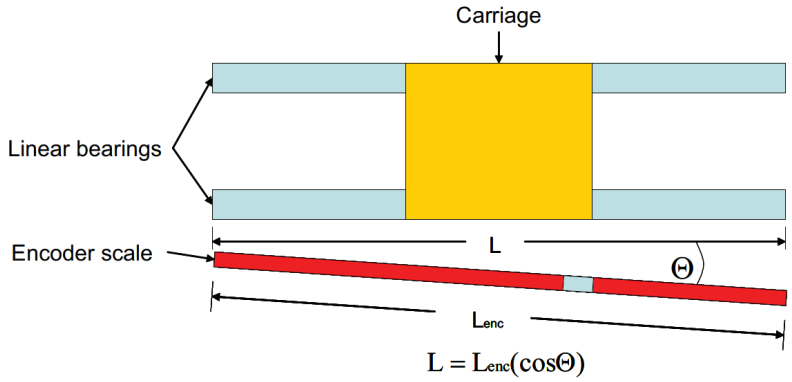

Figure 9-4 Misalignment of encoder and scale [53]

The actual distance traveled will be L, where L=Lenc(cosΘ). The size of the error will be Lenc(1 – cosΘ). Thus, it is important to pay attention to the mounting of the read head as well as providing robust attachment and accurate alignment of the linear scale. While mounting the linear encoder, the misalignment should be measured and care should be taken to mount

the encoder within the specified tolerances. During developing the test rig, the encoder mounting and scale mounting was marked to an accuracy of 50 microns before mounting the system.

An incremental magnetic linear encoder with a 5 micron resolution is used to detect the displacer position in the ASE test rig. The system has a homing routine to home the displacer to a reference position every time the test rig power is switched on. The data acquisition system uses incremental optical encoders to detect the instantaneous positions of displacer and power piston. The magnetic and optical encoders are shown in their mounted positions in Figure 9-5

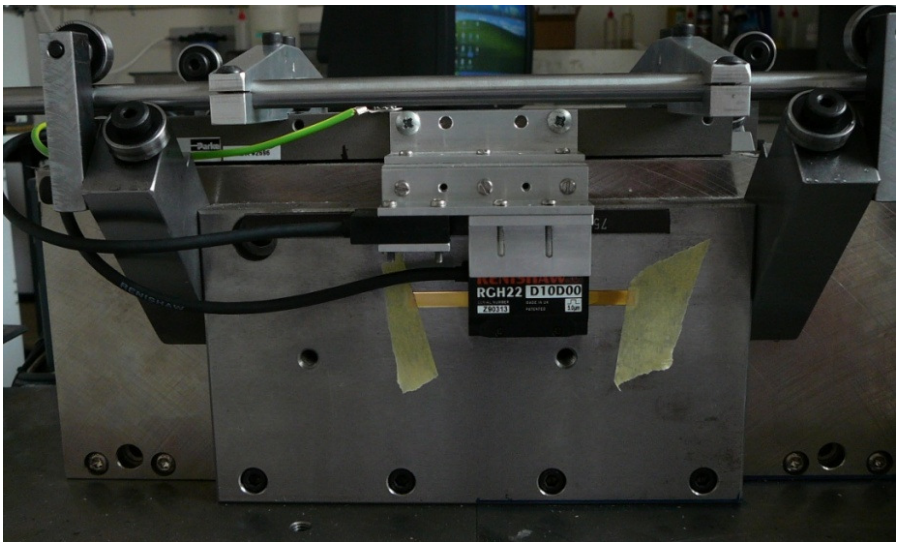

Figure 9-5 Magnetic and optical encoders mounted on the linear motor

The ASE test rig uses three linear encoders and two rotary encoders in total for providing feedback and to have redundant signals to the data acquisition system. Mounting, calibration and proper setting up of these encoders were done with great care to avoid measurement errors and system inaccuracies. Same signal is read with multiple systems and cross checked to make sure that the encoders provided reliable position information under conditions of high speed and vibrations.

10. Instrumentation

The ASE test rig is instrumented with pressure sensors, temperature sensors, position encoders and a coolant flow sensor. Three absolute pressure sensors measure the pressure at the hot end, cold end and the crank-case. Pressure sensors were connected to the hot and cold end to know the pressure loss in regenerator. As the regenerator was very well designed, the pressure loss was minimal and the pressure of the compression space was used in all efficiency calculations. The difference in pressure between the hot and cold end was less than 0.3%. The pressure sensors were cooled with circulating cold water at the gas inlet side so that the diaphragm is cooled and the temperature of the working gas does not cause additional errors. The temperature of the pressure sensors was monitored to make sure that it always stay well within the specified temperature of 80°C.

Three encoders measure the displacer position, piston position and the shaft position. The flow sensor measures the flow of coolant through the cold end of the test rig. The temperature sensors measure the temperature of the heater head, temperature of coolant in, temperature of coolant out and ambient temperature. All transducers are connected to a National

Instruments LabVIEW™ [57] based NI CompactDAQ [58] data acquisition system.

Figure 10-1 Two encoders mounted at the end of the rotary shaft of 3phase alternator.

The pulses from a trigger encoder connected to the shaft trigger data capture. The DAQ system acquires linear encoder positions on the power piston and the displacer, pressure at the expansion space, compression space and the crank case, temperature of the heater head, coolant in, coolant out, and ambient. Figure 10-1 shows the shaft position encoder and the data acquisition trigger encoder. The top one is a 1000 pulse per revolution encoder for triggering the data acquisition system. The smaller encoder is an SSI encoder providing shaft position information to the linear servo. All sensors are read 1000 times per shaft rotation. The volume

information is derived from the position encoder data. The pressure and volume information is used to plot a PV diagram.

Work done by the engine is the area enclosed by the PV diagram and can be easily calculated by numerical integration. Shaft or electrical power output is not measured, as the indicated power is the most reliable comparative measure.

The ASE is started using the 3phase induction generator acting as a motor. The linear servo driving the displacer follows suit depending on the programmed motion profile. Once the system is thermally stabilised, the data acquisition system is triggered to capture the power piston and displacer positions, pressure, temperature and coolant flow data.

The drive of the 3phase induction generator controls the speed of the test rig. An encoder tracks the position of the piston and commands the servo to drive the linear motor in a preprogrammed trajectory to control displacer motion. ASE displacer can be driven sinusoidally with optimum phase angle (usually 90 degrees) to collect a reference PV diagram at a particular speed. The linear servo system then drives the displacer in non-linear fashion with specified dwell at both the ends of the stroke, to increase the area within the PV diagram. Also the displacer phasing with respect to the

piston can be varied to study the overall controllability of the microCHP system.

Data Acquisition inputs	Transducer used	Output of DA System
Temperature sensor of heater head	Thermocouple	Power input
Temperature sensor of coolant inlet	Thermocouple	Reject power
Temperature sensor of coolant outlet	Thermocouple	PV (Output) power
Ambient temperature sensor	Thermocouple	Head temperature
Position of displacer	Optical linear encoder	Coolant flow rate
Position of power piston	Optical linear encoder	Engine speed
Position of shaft	Rotary encoder	Displacer Phase
Coolant flow	Turbine type flow meter	Displacer motion profile
Hot end pressure	Pressure Transducer	PV Diagram (1000 Points)
Cold end pressure	Pressure Transducer	Displacer stroke
Crankcase pressure	Pressure Transducer	Piston stroke
Heaterhead voltage	Resistor divider	Engine pressure
Heaterhead current	Current shunt	Crankcase pressure
		Pressure drop in regenerator

Table 10-1 Sensor inputs and post-processed outputs from the data acquisition system

The inputs and outputs of the data acquisition system are shown in Table 10-1. The data collected by the LabVIEW™ based Compact DAQ system is exported to MS-Excel for post-processing. Five cycles of data are averaged before numerical integration is used to calculate the indicated PV power. The input power to the heater head and the reject power are calculated from the incoming sensor data.

10.1 Data acquisition system details

A CompactDAQ chassis was used, with modules for analog inputs, thermocouple inputs and digital inputs. The CompactDAQ chassis

communicates via USB to a host PC running the LabVIEW™ application that controlled the data acquisition.

Data capture was synchronised with the output of the rotary incremental encoder on the ASE main shaft. This ensured that a fixed number of samples (1000) would be acquired during each shaft revolution, and if required averaging of the data over many revolutions could be easily achieved to improve the data quality. Since the main shaft has significant inertia and its angular speed is almost constant, the data points could also be treated as being almost equally spaced in time if Fourier analysis was required.

10.2 Different data acquisition modes

The LabVIEW™ application as shown in Figure 10.3 has a Front Panel allowing the user to select different modes of operation, initiate data capture and when desired to write the results to file in a tab-delimited form suitable for subsequent viewing and processing in a spreadsheet. The most commonly used mode is the "Shaft-based Acquisition", meaning the capture of N revolutions (N x 1000 data points) during operation and when the operating conditions of the Stirling engine have settled to a steady state.

The graphs and data displays on the LabVIEW™ application front panel allow the user to see much of what is happening, to judge how to operate the test rig and when to capture data files for later analysis.

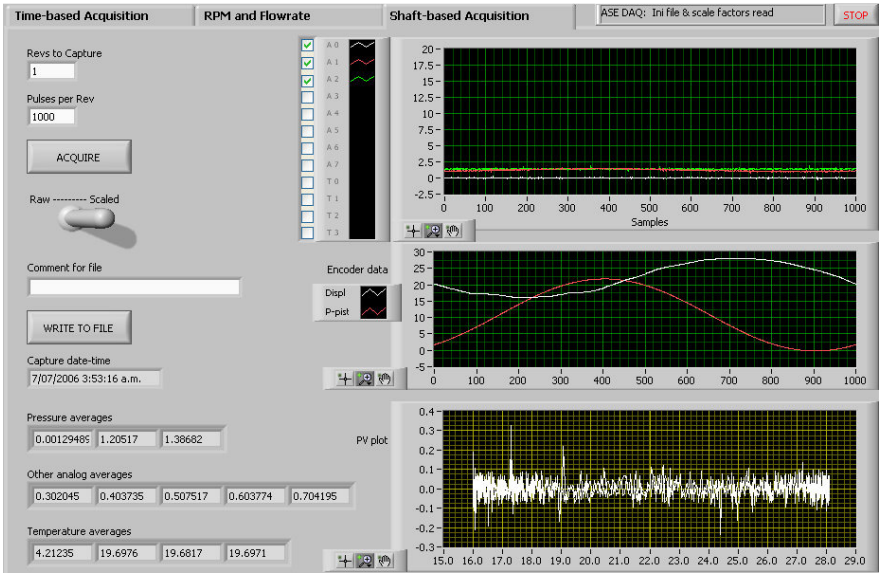

Figure 10-2 LabVIEW™ User interface for shaft based acquisition

However before this it is desirable to calibrate the system. To facilitate calibration exercise a time-based capture mode as shown in Figure 10-4 was included in the LabVIEW™ application, so data could be collected without any signal from the rotary encoder, averaged and displayed.

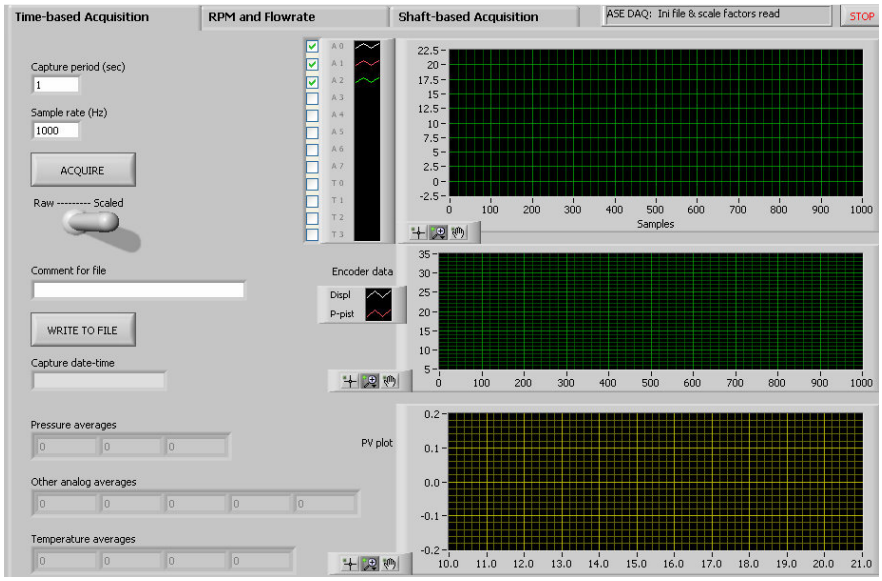

Figure 10-3 LabVIEW™ User interface for time based acquisition

The internal design of the LabVIEW™ application is fairly simple but required some trial and error to achieve the required functions. A Case structure is used to allow the user to select the different operating modes. The core functionality is contained in the "Shaft-based Acquisition" block diagram.

Synchronisation of the data points with engine rotation is achieved by clocking the analog and thermocouple input capture from the main shaft rotary encoder. Since that encoder has an index pulse that occurs only once per revolution, the commencement of data capture is triggered from this pulse. The result is that all data files commence at the same angular position of the main shaft, and this can be easily related to top dead centre

of the power piston etc. This is essential for the calculation of indicated power.

The displacements of power piston and displacer were measured with quadrature linear encoders, interfaced to the Compact DAQ digital module. Standard library functions in LabVIEW™ allowed the displacements to be easily read and scaled to engineering units. The hardware functions in the digital module and chassis keep track of linear position at all times, and the current displacement value is read synchronously with the analog measurements. This is achieved, as shown in Figure 10-5, by using the analog sampling clock to also control the encoder sampling.

10.3 LabVIEW™ application block diagram

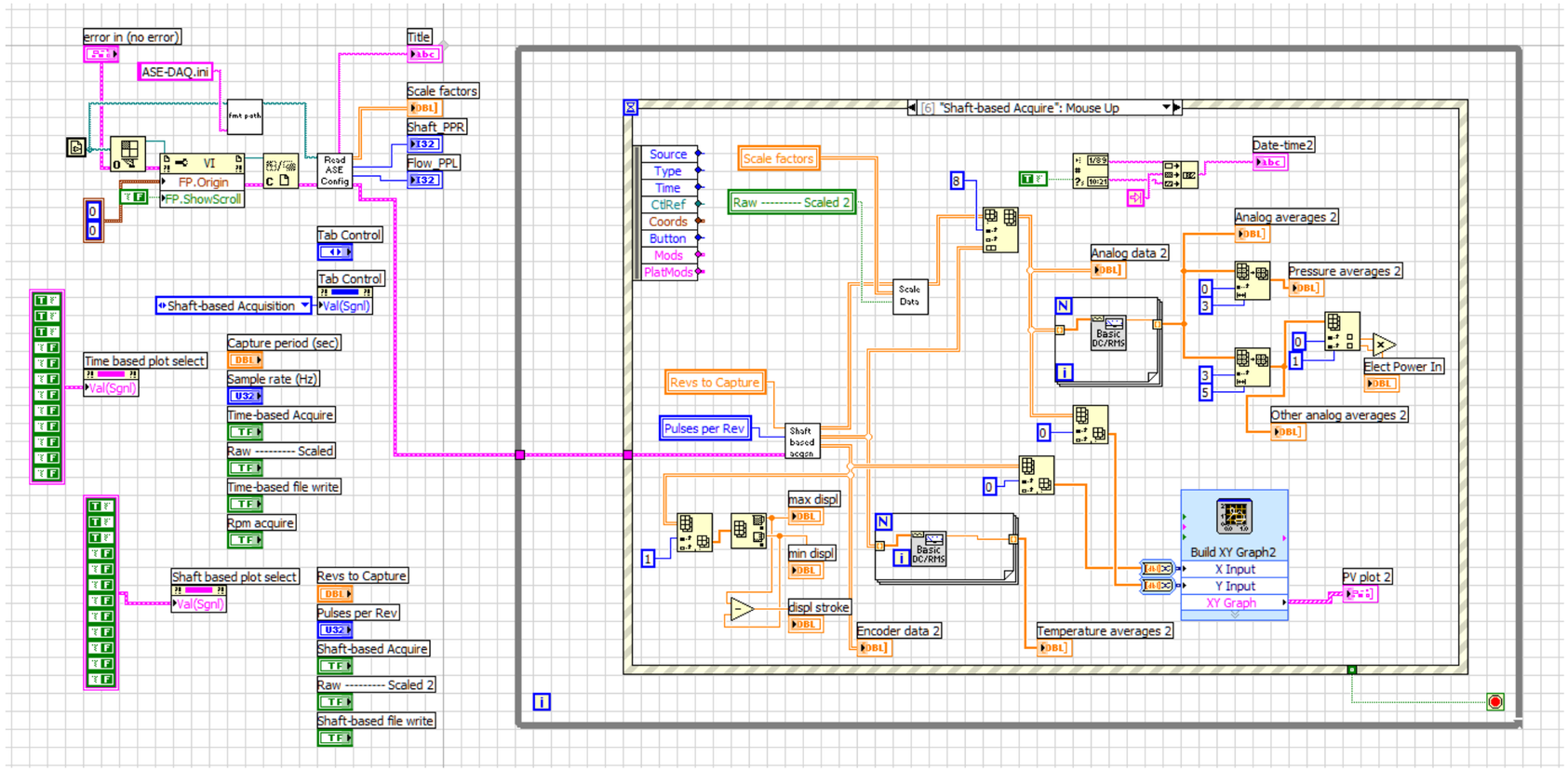

Figure 10-4 LabVIEW™ Block diagram

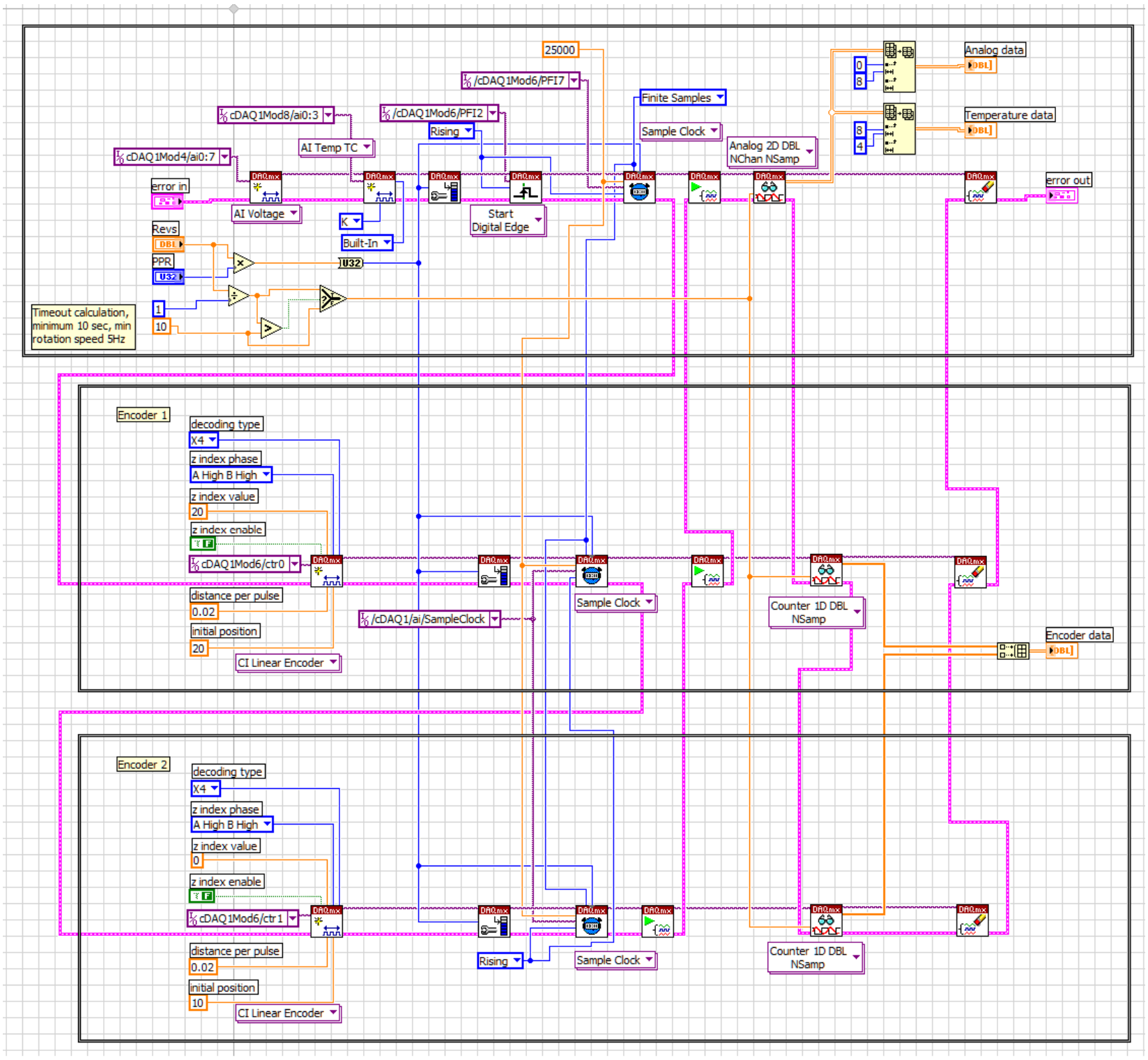

Figure 10-5 LabVIEW™ Block diagram continued

11. Calibration

The systems that require calibration are the pressure sensors, thermocouples, flow sensor, heat input to the heater head and the stroke of the displacer. Primary coolant temperature is controlled through a PID temperature control system so that all the measurements are taken with very similar primary coolant temperatures. The primary coolant temperature is controlled using a secondary heat exchanger with a heating coil and a secondary cooling circuit. The primary coolant is always maintained between 25°C and 35°C to avoid any significant variation in reject temperature. All readings are normalised to Carnot efficiency [99] to eliminate any discrepancy in the reject coolant temperature.

11.1 Pressure sensor calibration

The pressure sensor used is a GEMS® sensors and controls 2200RGB2508A3UB [100]. The pressure sensors are cooled by a separate cooling circuit, which will keep the operating temperature close to the coolant temperature. The engine is pressurised to a series of static pressure values, reading the acquired analog values, and calculating offset and scale factors to convert each sensor output to engineering units (Bar). These calibration factors are then stored in an .ini file.

To calibrate the pressure sensor, the ASE test rig is started and allowed to reach steady state. The heater head is powered from the laboratory power supply. When the heater head temperature has reached steady state, the engine is stopped. A pressure reading is taken after the pressure fluctuations have died out and the results compared with a calibrated pressure sensor. To confirm the calibration, the system is run as a Stirling refrigerator and stopped once the temperatures are stabilised around -100°C. Another pressure reading is taken after the fluctuations have died out and the measured value is compared against a calibrated sensor to ensure that the linearity is better than 0.1% between extremes. A test to evaluate the dynamic performance of the pressure sensor is detailed in Appendix -3

11.2 Thermocouple and Flow sensor calibration

The thermocouples [101] are calibrated using a similar two point calibration against a calibrated temperature source. Two thermocouples (coolant in and coolant out temperatures) form the integral part of the reject heat measurement system along with the flow sensor. To calibrate the flow sensor and the reject heat measurement system, an additional test rig was developed. The flow sensor used is a GEMS® sensors and controls FT-210 with turbine type flow measurement [102].

An insulated tube with the same material and diameter of the coolant circuit was used. A heating coil, two thermocouples and a flow meter is connected to the tube. The heating coil is placed inside the tube with its electrical contacts taken out through insulated cable glands.

Thermocouples are placed at the inlet and outlet of the tube and the flow meter is placed in the tube. A known amount of power is provided into the heating coil. Once the system has stabilised, the data acquisition system is used to acquire the signals from the thermocouples and the flow sensor to calculate the power. The reject power was measured at different flow rates and a two-point calibration used for accounting for power differences at different flow rates.

11.3 Test to account for ambient heat loss

Heater head power is provided from a 1kW DC laboratory power supply to a heating coil as shown in Figure 11-1. Power measurement is performed with an error less than 0.1%. The heat loss component of power delivered to the head is split in two ways. Heat delivered to the system has to either get transferred to the coolant or lost to the ambient. Heat is conducted through the walls of the engine directly into the coolant without taking part in the thermodynamic heat transfer process through the working fluid. Part of the heat delivered is also lost to the ambient

through convection and radiation. To quantify these two losses, a series of tests were carried out.

Power is supplied to the heater head to continually keep the heater head at 600°C while the Stirling engine is switched off to avoid thermodynamic heat transfer through the working fluid.

Figure 11-1 Photograph of heating coil wound over the heater head. The coil is held in place by a metallic sleeve

Once the system is stabilised, the power to the heater head and the reject power are acquired by the time based acquisition module of the data acquisition system. The test is repeated at 25 °C intervals until the heater head temperature reaches 1000°C. The data is plotted and the relationship between the loss to the ambient and direct reject heat with

respect to the temperature is obtained. During post processing, heat lost to the ambient is accounted for to assist in calculating the total energy balance of the system.

11.4 Motion control system calibration

The motion control system needs to track the phase and commanded stroke to a good degree of accuracy. A second linear encoder was used to couple the displacer to the data acquisition system. The commanded phase and the actual phase were recorded at different speeds. The velocity feedback and feed-forward parameters were tuned to obtain a phase error less than 2%.

Similarly the stroke was measured using the linear encoder with 50 micron resolution. The system gains and the integral windup limit were tuned. A limit was set on the correctional control signal that results from the integral gain action trying to compensate for a position error that persists too long. The stroke error was controlled within 3% at all operating conditions.

The piston is connected to a linear encoder. A cylindrical rod is connected to the piston and is brought out through a seal and is connected to an optical linear encoder as shown in Figure 11-2. This encoder measures the actual position of the piston for the data acquisition system to calculate swept volume.

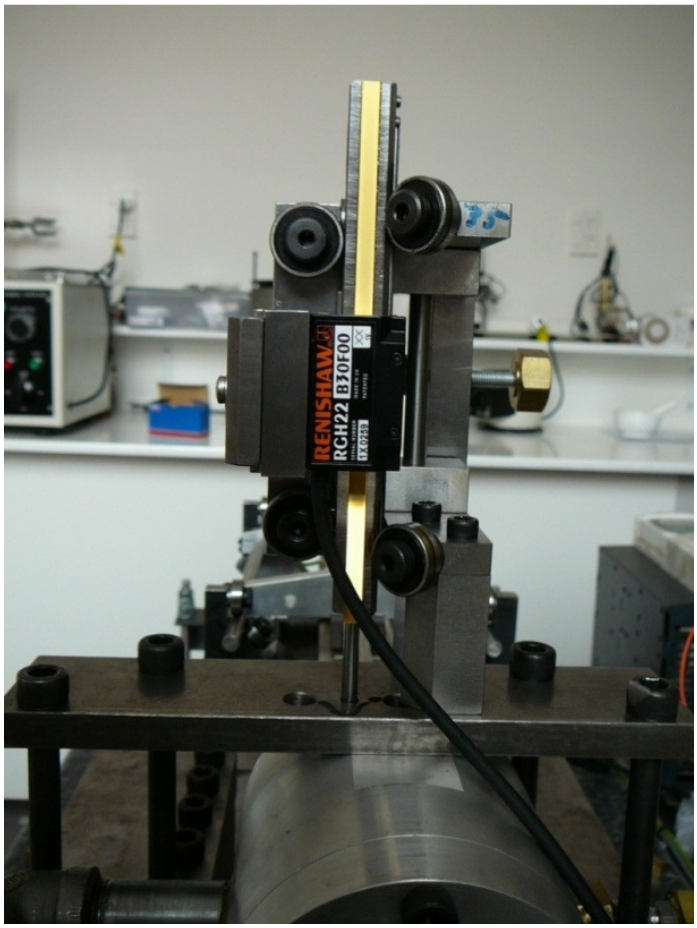

Figure 11-2 Picture of the optical linear encoder measuring piston position

11.5 Analysis of errors and methodology

A table listing the errors involved with sensors and measurement systems are shown in table 11-1.

Sensor	Type	Mfr.	Resolution	Accuracy
Displacer position encoder DAQ	Optical	Renishaw	5 Microns	
Piston position encoder DAQ	Optical	Renishaw	5 Microns	
Encoder scale optical	Optical	Renishaw	5 Microns	1 Micron
Displacer position feedback encoder	Magnetic	Siko	5 Microns	
Encoder scale magnetic	Magnetic	Siko	5 Microns	1.6 Micron
Trigger encoder	Digital	US Digital	0.36°	0.36°
Piston position for feedback encoder	SSI	Siko	12 Bits	0.18°
Heater head thermocouple	K	Omega	24 Bits	1.1° or 0.4%
Coolant in thermocouple	K	Omega	24 Bits	1.1° or 0.4%
Coolant out thermocouple	K	Omega	24 Bits	1.1° or 0.4%
Hot end pressure sensor	Diaphragm	Gems	12 Bits	0.15% Full Scale
Cold end pressure sensor	Diaphragm	Gems	12 Bits	0.15% Full Scale
Crank case pressure sensor	Diaphragm	Gems	12 Bits	0.15% Full Scale
Coolant flow sensor	Turbine type	Gems	0.05 mL	0.5% of full scale

Table 11-1 Sensors used, resolution and accuracy

Indicated power is calculated from the PV diagram. This utilizes the pressure sensors and the encoders. Pressure sensors have a 12bit resolution and 0.15% full scale accuracy. Encoders have a 5-micron resolution out of 16.8mm stroke. Even a 16.8-micron error will result in 0.1% accuracy. The input power to the heater head is provided by an electrical coil. The current in the heating coil is measured using a calibrated shunt and a 12 bit ADC system. The voltage of the heating coil is also measured by a 4 wire system with better than 0.1% accuracy connected to a 12 bit ADC. The combined error in calculating the efficiency is less than 1%. The sensor inputs are connected to a data acquisition system as explained in chapter 10. The LabVIEW™ system will export a raw data file with the actual data collected from the sensors. This will contain 5000 rows corresponding to 1000 rows per cycle and 14 columns in width. The columns include data

from the piston and displacer encoders, 8 analog channels reading in three pressure sensors (compression space, expansions space and the crank case), voltage and current to the heater head and four temperature channels (heater head temperature, coolant in, coolant out and ambient temperature). Three channels are not used on the available 8 analog channels. This raw data file is read into MS Excel and is post processed. “Enc” is the encoder channels, “A” is analog channels and “T” is temperature channels in Table 11.2

	Enc0	Enc1	A0	A1	A2	A3	A4	A5	A6	A7	T0	T1	T2	T3	
1	16.135	8.375	15.4553	15.1661	19.8974	31.6345	26.3337	0.00346352	0.00337675	-0.00159455	769.982	29.5307	32.2723	18.7	
2	16.16	8.42	15.4142	15.1661	19.8562	31.5885	28.1851	0.00346352	0.00337675	-0.00159455	769.982	29.5307	32.2723	18.7	
3	16.185	8.465	15.4142	15.125	19.8562	31.6345	30.0366	-0.00682219	-0.00176483	0.00354759	769.982	29.5307	32.2723	18.7	
4	16.21	8.515	15.4553	15.1661	19.8562	31.5885	28.1851	0.00346352	-0.00176483	0.00354759	769.982	29.5307	32.2723	18.7	
5	16.24	8.565	15.3731	15.1661	19.8562	31.5885	30.0366	0.00860638	0.00851832	-0.00159455	769.982	29.5307	32.2723	18.7	
6	16.265	8.615	15.4965	15.1661	19.8562	31.5885	28.1851	0.00346352	-0.0069064	0.00354759	769.982	29.5307	32.2723	18.7	
7	16.29	8.67	15.4965	15.1661	19.8562	31.6805	28.1851	0.00346352	0.00337675	0.00354759	769.982	29.5307	32.2723	18.7	
8	16.32	8.725	15.4965	15.1661	19.8562	31.6345	28.1851	-0.00682219	0.00337675	-0.00159455	769.982	29.5307	32.2723	18.7	
9	16.345	8.78	15.4965	15.2073	19.8562	31.5885	30.0366	-0.00167934	0.00337675	0.00354759	769.982	29.5307	32.2723	18.7	
10	16.375	8.84	15.5376	15.1661	19.8562	31.5885	30.0366	0.00346352	0.00337675	0.00354759	769.982	29.5307	32.2723	18.7	
11	16.4	8.9	15.5376	15.1661	19.7328	31.6345	28.1851	0.00346352	0.00337675	0.00354759	769.982	29.5307	32.2723	18.7	
12	16.43	8.955	15.4965	15.1661	19.8562	31.5885	28.1851	0.00346352	0.00851832	-0.00159455	769.982	29.5307	32.2723	18.7	
13	16.46	9.015	15.4965	15.2073	19.8562	31.5885	28.1851	-0.00167934	0.00337675	-0.00159455	769.982	29.5307	32.2723	18.7	
14	16.49	9.075	15.4965	15.2073	19.8974	31.5426	28.1851	0.00346352	0.00337675	0.00354759	769.982	29.5307	32.2723	18.7	
15	16.52	9.135	15.5376	15.1661	19.8151	31.5885	30.0366	0.00346352	0.00337675	-0.00159455	769.982	29.5307	32.2723	18.7	
16	16.55	9.195	15.5376	15.1661	19.8562	31.6805	30.0366	0.0137492	0.00851832	0.00354759	769.982	29.5307	32.2723	18.7	
17	16.58	9.255	15.4965	15.1661	19.8974	31.5885	26.3337	0.00346352	0.00337675	0.00354759	769.982	29.5307	32.2723	18.7	
18	16.61	9.315	15.4965	15.1661	19.8974	31.5885	26.3337	0.00346352	0.00337675	-0.00673669	769.982	29.5307	32.2723	18.7	
19	16.645	9.38	15.4965	15.1661	19.8151	31.5885	28.1851	-0.00682219	-0.00176483	0.00868973	769.982	29.5307	32.2723	18.7	
20	16.675	9.44	15.5376	15.1661	19.8562	31.5885	30.0366	0.00346352	0.00851832	0.00868973	769.982	29.5307	32.2723	18.7	

Table: 11-2. Raw data file. Only 20 rows are shown instead of 5000

First the 5 cycles of data is averaged to a total of 1000 rows. Stroke, phase and volume are calculated from the encoder data and the pressure volume diagram is calculated through numerical integration of the calculated volume and compression space pressure.

The post-processed worksheet is updated with command values for stroke, phase and dwell. The experimental values are compared against the command values and if any discrepancy occurs due to data corruption or any experimental error, the post processed workbook will flag the mistakes and the experiment is repeated after correcting the error. This provided a foolproof method to ensure that the data collected is accurate.

Summary sheet. 900W input power, 750 RPM, 16.4mm stroke and 50% dwell										
Master Sheet ID	20750082060000CC00900	20750082050500CC00900	20750082060500CC09000	20750082070500CC09000	20750082080500CC09000	20750082080500CC00900	20750082090500CC00900	20750082110500CC00900	20750082120500CC00900	Engine
Input Parameters										
Parameter	Value	Value	Value	Value	Value	Value	Value	Value	Value	Units
Speed	752	749	751	749	750	749	751	750	751	RPM
Flow	0.0475	0.0475	0.0475	0.0475	0.0474	0.0472	0.0475	0.0474	0.0473	Lit/Sec
Phase angle °	40	50	60	70	80	90	100	110	120	Degrees
Command stroke amplitude	16.4	16.4	16.4	16.4	16.4	16.4	16.4	16.4	16.4	mm
Dwell	50	50	50	50	50	50	50	50	50	%
Experimental results										
Parameter	Value	Value	Value	Value	Value	Value	Value	Value	Value	Units
Crank case average pressure	19.8	19.8	19.8	19.9	19.9	19.9	19.8	19.8	19.8	Bar
Measured stroke	16.41	16.42	16.39	16.42	16.41	16.41	16.39	16.41	16.41	mm
Measured Phase	40.0	50.0	60.0	70.0	80.0	90.0	100.0	110.0	120.0	Degrees
Head temperature	896	853	827	802	780	753	718	705	712	°C
PdV	6.32	7.72	8.41	8.80	9.08	8.52	7.86	6.78	5.95	Joules/Cycle
Indicated PV power	79	96	105	110	113	106	98	85	75	W = (J/Cycle)*(RPM/60)
Power to the head	901	902	901	901	900	900	901	901	902	Watts (V*I)
Power loss to ambient	259	244	237	231	227	224	221	221	221	Watts
Reject power	543	532	541	547	526	564	525	582	561	Watts= M.C. dθ
Indicated efficiency	8.8%	10.7%	11.7%	12.2%	12.6%	11.8%	10.9%	9.4%	8.3%	PV Power/Input power
Thermal efficiency	60.3%	59.0%	60.0%	60.7%	58.4%	62.7%	58.3%	64.6%	62.2%	Reject /Input Power
Carnot efficiency	74.5%	73.3%	72.5%	71.7%	70.9%	70.6%	69.5%	69.4%	68.9%	(Th-Tc)/Tc
% of Carnot	11.8%	14.6%	16.1%	17.0%	17.8%	16.7%	15.7%	13.5%	12.0%	% Relative to Carnot
Total power accounted for	98%	99%	99%	99%	101%	99%	99%	99%	101%	Cross Check

Table: 11-3. Post processed master worksheet averaging results of multiple experiments performed with the same parameters

Multiple experiments are performed for the same case and the results are averaged in a master worksheet (as shown in Table 11-3) which will calculate the input power, output power, thermodynamic efficiency, loss

calculations, thermal efficiency and performs a cross check between the numbers to make sure that the experimental data is good to use.

12. Displacer motion control system and tuning

Displacer motion control is achieved by programming the ACR controller [53]. This is done through the ACR View software [59] which is an environment running a programming language AcroBASIC [59]. The AcroBASIC programming language accommodates a wide range of needs by providing basic motion control building blocks, as well as sophisticated motion and program flow constructs. The language comprises of 172 ASCII mnemonic commands, with each command separated by a command delimiter (carriage return, colon, or line feed). The command delimiter indicates that a command is ready for processing. The AcroBASIC programming language uses a parent daughter approach. A parent can have daughter statements; a daughter statement is considered a sub-statement of the parent. Code is executed sequentially, following the order in which it is written. But based on some input, one can shift code execution elsewhere in a program using conditional statements. Using conditional statements, one can create code that tests for specific conditions and repeats code statements.

The conditional statement provides a logical test—a truth statement—allowing decisions based on whether the conditions are met. In the code, an expression is created and tested whether the result is true. A conditional

statement can be divided into two sub-categories, selection and repetition. The selection structure controls the direction of program flow. This can be thought of as a branch in a program. When the conditions are met, the program moves to a different block of code. The repetition structure—known as a loop—controls the repeated execution of a statement or block of statements. While the conditions remain true, the program loops (or iterates) through the specific code. Typically, the repetition structure includes a variable that changes with every iteration. A test of the value determines when the conditions of the expression are satisfied. The program then moves to the next statement past the repetition structure. If the condition is not met, the loop does not execute. In many cases that is acceptable behavior. Conversely, if the condition is always met, then the loop does not end.

After proper installation, it is necessary to configure the system. This will deactivate any unused axes, sets the motor type, encoder resolutions, primary feedback port, secondary feedback port, acceleration and velocity limits, communications ports, kill all motion settings, home position, temperature limits for trip and acceptable position error. Once the configuration code is in and the system is ready to execute basic move commands, the servo needs to be tuned. Servo tuning needs to be done

initially without load and then the process has to be repeated at load under working pressure.

12.1 Servo tuning tutorial

The tuning process lets the user home the servo response and settling for the motion control application [60]. Settling and responsiveness are the main components that determine performance. Generally, the goal of servo tuning is good settling with a secondary goal of good responsiveness. Ultimately, the designer can determine which aspect is of prime importance, and when the tuning is "good enough" for the motion control system. For safety, servo system is tuned in an unloaded condition. Once the servo is stable and responsive, the displacer load is added and the servo is tuned again. The process is repeated with the system pressurized to obtain servo tuning under pressure.

Proportional and derivative gains work against each other—an increase to one gain affects the other. With this in mind, tuning is treated as an iterative process: alternate between adjusting proportional and derivative gains. The parameter PGAIN is proportional gain and it adjusts servo response. One can always try to increase responsiveness, though mechanics ultimately limit response time. The parameter DGAIN is differential gain and it adjusts settling time. The goal is always good settling. The parameter

IGAIN is integral gain and it adjusts steady-state errors. Adding integral gain also increases responsiveness, though the increase might not be noticeable.

The motion control software flowchart in Figure 12-10 explains the normal operation mode. Each of the blocks is simplified to gain a better understanding of the functions involved. Initially the servo controller and the motor drive are powered up and the communication link with the PC is tested. Once the communications is established, the user interface is activated and the program and the configuration files are downloaded into the servo controller. The user commands to start the program through a terminal emulator, which is used as the user interface. The configuration settings are loaded into the working memory during initialization. Then the homing routine is initialized.

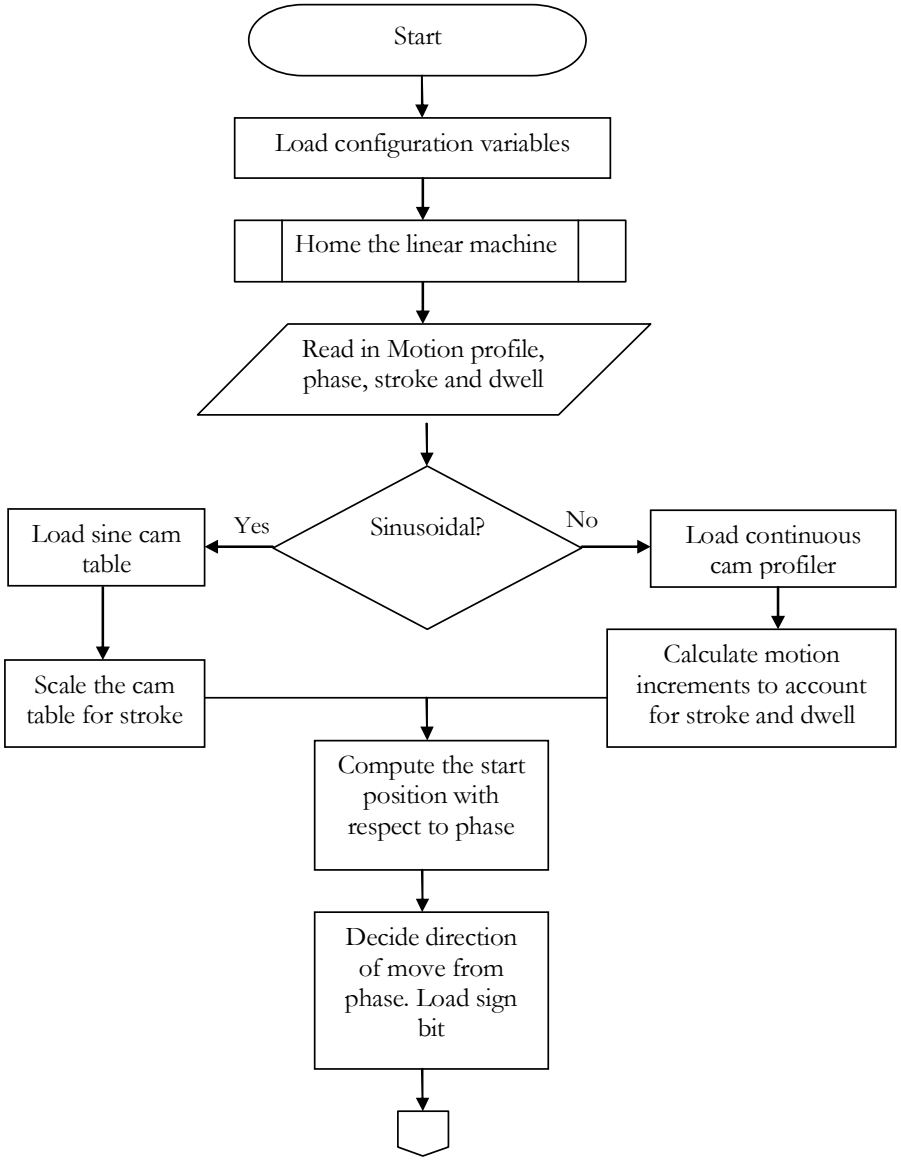

Figure 12-1 Motion control software algorithm; continued

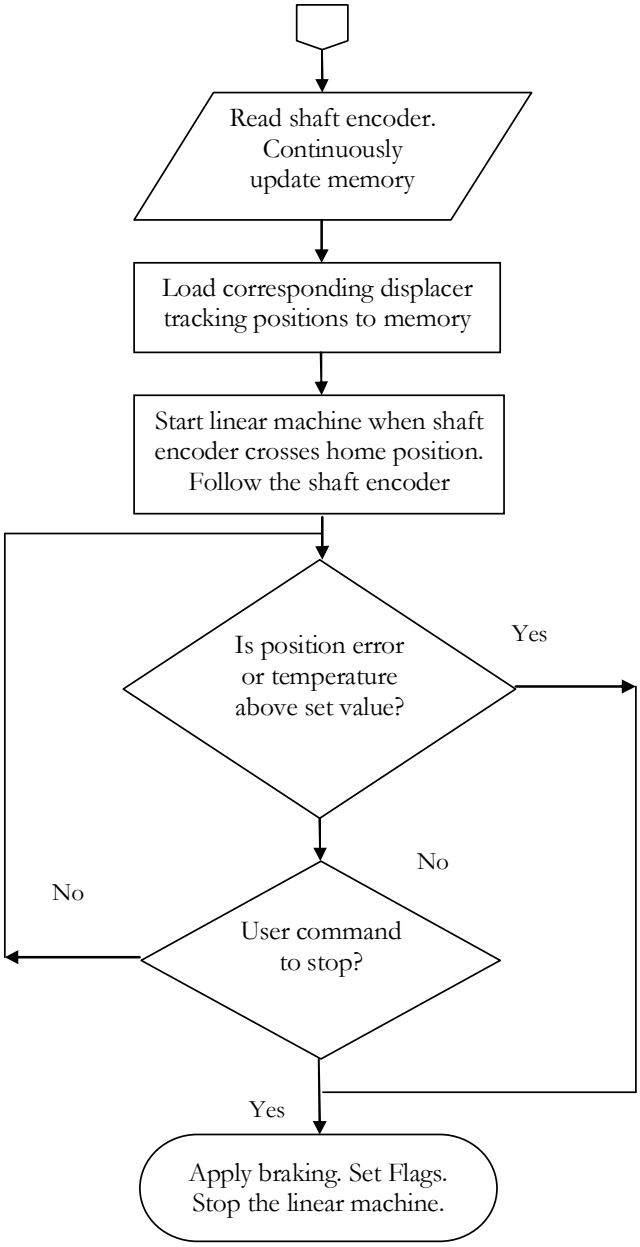

Figure 12-2 Motion control software algorithm

12.2 Homing procedure for the linear motor

The linear machine is moved in one direction slowly until the home reflective sensor is activated. If the positive or negative sensor is activated, the linear machine reverses direction and searches for the home signal. Once the home sensor is triggered, the machine is stopped and the position corrected if necessary. Once the system is homed, the user interface is notified that the system is homed and is ready to take further inputs.

The program asks to input the motion profile, stroke, phase and dwell. If the motion profile is sinusoidal, then the dwell has to be zero, otherwise an error is flagged. If the motion profile is "Dwell" then the cam table positions are calculated for the specified stroke movement and loaded in memory. For a sinusoidal input, the sinusoidal cam table is loaded and scaled according to the stroke. These values are loaded in memory. The start position corresponding to the home position is calculated and is loaded in memory. Depending on the phase input, the direction of movement is also calculated. The sign bit is set to indicate the multiplying factor for the direction bit. At this point if the 3phase rotary machine is not started, the program waits for the shaft encoder to change values. Or in other words, the linear machine is armed and ready to go. Once the rotary machine is started, the incoming signals from the shaft encoder are mapped

and the linear machine is started at the appropriate encoder count. It then tracks the shaft encoder with the correct stroke, phase and dwell. The shaft encoder is an absolute encoder with an SSI interface. If it was an incremental encoder, a homing routine should have been used for the piston also.

12.3 Closed loop feedback control

Once the shaft encoder data comes in, the program [Appendix-4] loads the appropriate displacer positions to the cam profiler and the linear machine follows the shaft encoder. Speed of the system can be changed by the settings on the drive of the 3phase rotary machine. The displacer linear drive is speed blind and just follows the shaft encoder. If the shaft encoder speeds up or slows down, the displacer also follows suit. As such there is no speed control for the displacer. It follows the shaft encoder at the appropriate phase and moves with the commanded stroke and motion profile.

Due to complications in calculating the scaled cam table for different non linear functions, dwell was predetermined to be 5.9%, 14.3%, 20%, 33% and 50%. These positions provided round functions with very low truncation errors, which made the programming easy. These dwells provided a wide variation from a low dwell to a high dwell of 50% to

adequately examine the performance variation with non linear displacer motion.

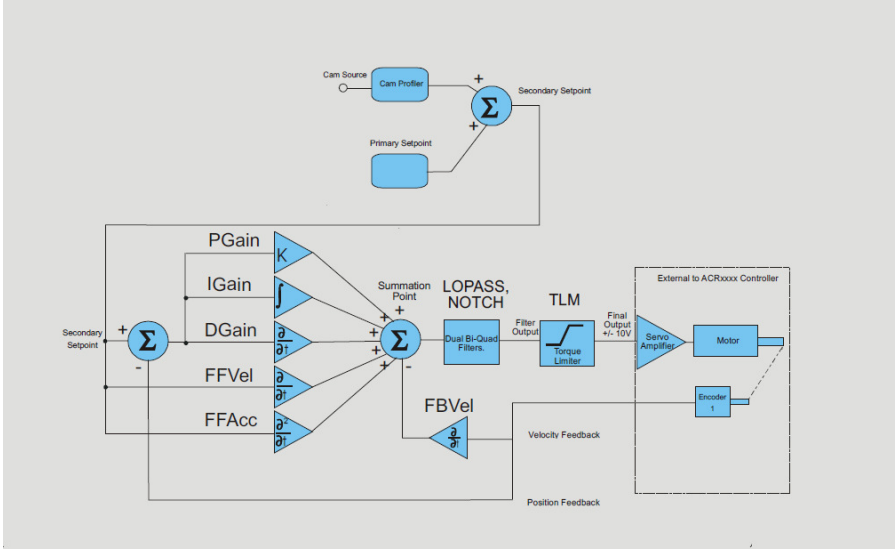

Figure 12-3 Motion control system with closed loop feedback control

The primary set point is provided to the system through the user interface. It will include the information about motion profile (sinusoidal or non linear), amount of dwell if the motion profile is non linear, displacer stroke and phase angle. Speed is not input to the system as the displacer motion control blindly follows the shaft speed.

If the motion profile is sinusoidal, the software scales the cam table to the required dimension depending on the stroke. The corresponding gain parameters and feed forward parameters are loaded. The system waits for

the shaft to cross a predetermined position and the displacer follows suit at the commanded phase angle and stroke. At every point, the control system calculates the future position, time to reach the future position and adjusts the servo continuously to make sure that the payload (displacer) is at the right place at the right time. The integral gain corrects the steady state error and the total following error is limited to a maximum value of 10 microns. Velocity and acceleration feed forward is used by the control system to achieve the acceptable error in an acceptable time so that the speed of response is not affected. In the case of 750RPM, the cycle time was 80 milliseconds and the settling time was 75 microseconds. For sinusoidal motion, the scaled cam table provides the command positions and the control system tries to achieve displacer positions corresponding to the respective piston positions.

For non sinusoidal motion or nonlinear motion, the positions are calculated depending on the dwell and the stroke values, which can define the non linear motion completely. The control system loads the values of command positions in memory. The rest of the operation is same as that for the sinusoidal case where the command positions are provided from a long array instead of a scaled cam table.

13. Test method and matrix

13.1 Introduction to testing as an engine and a refrigerator

If heat is supplied to the heater head, the 3phase machine generates motive power while heat is being absorbed from the heater head and rejected to the circulating coolant. If the heater head is not supplied with heat, the system works as a refrigerator taking input power from the 3phase rotary machine and pumping heat from the heater head to the circulating coolant.

13.2 Work done by the Stirling engine and numerical integration

While working as an engine, the integrated PV diagram denoting the work done, will be positive and while working as a refrigerator the integrated PV diagram will be negative indicating power absorbed. One of these will be positive and the other negative depending on the direction of numerical integration performed. During initial tests, it was observed that the highest efficiency was observed at around a phase angle of 80°. The refrigerator tests were done at this phase angle.

13.3Engine testing

Tests running as an engine were done as follows. The heater head was supplied by power from a 1kW variable power supply. The variables of

interest are the phase angle and dwell. A test was designed to study the impact of both these variables on engine performance. The speed was set as 750RPM. The heater head was supplied with 900W through a heating coil. The heater head was insulated to minimize the heat loss through convection and radiation. The motion profile was set as sinusoidal. The stroke was set at 16.4mm. The system was operated at 40°phase angle. Coolant temperature control was employed during the test. Primary coolant was heated to 25°C before start of the tests. If the temperature rose above 35°C during the tests (which it did always), a secondary heat exchanger was activated to cool the primary coolant to less than 30°C. This ensured that the coolant always stayed at around the same temperature to avoid the effect of reject temperature on the data collected.

The data acquisition system was activated through its LabVIEW™ interface to acquire the head temperature, coolant in temperature, coolant out temperature, ambient temperature, pressure at the expansion space, pressure at the compression space, pressure at the crank case, position reading from the displacer encoder, position reading from the piston encoder and the coolant flow. Every time the data acquisition system is activated, it reads all the sensors and collects data for five cycles. The data acquisition system is triggered off the shaft encoder and 1000 points per cycle is collected.

After collecting the data at 40° phase angle, the system was stopped and the displacer phase was set to 50° before repeating the test with all other variables remaining the same. The test was repeated for every 10° phase angle until 120°.

Once a set of readings were taken for displacer phase angles of 40° to 120°, the motion profile was changed from sinusoidal to 5.9% dwell. The test was repeated for displacer phase angles of 40° to 120°. The tests were similarly repeated for 14.3%, 20%, 33% and 50% dwell. All these tests were conducted at 750RPM and 900W heater head power. To summarize, 9 tests (40° displacer phase angle to 120° displacer phase angle in steps of 10°) were carried out at each motion profile. This was repeated for 6 motion profiles (sinusoidal and 5 non linear motion profiles with dwell). In total 54 tests were carried out at 750RPM and 900W heater head power

To confirm that there are no gross errors in testing and critical points were not missed, the tests were repeated at 500RPM and 800W heater head power. 54 tests similar to the above were carried out at 500RPM and 800W heater head power.

Tests were conducted at 750RPM and 500RPM as they are synchronous speeds for 8 pole and 12 pole machines working from a 50 Hz AC source.

Electrical machines are manufactured around synchronous speeds for commercial applications

In the above series of tests, the heater head power was kept constant at a particular speed and the temperature of the heater head was allowed to vary. This was to mimic a burner with a constant heat source, which provides a constant fuel rate and hence constant power. In microCHP applications, certain operating modes demand the fuel supply to be controlled to keep the heater head temperature constant. To explore this system, tests were carried out with constant head temperature. They were conducted as follows.

Speed was set to 750RPM, stroke was 16.4mm, sinusoidal motion profile was chosen. Power was adjusted to control the heater head temperature to 800°C. Displacer phase was set to 40° as before. The system was allowed to settle while the power was continuously adjusted to maintain the heater head at 800°C. Readings were taken as before. The test was repeated at 10° displacer phase intervals to 120° phase. 9 tests were carried out (40° displacer phase angle to 120° displacer phase angle in steps of 10°) with sinusoidal motion profile. The test was repeated with 50% displacer dwell. In total, 18 tests were performed at constant heater head temperature.

13.4 Test Matrix-Engine

In total 126 engine tests (54 tests at 900W heater head power at 750RPM, 54 with 800W heater head power at 500RPM and 18 with 800°C heater head temperature at 750RPM) were carried out as an engine. These tests provided the data to comprehensively study the effects of phase and dwell changes in an Active Stirling Engine.

13.5 Refrigerator testing

The primary interest in the refrigeration tests is to find out the lift capacities at different temperatures while the system is having a sinusoidal displacer motion and while the system is having a non linear displacer motion with maximum dwell. To find this out, a refrigeration test was planned as follows.

The stroke was set at 16.4mm (this was the stroke for all the refrigerator and engine tests carried out) and the phase at 80°. This means that the displacer leads the piston at 80° with a displacer stroke of 16.4mm. Speed was set to 750RPM. Initially the motion profile was commanded as sinusoidal. The system was run until the head temperature dropped and stabilized without any further drop. The head acquired frost and is close to cryogenic temperatures at this stage.

Then 5W was applied to the heater head through the electric heater wound on the heater head. The system was allowed to settle at the new temperature. The data acquisition system was activated to read 5 cycles worth of data. Similarly, readings were taken at 10W, 15W, 20W, 30W, 40W, 50W, 60W, and 70W lift. At each operating point, speed was finely adjusted on the drive of the 3phase rotary machine. Once the system settled at each of these points, the data acquisition system was activated to collect data.

The system was stopped and the motion profile of the displacer was changed to 50% dwell. The system was restarted and the same experiment was repeated to collect the data with non linear displacer motion.

13.6 Test Matrix- Refrigerator

Test #	Dwell	Lift power	Stroke	Speed	Phase
1		Final	16.4mm	750RPM	80°
2		5W	16.4mm	750RPM	80°
3		10W	16.4mm	750RPM	80°
4		15W	16.4mm	750RPM	80°
5	Sine	20W	16.4mm	750RPM	80°

6		30W	16.4mm	750RPM	80°
7		40W	16.4mm	750RPM	80°
8		50W	16.4mm	750RPM	80°
9		60W	16.4mm	750RPM	80°
10		70 W	16.4mm	750RPM	80°
11		Final	16.4mm	750RPM	80°
12		5W	16.4mm	750RPM	80°
13		10W	16.4mm	750RPM	80°
14		15W	16.4mm	750RPM	80°
15		20W	16.4mm	750RPM	80°
16		30W	16.4mm	750RPM	80°
17		40W	16.4mm	750RPM	80°
18		50W	16.4mm	750RPM	80°
19		60W	16.4mm	750RPM	80°
20	50.0%	70 W	16.4mm	750RPM	80°

Table 13-1 Test matrix for refrigerator

14. Engine test results

14.1 Introduction to presentation of results

The following pages illustrate the test results from running the Active Stirling Engine test rig. This chapter looks at the comparative results of sinusoidal motion and non-linear motion (at 50% dwell only, results at other dwells are not presented to avoid clutter). Also the 3D graphs showing Dwell vs. Phase vs. efficiency are plotted. Efficiency is calculated as the ratio between the indicated power and the input heater head power.

The PV diagram, which is the indicator of the work done, is examined for sinusoidal and non linear displacer motion. The heater head temperature, input power and reject power is plotted. PV power and thermodynamic efficiency is also plotted. The results are discussed along with the respective plots.

All the above mentioned plots are graphed for 750RPM speed and, 500RPM speed at constant power input. They are also plotted at 750RPM for a constant temperature of the heater head which is a common control mode in microCHP systems.

Prediction of the theoretical Sage model vs. experimental results for sinusoidal motion is presented in Figure 14-20.

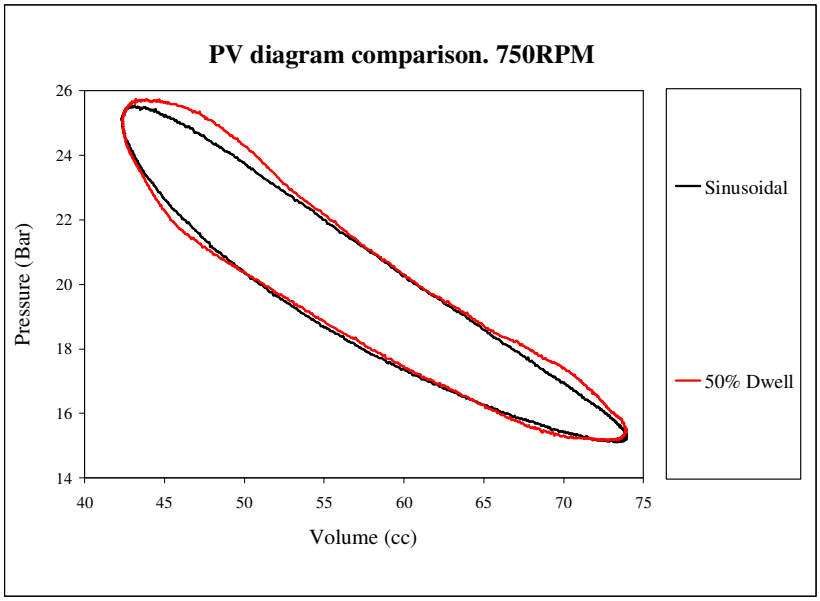

Figure 14-1 PV diagram comparison with sinusoidal displacer motion and non-linear displacer motion at 750 RPM and constant power input

The PV diagram comparison between sinusoidal operation and with 50% displacer dwell at 750 RPM and constant power input is shown in Figure 14-1. Improvement in the work done is observed while operating with 50% dwell. The efficiency (not work done) increase is 13.5% (at 750RPM) with non linear motion compared to sinusoidal motion of the displacer. The

efficiency improvement has a higher impact at lower speeds (15% at 500RPM).

Heater head temperature, reject power and thermal efficiency vs. phase is plotted in Figure 14-2 for sinusoidal and non linear operation with 50% dwell at 750RPM. As the phase angle increases, the head temperature reduces. This input might be useful in production engines to avoid using costly materials capable of withstanding higher temperatures for heater head design.

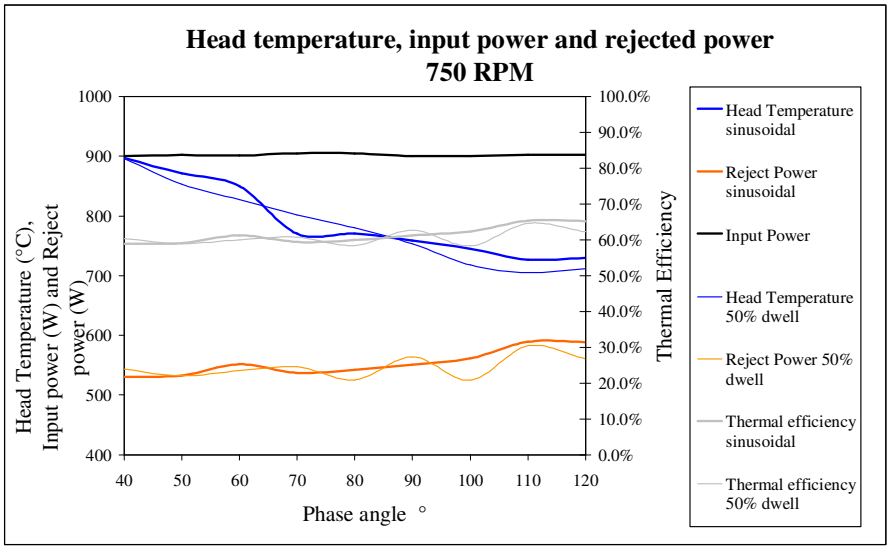

Figure 14-2 Heater head temperature, Input power and rejected power with respect to the phase angle at 750 RPM and constant power input

Considerable ripple is present in the curves as seen from Figure 14-2. Components (piston, cold end, displacer, heater head, lower housing,

transmission, etc) from the WhisperGen® engine which is optimised for 1500RPM, 90 degrees phase angle and sinusoidal motion were used to build the ASE test rig. The ASE is operated at lower speeds (750RPM and 500RPM), and varying phase angle for all these tests. The impact of lower speeds and varying phase angle is contributing to the ripple present in many of the readings. Mechanical resonance variations, gas resonances and gas elasticity variations with phase are causing the ripple in the readings. The secondary coolant circuit is also having a large thermal time constant which is contributing to the ripple in the curves.

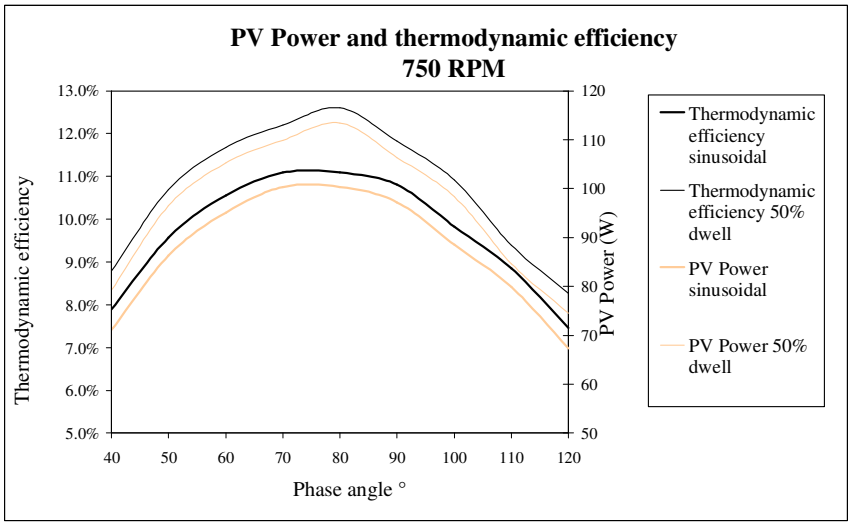

Figure 14-3 PV Power and Thermodynamic efficiency with respect to phase angle at 750 RPM and constant power input

Figure 14-3 shows the relationship between PV Power and efficiency vs. phase angle at 750 RPM speed for sinusoidal displacer motion and with

50% dwell. When the ASE is operated with displacer dwell, the efficiency is higher compared to sinusoidal operation. The curve has a peaky nature at the point of highest efficiency while operating with 50% displacer dwell. As dwell reaches close to 50%, the efficiency increases non-linearly and hence the peaky nature.

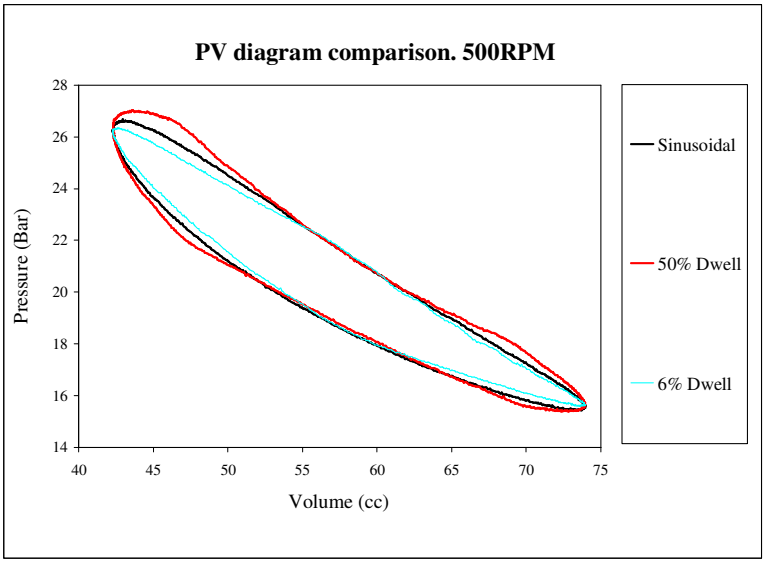

Figure 14-4 PV diagram comparison with sinusoidal displacer motion and non-linear displacer motion at 500 RPM and constant power input

The PV diagram comparison between sinusoidal operation and with 50% displacer dwell at 500 RPM is shown in Figure 14-4. The efficiency improvement over sinusoidal operation is 15% in this case.

Heater head temperature, reject power and thermal efficiency vs. phase is plotted in Figure 14-5 for sinusoidal and non linear operation with 50% dwell at 500RPM. The ripple caused at 750RPM due to various parameters as mentioned earlier is also present at 500RPM also. Figure 14-6 shows the relationship between PV Power and efficiency vs. phase angle at 500 RPM speed for sinusoidal displacer motion and with 50% dwell. The results are similar to 750RPM.

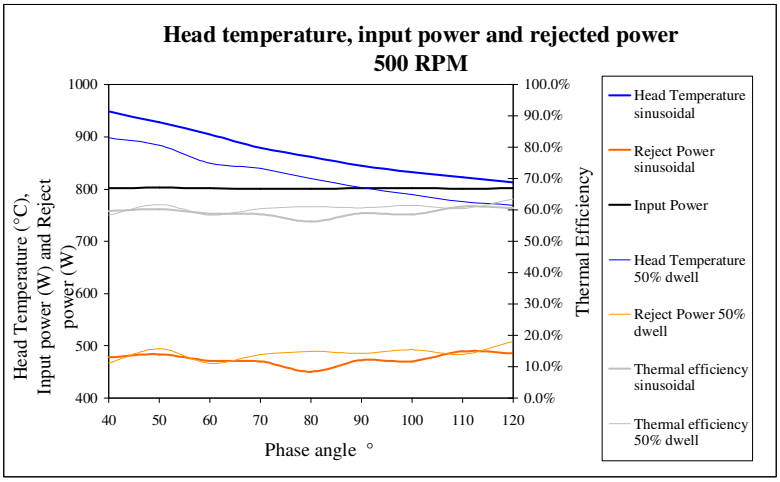

Figure 14-5 Heater head temperature, Input power and rejected power with respect to the phase angle at 500 RPM and constant power input

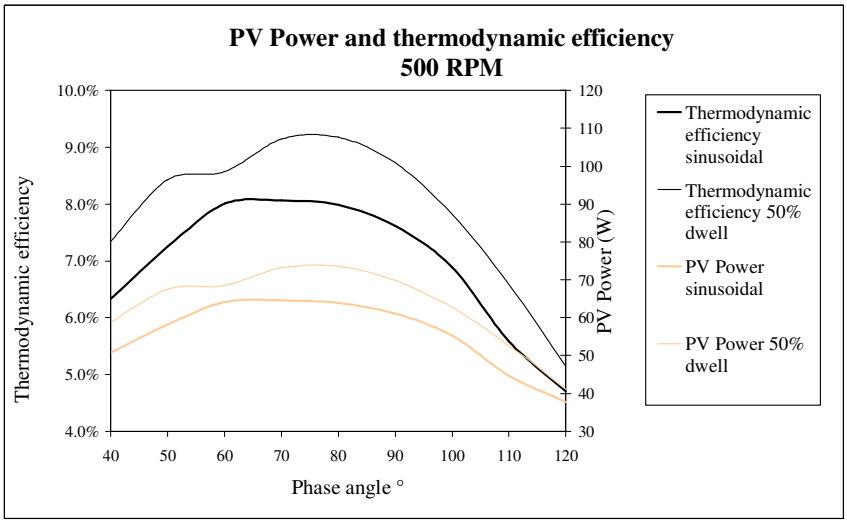

Figure 14-6 PV Power and Thermodynamic efficiency with respect to phase angle at 500 RPM and constant power input

It can be seen that the curve departs from 60° phase angle while operating with 50% displacer dwell. This can be caused by mechanical resonance variations, gas resonances, gas elasticity variations with phase and the time constant of the secondary coolant circuit affecting the reject temperature.

In all the above tests, the input power to the heater head is kept constant and the temperature is monitored. In the following tests, the heater head temperature is kept constant while adjusting the power to maintain the head temperature at different operating conditions. Constant temperature tests are performed only at 750 RPM.

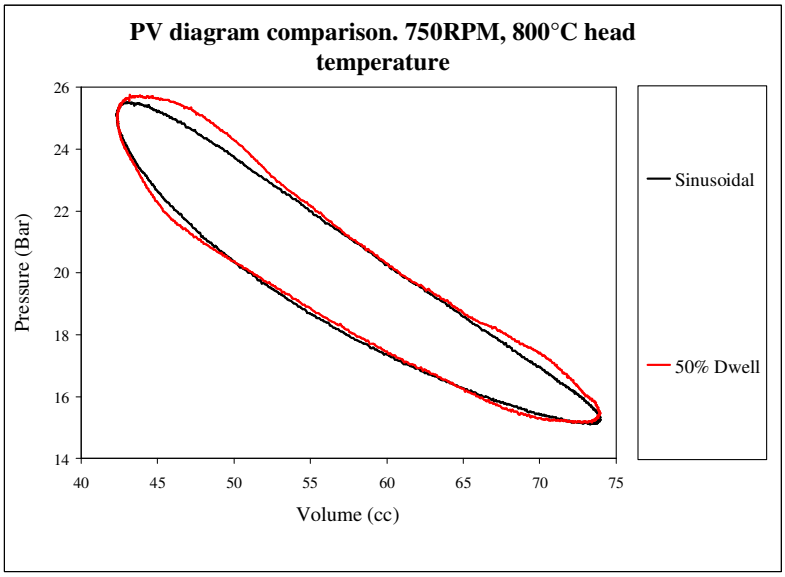

Figure 14-7 PV diagram comparison with sinusoidal displacer motion and non-linear displacer motion at 750 RPM and constant heater head temperature

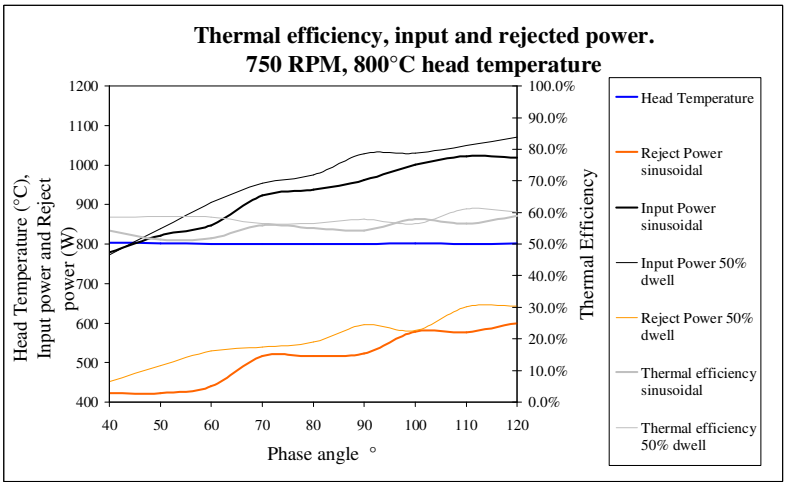

Figure 14-8 Heater head temperature, Input power and rejected power with respect to the phase angle at 750 RPM and constant heater head temperature

PV diagram with sinusoidal displacer motion and with 50% dwell is shown in Figure 14-7. The results are similar to the constant power tests. Heater head temperature, reject power and thermal efficiency vs. phase is plotted in Figure 14-8 for sinusoidal and non linear operation with 50% dwell with constant heater head temperature at 750RPM. Considerable ripple is present in the curves as seen earlier with constant power tests due to the same reasons as described earlier.

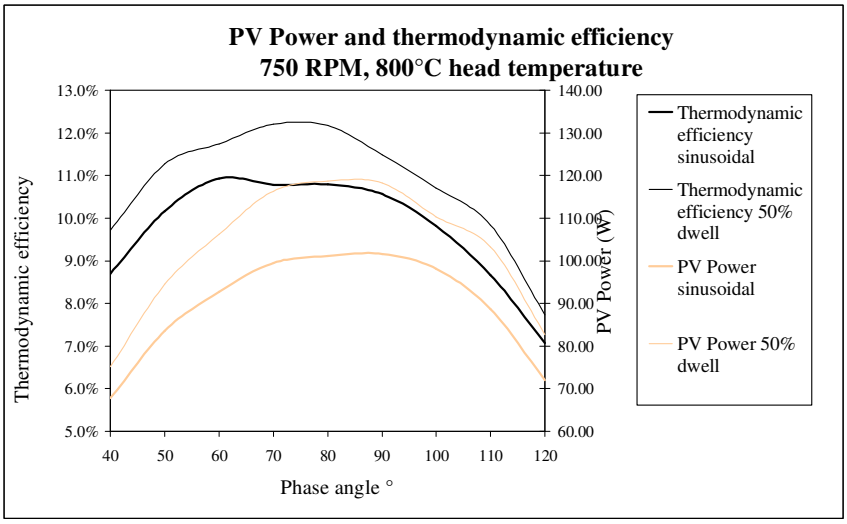

Figure 14-9 PV Power and Thermodynamic efficiency with respect to phase angle at 750 RPM and constant heater head temperature

Figure 14-9 shows the relationship between PV Power and efficiency vs. phase angle with constant heater head temperature at 750 RPM speed for sinusoidal displacer motion and with 50% dwell. The peak efficiency has shifted to a lower phase angle compared to the tests performed at constant

power input. This is due to the fact that a higher power level is needed to maintain the head at 800°C compared to the constant power case. As input power vs. efficiency is not studied, this cannot be commented in detail.

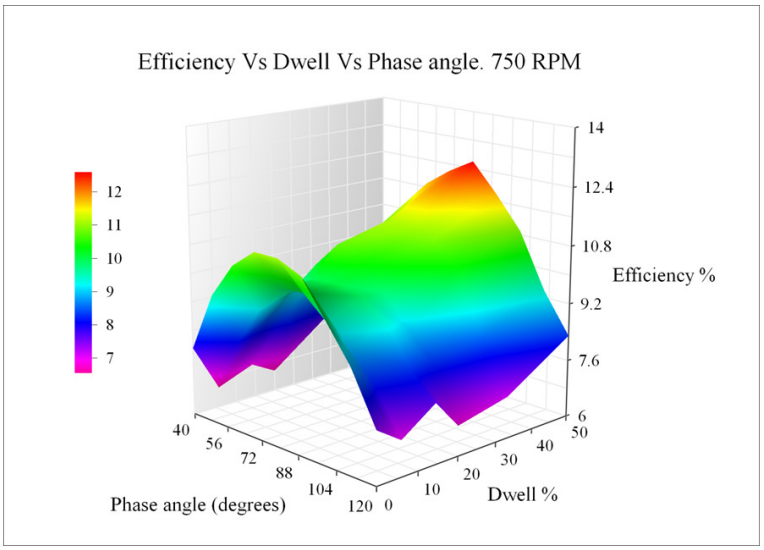

Figure 14-10 Efficiency vs. Phase angle vs. dwell at 750 RPM and constant power input

Figure 14-10 shows a 3D plot showing the efficiency variation vs. dwell and phase angle at 750RPM with constant power input. Figure 14-11 shows the variation in heater head temperature with dwell and phase angle at constant power input. Interestingly, the head temperature with dwell is lower than that with sinusoidal motion. Another observation is that at constant power input, the highest thermodynamic efficiency is not obtained at the operating point with the highest Carnot efficiency (higher temperature differential between hot and cold ends). Also when the phase

angle is increased, the heater head temperature comes down. These inputs are useful in designing Stirling engines as usage of exotic materials to withstand higher temperatures can be avoided.

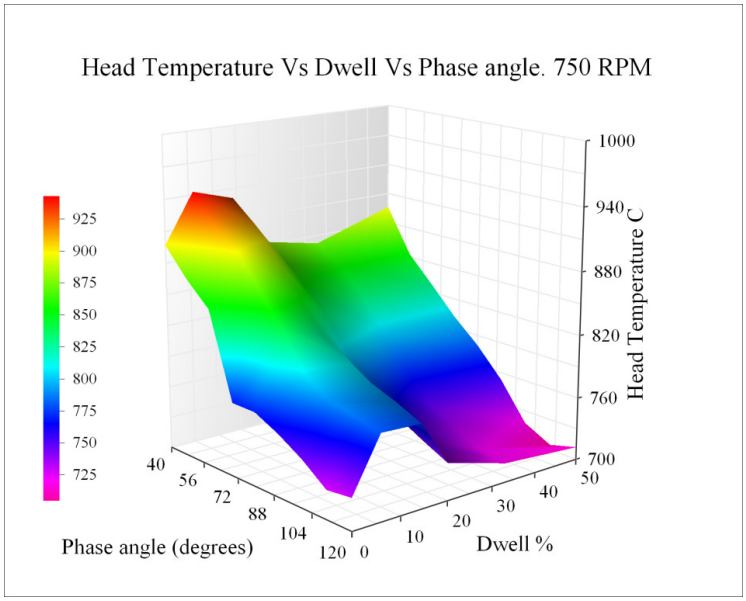

Figure 14-11 Heater head temperature vs. Phase angle vs. dwell at 750 RPM and constant power input

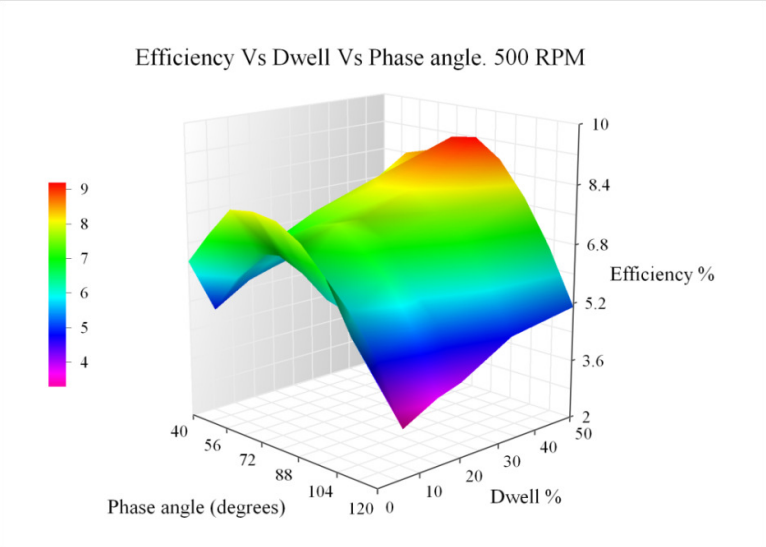

Figure 14-12 Efficiency vs. Phase angle vs. dwell at 500RPM and constant power input

Figure 14-12 shows a 3D plot showing the efficiency variation vs. dwell and phase angle at 500RPM with constant power input. Figure 14-13 shows the variation in heater head temperature with dwell and phase angle at constant power input. These curves look very similar to the ones at 750RPM. Tests were performed at 500RPM to validate the measurements done at 750RPM for cross correlation. At 500 RPM also, the temperature of the heater head comes down with increasing phase angle.

Figures 14-1 to 14-13 shows the variation in thermodynamic efficiency, thermal efficiency, PV power and heater head temperature of a Stirling engine to varying phase and dwell. All the above information should assist

the designer to optimise the design of a production Stirling engine for microCHP applications.

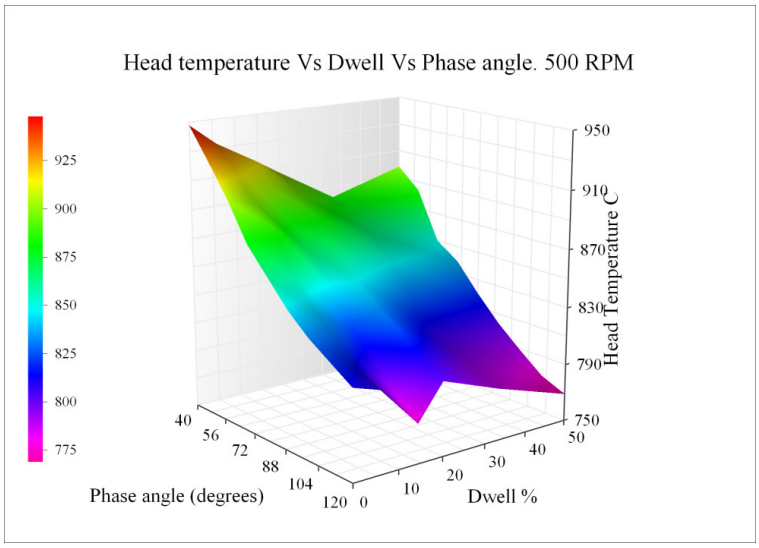

Figure 14-13 Heater head temperature vs. Phase angle vs. dwell at 500 RPM and constant power input

Figure 14-14 shows the PV diagram at various phase angles for sinusoidal displacer motion. The pressure excursions increase with increasing phase angle. The motion profile of the piston and the displacer is shown in Figure 14-15. The displacer motion profile is displayed only for three phase angles to avoid cluttering the graph. The displacer motion shows the chattering at the end of stroke due to the high velocities encountered.

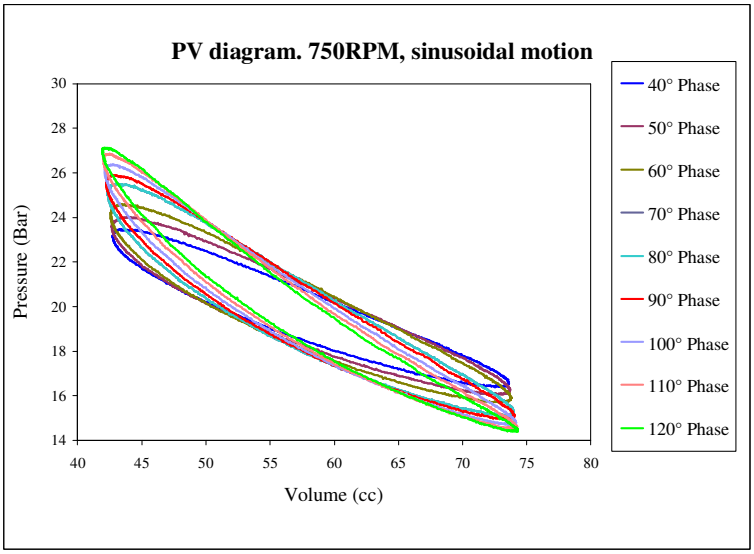

Figure 14-14 PV diagram at different phase angles for sinusoidal motion at 750 RPM

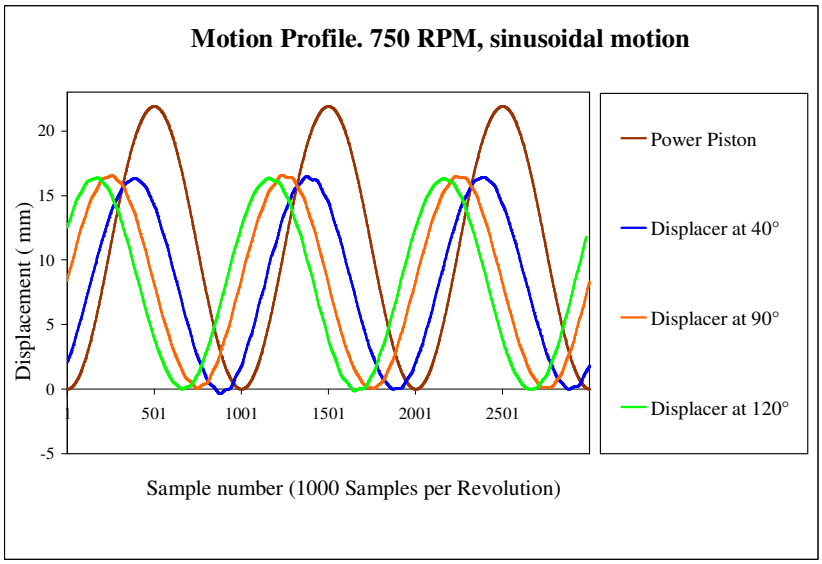

Figure 14-15 Motion profile showing piston motion and displacer motion at different phase angles at 750RPM

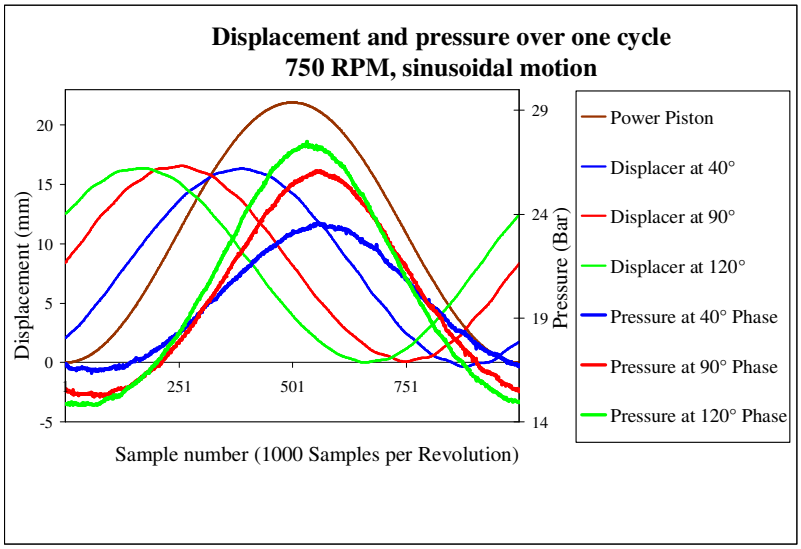

Figure 14-16 Piston position, displacer position and engine pressure at various phase angles for sinusoidal motion

The positive and negative excursions at end of stroke (chattering) cancel each other thermodynamically and do not have any significant effect on the performance of the system.

The pressure over one cycle at different phases along with the corresponding displacement of the piston and displacer is shown in Figure 14-16. This is for the test performed with sinusoidal motion at 750RPM with constant power input to the heater head. Phase angle of the engine pressure wave does not vary with changes in phase to the displacer. The pressure wave follows the phase of the piston with a slight lag. The amplitude of the pressure wave changes with changes in the phase angle of

the displacer. These are quite clear from the fact that the displacer does not contribute to the volume changes in the machine and influence the pressure only due to its phase. Another interesting observation from Figure 14-16 is that the highest efficiency or power does not occur at the displacer phase angle which produces maximum pressure differential. This is also evident from the PV diagram shown in Figure 14-14. At operating points with maximum pressure differential, the corresponding swept volume is lower and effectively produces a lower output power compared to the optimum pressure –volume combination at optimum operating phase.

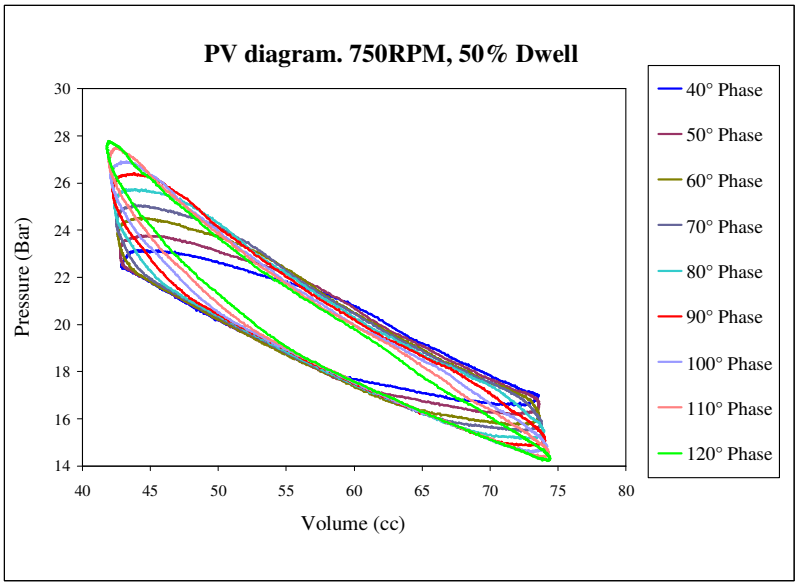

Figure 14-17 PV diagram at different phase angles for 50% dwell at 750 RPM

This is also true for operating points with a lower pressure differential compared to the operating point with the optimum phase angle.

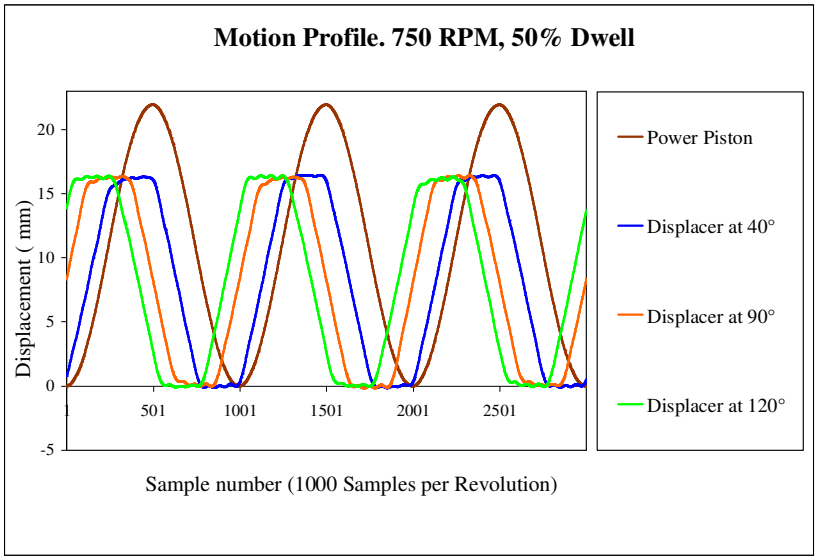

Figure 14-18 Motion profile showing piston motion and displacer motion at different phase angles for 50% dwell

Figure 14-17 shows the PV diagram at various phase angles for non-linear displacer motion with 50% dwell. The pressure excursions increase with increasing phase angle as in the case of sinusoidal motion. The motion profile of the piston and the displacer is shown in Figure 14-18. The displacer motion shows the chattering at the end of stroke due to the high travel velocities and end of stroke braking encountered by the linear motor. The positive and negative excursions at end of stroke cancel each other thermodynamically as in the sinusoidal case.

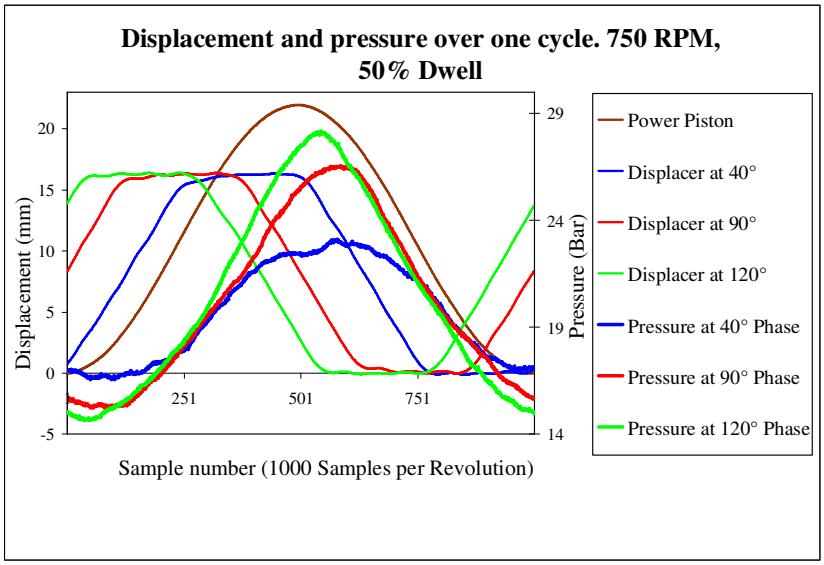

Figure 14-19 Piston position, displacer position and engine pressure at various phase angles for 50% dwell

The pressure over one cycle at different phases along with the corresponding displacement of the piston and displacer is shown in Figure 14-19. This is for the test performed with non linear motion with 50% dwell at 750RPM with constant power input to the heater head. Phase of the engine pressure wave slightly vary with changes in phase to the displacer. The pressure wave follows the phase of the piston with a slight lag. The amplitude of the pressure wave changes with changes in the phase angle of the displacer as in the sinusoidal case. One interesting observation is the unusual bump in the pressure wave at lower phase angles. When the acquired data is closely inspected, this bump is present in all the cycles acquired at lower phase angles at higher dwells.

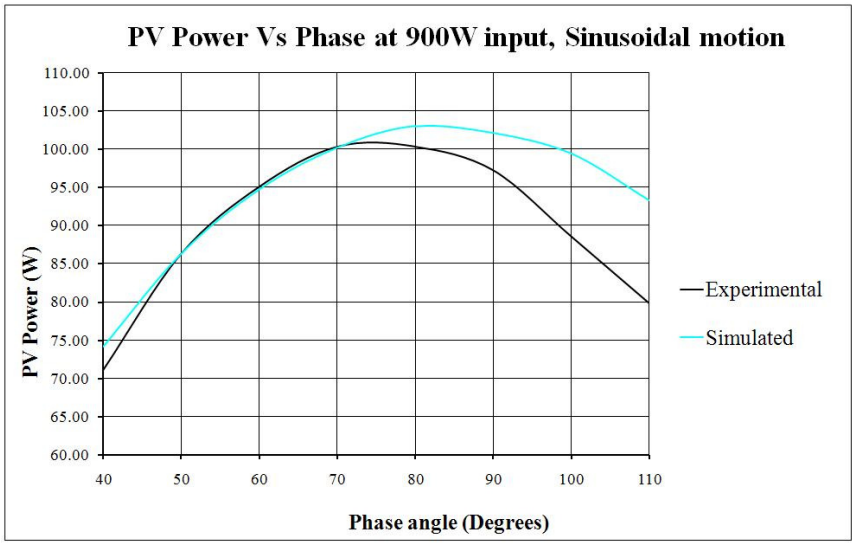

Figure 14-20 PV Power vs. Phase angle at 750RPM. Simulation and experimental.

Figure 14-20 compares the thermodynamic power obtained by experiment against theoretical values generated via simulation using SAGE. Simulation and experimental results tightly correlate at lower phase angles. At peak power, the variation is only 3% and even at the highest phase angle, the difference is only 17%. The simulations were not performed for non linear motion of the displacer. This needs to be taken up in a future work.

Simulation was performed in SAGE to check the validity of the simulator and the modelling techniques to assist in designing production engines. A validated simulator will be a useful tool for optimising designs before

going into prototyping and production. Figure 14-20 proves that the SAGE simulator is very accurate for Stirling engine designs which does not use very high phase angles. The simulator and its input model need to be further tuned for making more accurate predictions at higher phase angles.

The above 20 diagrams summarises the data collected with the ASE test rig operating as an engine. Thermodynamic efficiency is found to increase with dwell (except at very low dwells). Peak efficiency occur around 80° phase angle for sinusoidal and non linear motion of the displacer. Head temperature reduces, and reject power increases with increasing phase angle. The above graphs provide a very good understanding of the Active Stirling Engine operation with respect to varying dwell and phase.

14.2 Refrigerator test results

Refrigerator tests were carried out at 80° phase angle and at 750RPM. The test procedure is explained in detail in this thesis. Investigation was on the benefits of non linear displacer motion and whether the COP improves with nonlinear displacer motion. In refrigerator testing, PV diagram indicates the input thermodynamic power and the lift indicates the output at the particular lift temperature. Non linear motion improves the lift capacity and efficiency when an Active Stirling Engine operates as a refrigerator. This is evident from the Figures 14-21, 14-23 and 14-24.

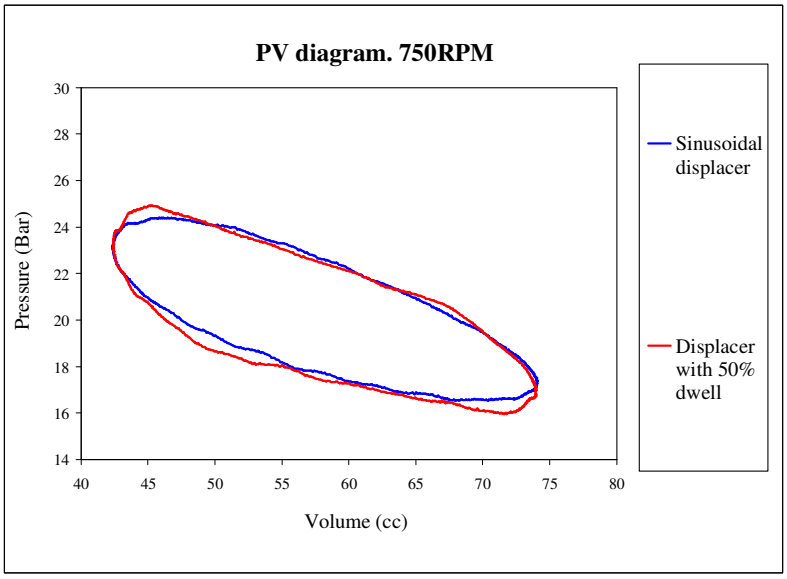

Figure 14-21 Plot 100. PV Diagram with sinusoidal displacer motion and with 50% dwell.

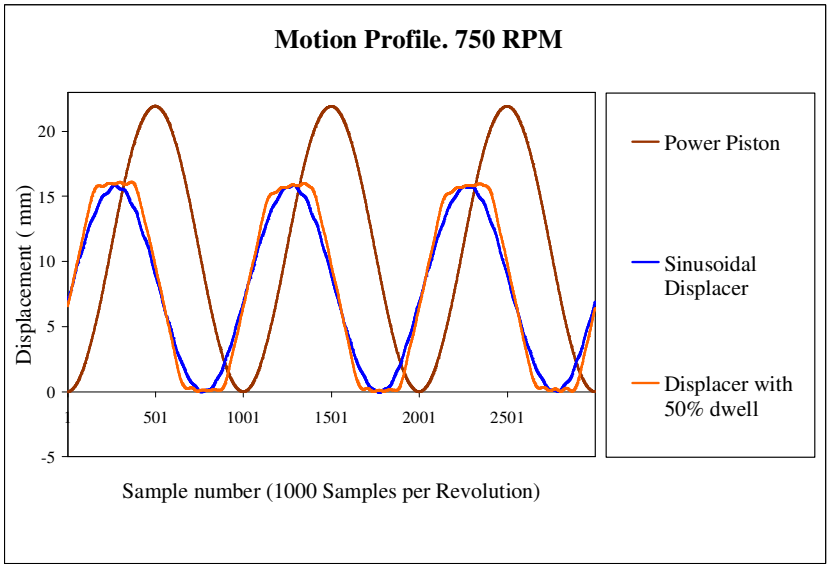

Figure 14-22 Plot 101. Motion profile of piston and displacer

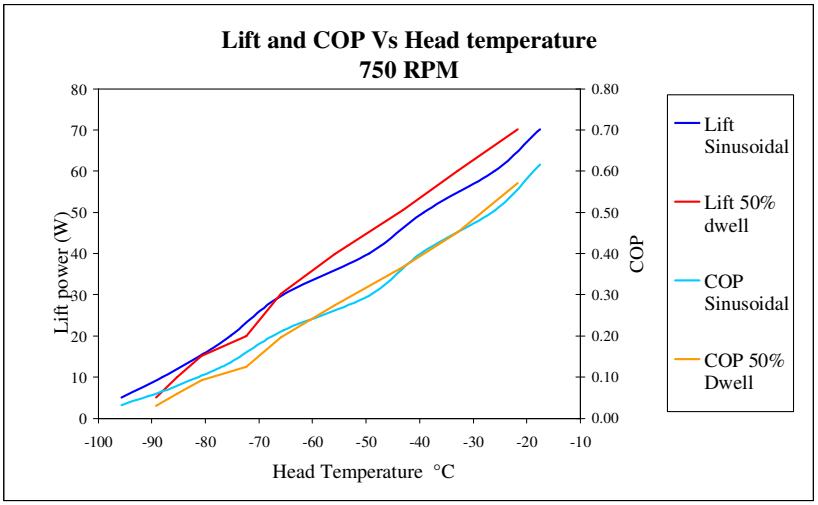

Figure 14-23 Plot 102. Lift and COP of the refrigerator with respect to the head temperature at sinusoidal and 50% dwell

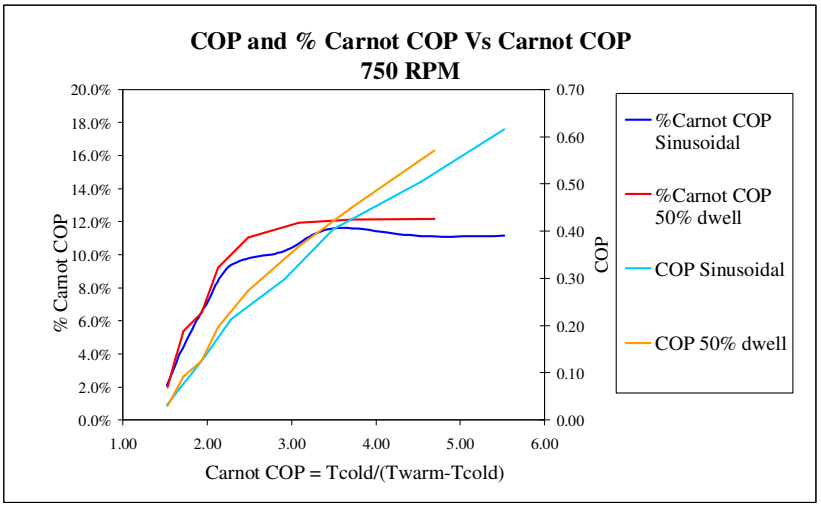

Figure 14-24 Plot 102. COP and %Carnot COP vs. Carnot COP for sinusoidal displacer motion and with 50% dwell.

The primary purpose of the experiments conducted was to test the test rig as an engine. As the Stirling engine is a four quadrant machine, operation of the system as a refrigerator was briefly examined and the above graphs (Figure 14-21 to Figure 14-24) summarises the data collected. This was included as a guideline or starting step for future researchers interested in pursuing active control of Stirling refrigerators or cryocoolers.

14.3 Effect of working gas on Stirling engine performance

In the experiments conducted, nitrogen was used as the working fluid since the test rig was designed for using nitrogen. Helium was tried as an experiment and degradation in efficiency was observed.

Different engines are designed for different gases. Normally Nitrogen, Helium, Hydrogen and Air are used. Researchers try to charge different gases to a Stirling engine and do comparative studies. This is not a good practice as each Stirling engine is designed for a particular working gas and will respond favorably to that gas.

Hydrogen and Nitrogen are diatomic gases while Helium is monatomic. The thermodynamic properties of working gas of Stirling engines have the biggest influence of possibility to achieve high energetic efficiency. Fast exchange of heat is the main factor of working gas selection. Some

construction options can increase or decrease speed of heat exchange. The special regenerators are built and used in Stirling engines to increase speed of heat exchange. Often they are built in special technology from special materials. The highest pressure of working gas increases the speed of heat exchange as well. But in every constructional option the properties of the working gas are of great importance. The gas heat capacity is the most important factor. From all the gases hydrogen has the highest heat capacity. But hydrogen is dangerous because the possibility of explosion and burning in the air is very high. Moreover, hydrogen is chemically active, embrittles many materials, mainly metals, can penetrate through any materials, metals included, and can decrease construction and fatigue properties of different materials including materials of seals. In spite of many difficulties hydrogen is used in cooling systems of generator of power plants. This shows possibility of effective usage of hydrogen.

Helium has very low chemical reactivity and is included to the noble gases. It means that helium contributes to burning and explosive safety. From the noble gases helium is the cheapest. Moreover, helium has three time worse heat capacity than hydrogen and in that mater it is in the second place after hydrogen.

Practical factors often decided about the usage of compressed air or nitrogen as the main working gas of Stirling engines. Nitrogen is the cheapest incombustible gas.

15. Applications of Phase and Dwell control in microCHP

At 750 RPM, non linear motion of the displacer as demonstrated improves the efficiency by 13.5% and at 500 RPM by 15%. Some preliminary tests conducted at 300 RPM indicated an efficiency improvement above 20%. Very low speed engines are not commercially attractive in a microCHP space and hence not investigated. But these might be useful for low temperature differential Stirling engine researchers interested in extracting geothermal energy or low temperature sources [103]. Low speed machines are easy to control; they generally work on low temperature differential and have lower wear and tear. They also operate at a lower charge pressure in general. The main drawback of low speed machines is the low specific power. Low speed machines tend to be very large and for a particular power output, tend to have a lower efficiency for higher power levels compared to a high speed machine. Due to these reasons for microCHP applications, low speed machines are not suitable.

Even a 10% efficiency increase is very good for our planet. Dwell control is clearly something that can be implemented in commercial Stirling engines for different applications. A fixed dwell can be implemented using mechanical cams without the need for active control.

Phase angle control actually detunes the engine. It can be used to control the heat to power ratio in microCHP applications. If the intention is to obtain the best efficiency, the optimum phase angle can be hunted for and the microCHP system can be operated at the operating point where the efficiency is highest. Similarly the system can perturb and observe for the optimum dwell and operate at the region of best net efficiency. In the case where dwell is changed, the system needs to consider the power required for displacer motion as well. The power requirement for the displacer motion will depend on the specific design of the microCHP system. The mass of the displacer, speed, stroke, charge pressure and the amount of springing used will decide the overall power required to drive the displacer.

In markets where the exported energy is not paid for or if the incentive is less, it might be ideal to generate electricity only when it is consumed in house. The phase control scheme allows the system to respond to the situation and make sure that only enough power consumed in the house is generated. Also when there is time of day metering or demand response

kind of systems in action, electricity for export need to be only generated during the time of highest incentive or above breakeven incentive.

Active Stirling Engines open new avenues in microCHP design as it will allow the development of algorithms to evaluate various inputs like electricity pricing, usage and command the microCHP to response accordingly without using start stop control. This system can be integrated to a heat management module to make it a heat and electricity management module. These modules can even download real time pricing; when it becomes a reality in future; and allow the microCHP system to respond proactively to maximize the financial incentive to the user and the utility. Another driver for using ASE will be the electricity provider, who needs to ensure grid stability.

This thesis provides the basic ground work for designing algorithms and guidelines to design real microCHP systems and provides a wealth of data for designers of various systems. It encourages the user to look for new solutions in the conventional microCHP applications space.

16. Conclusions and future work

This thesis provides a “first of its kind data” and a detailed look on actively controlled Stirling engines. Several hundreds of tests were carried out tuning and calibrating the system before going into actual data collection. The importance of collecting good data in multi discipline environments cannot be overstated. In this experiment, application software is commanding a DSP which in turn monitors the control loop and generates the command signals to drive a linear motor which in turn drives a displacer of a gamma Stirling engine. Position, pressure, flow and temperature sensors, electrical machines and an engine work in a coordinated fashion to provide valuable data, which is the basis of this thesis.

This thesis proves that the efficiency of Stirling engines can be improved by using non linear control of the displacer. Up to 15% efficiency improvement is demonstrated. This thesis also provides information on the

impact of phase control on Stirling engine operation. The data and analysis presented should assist in designing a production machine with non linear displacer motion and utilizing phase control. Non linear motion increases the work done and efficiency by altering the thermodynamics, and phase control provides operational control of the Stirling engine for a production machine.

A displacer machine has to be realized to integrate this concept into a product. Dynamic balancing is going to be very important to practically implement phase control and non linear motion. Don Clucas discloses different ways to realize such a machine [104]. All the designs disclosed by Dr. Clucas have the potential to balance adequately and can be used to drive the displacer (or even the power piston). A balanced displacer drive machine and its control electronics are important to integrate the concept of ASE in a microCHP product. An example of a similar machine, named the "Oscillomotor" is briefly explained in Appendix 2.

Another area of future work is the algorithms for heat management and power export. Conventional heat management algorithms are designed to work with a domestic boiler for heating purposes. These algorithms make use of the heat demand signal of the central heating controller as the primary control. They also have a boost demand signal at times of high

heat requirement. It is similar to a two step on off control. Some of the central heating controllers issue a PWM signal for heat demand and the amount of heat requirement can be decoded from the PWM.

Conventional PWM controllers (on – off or PWM) are not ideal for utilizing dwell and phase control. New algorithms utilizing dwell and phase control needs to be developed for utilizing the concept of ASE in microCHP applications. The algorithm should consider the export incentives depending on time of day, price differential between the fuel used and the electricity exported and the heat demand history. These inputs should be used to effectively control the microCHP to optimize usage.

The utilization of phase and dwell control can also be explored for refrigeration applications. Cryocoolers might be benefitted from the non linear motion of the displacer. Efficiency comparison studies need to be taken up for conventional reciprocating and rotary refrigeration compressors, and ASE based cooling to evaluate the advantages of ASE in refrigeration and cryocooler applications. Refrigeration and air conditioning is an area where large potential exists for improving energy utilisation efficiency.

Nonlinear motion of the power piston is another area which needs investigation. A test rig where the power piston and the displacer can

achieve non linear trajectory needs to be built and investigated. This can be initially evaluated in SAGE or similar simulation software before a prototype is built to validate the simulations.

The current ASE test rig is a Gamma configuration system. Similar test rigs can be built for Alpha and Beta configurations to find out whether there are any significant differences in the results achieved.

In the current tests, most of the experiments are carried out at constant input power or at a constant temperature. Studies can be carried out on the effects of phase and dwell at different power levels and heater head temperatures. This will be suitable for concentrator type solar dish Stirling systems as they do not have a constant input power or constant head temperature.

The speed control, stroke control and bias control (whether the displacer shuttles towards the top dead centre or the bottom dead centre breaking away from symmetry) should be investigated to find out their effect on energy flows. Effects of asymmetric displacer motion also need to be investigated (moving up slowly and coming down faster or vice versa). These studies will open up new venues in energy efficiency improvement and control for microCHP systems of the next generation.

17. References

[1] I. Urieli, "The Regenerator and the Stirling Engine," *Proceedings of the Institution of Mechanical Engineers,* vol. 212, p. 531, 1998.

[2] H. Liu and S. Kakac□, *Heat exchangers: selection, rating, and thermal design*. Boca Raton, Fla: CRC Press, 1998.

[3] A. C. Baisden, "Generalized Terminal Modeling of Electro-Magnetic Interference," Dissertation/Thesis, VT, 2009.

[4] A. J. Organ and T. Finkelstein, *Air engines*. London: Professional Engineering Pub, 2001.

[5] G. T. R. a. C. Hooper, *Stirling Engines*: E&F N Spon, 1991.

[6] K. Hirata. *Stirling Engine*. Available: http://www.bekkoame.ne.jp/~khirata/english/history1.htm

[7] J. Ericsson, "The caloric engine," *Journal of the Franklin Institute,* vol. 18, pp. 48-53, 1834.

[8] G. R. Walker, G. Fauvel, O R.Bingham, E.R, *The Stirling Alternative*: Gordon and Breach Publishers Inc, 1994.

[9] T. Finkelstein, "Air Engines," *Engineer,* vol. 207, pp. 492-297, 522-527, 568-571,720-723, 1959.

[10] R. Sier, *A history of Hoty Air and Caloric engines*. London: Argus Books, 1987.

[11] C. M. Hargreaves, *The Philips Stirling Engine*. Amsterdam: Elsevier Science Publishers B.V., 1991.

[12] G. R. Graham Walker, Owen R. Fauvel, Edward R. Bingham, *Stirling Alternative*: Gordon & Breach Science Pub, 1994.

[13] G. Walker and J. R. Senft, *Free piston Stirling engines* vol. 12. New York: Springer-Verlag, 1985.

[14] W. R. Martini, C. Lewis Research, V. United States. Dept. of Energy. Office of, R. Engine, and Development, "Stirling engine design manual," The Office, Springfield, VA1983.

[15] Anonymous, "California Unions for Reliable Energy Partners with K Road Calico Solar Project," in *Business Wire*, ed. New York: Business Wire, 2011.

[16] G. F. Nellis, "Stirling-magnetic cryocooler," Dissertation/Thesis, Massachusetts Institute of Technology, 1997.

[17] T. Flynn, *Cryogenic Engineering*. Hoboken: Informa Healthcare, 2004.

[18] G. Walker, *Cryocoolers: Fundamentals*: Plenum Press, 1983.

[19] J. Allison, *Electronic Engineering Semiconductors and Devices*. London: McGraw-Hill, 1990.

[20] H. A. Garratt, *Heat Engines*: E Arnold, 1912.

[21] A. Lightman, "The Second Law of Thermodynamics," *Physics Today,* vol. 58, p. 59, 2005.

[22] S. Dan, "Cogeneration," *Chemical Market Reporter,* vol. 251, p. SR6, 1997.

[23] J. Steigenthaler, *Modern hydronic heating for residential and light commercial builduings* vol. 1: Delmar Learning, 2011.

[24] S. Massucco, A. Pitto, and F. Silvestro, "A Gas Turbine Model for Studies on Distributed Generation Penetration Into Distribution Networks," *Power Systems, IEEE Transactions on,* vol. 26, pp. 992-999, 2011.

[25] B. Gou, W. K. Na, and B. Diong, *Fuel cells: modeling, control, and applications*. Boca Raton: CRC Press, 2010.

[26] W. W. Pulkrabek, *Engineering fundamentals of the internal combustion engine*, 2 ed. vol. 1: Pearson Prentice Hall, 2004.

[27] B. Murray, *Electricity markets: investment, performance, and analysis*. Chichester: Wiley, 1998.

[28] "UK govt investigates potential for dynamic demand management," *EU Energy,* p. 21, 2007.

[29] J. A. Orlando, *Cogeneration technology handbook*: Government institutes, 1984.

[30] C. R. Mischke and J. E. Shigley, *Power transmission elements: a mechanical designers' workbook*. New York [N.Y.]: McGraw-Hill, 1990.

[31] S. Fredette, "Squirrel cage induction machines in distributed generation and microgrids," Dissertation/Thesis, 2009.

[32] Drugasar. *Balanced flue*. Available: http://www.drugasar.co.uk/balanced_flue_system.htm

[33] G. Dastagir, "Voltage and frequency regulation of a stand-alone self-excited induction generator with an unregulated prime mover," Dissertation/Thesis, 2008.

[34] S. S. Wilson, "Sadi Carnot," *Scientific American,* vol. 245, pp. 134-145, 1981.

[35] G. Charles Coulston, "Science in the Eye of the Beholder, 1789-1820," *Transactions of the American Philosophical Society,* vol. 96, p. 223, 2006.

[36] Y. A. B. Wiki Cengel, Michael A, *Thermodynamics: an engineering approach*. Boston: McGraw-Hill, 2002.

[37] V. Y. Voskresenskii, "On quasistatic processes," *Russian Physics Journal,* vol. 40, pp. 554-557, 1997.

[38] Z. Ernest, Jr., "Power output of the Otto cycle engine," *The Physics Teacher,* vol. 22, p. 390, 1984.

[39] G. Ronald, "Real otto and diesel engine cycles," *The Physics Teacher,* vol. 21, p. 29, 1983.

[40] K. Lee, "Analysis, modification and improvement of performance of a closed, regenerative, reciprocating Brayton cycle engine," Dissertation/Thesis, Massachusetts Institute of Technology, 1978.

[41] G. Rajamohan, B. Chua Han, and K. Balasundaram Mohan, "Theoretical Analysis of Closed Rankine Cycle Solar Pond Power Generator," *Modern Applied Science,* vol. 2, 2009.

[42] S. W. Bancha Kongtragool, "A review of solar-powered Stirling engines and low temperature differential Stirling engines," *Renewable and Sustainable Energy Reviews,* vol. 7 (2003) 131–154, pp. 131-154, 2002.

[43] D. W. Kirkley, "Determination of the optimum configuration for a stirling engine," *ARCHIVE: Journal of Mechanical Engineering Science 1959-1982 (vols 1-23),* vol. 4, pp. 204-212, 1962.

[44] C. D. West, *Principles and applications of Stirling engines*. New York: Van Nostrand Reinhold company, 1986.

[45] V. K. Gopal, R. Duke, and D. Clucas, "Active Stirling engine," in *TENCON 2009 - 2009 IEEE Region 10 Conference*, 2009, pp. 1-6.

[46] B. Kongtragool and S. Wongwises, "Performance of low-temperature differential Stirling engines," *RENEWABLE ENERGY,* vol. 32, pp. 547-566, 2006.

[47] B. P. Nuel and S. P. Weaver, "Displacer motion control within air engines " US Patent 7,805,934, October 5 2010.

[48] J. S. Moloney, "Stirling cycle machine " US Patent 4,195,482, April 1, 1980

[49] M. M. Walsh, "Resonant free-piston Stirling engine having virtual rod displacer and linear electrodynamic machine control of displacer drive/damping " US Patent 4,458,489 July 10, 1984

[50] J. M. Beggs, "Stirling cycle cryogenic cooler " US Patent 4,389,849, June 28, 1983.

[51] M. M. Walsh, "Start-up and control method and apparatus for resonant free piston Stirling engine " US Patent 4,434,617 March 6, 1984

[52] J. Otters, "Variable cycle stirling engine and gas leakage control system therefor " US Patent 4,489,554, December 25, 1984

[53] D. G. Beremand, "Free-piston regenerative hot gas hydraulic engine " US Patent 4,215,548 August 5, 1980

[54] W. T. Beale, "Power piston actuated displacer piston driving means for free-piston stirling cycle type engine " US Patent 3,552,120 February 10, 1976

[55] W. T. Beale, "Free piston stirling machine having variable spring between displacer and piston for power control and stroke limiting " US Patent 5,385,021, January 31, 1995

[56] Y. Yamamoto, "Stirling engine and actuator " US Patent 6,843,057 January 18, 2005

[57] H. T. Jarvis, "Variable displacement and dwell drive for stirling engine " US Patent 5,782,084 July 21, 1998

[58] R. A. Frosch and A. R. McDougal, "Phase-angle controller for stirling engines " US Patent 4,240,256 December 23, 1980

[59] J. R. Senft, "Drive mechanism for Stirling engine displacer and piston and other reciprocating bodies " US Patent 4,339,960 July 20, 1982

[60] W. T. Beale, "Free piston stirling machine having a controllably switchable work transmitting linkage between displacer and piston " US Patent 5,502,968, April 2, 1996

[61] T. D. McWaters, "Kinematic stirling engine " US Patent 5,6,44,917

[62] W. G. Livezey, "variable power and variable direction engine and compound planetary phase changing device " US Patent 3,416,308 December 17, 1968.

[63] R. B. Wallis, "Phase relation control," US Patent 3,315,465, April 25, 1967.

[64] D. M. Berchowitz, "Double acting stirling engine phase control " US Patent 4,395,880, August 2, 1983

[65] K. D. Price, "Passive three state electromagnetic motor/damper for controlling stirling refrigerator expanders " US Patent 5,678,409 October 21, 1997.

[66] W. H. Bamberg and J. A. O'Neil, "Temperature staged cryogenic apparatus of stepped configuration with adjustable piston stroke," US Patent 3,802,211 April 9, 1974.

[67] K. H. Chien and L. M. Liou, "Stirling engine with variable stroke," US Patent US2004/0112048A1, June 17, 2004.

[68] K. Kocsisek, "Stirling engine " US Patent 6,729,131, May 4, 2004

[69] H. A. Jaspers, "Power control system for Stirling engines," US Patent 3,886,744 June 3, 1975.

[70] A. E. Biermann, "Variable Stroke Mechanisms," US Patent 2,873,611 February 19, 1957.

[71] S. A. S. Hakansson, "Stirling cycle engine power control system," US Patent 3,820,330 June 28, 1974.

[72] N. O. Young, R. Henderson, and P. J. Kerney, "Refrigeration system with linear motor trimming of displacer movement " US Patent 4,475,346 October 9, 1984.

[73] N. O. Young, "Linear drive motor control in a cryogenic refrigerator " US Patent 4,664,685 May 12, 1987

[74] A. Chertok, "Free piston Stirling engine control," US Patent 7, 200, 994 B2 April 10, 2007.

[75] B. J. Chagnot, "Apparatus and method for the speed or power control of stirling type machines " US Patent 4,856,280 August 15, 1989.

[76] E. S. Holliday, "Hybrid electrical source combining stirling engine driven alternator with supplementing energy storage," US Patent US2009/0206667 A1 August 20, 2009.

[77] A. C. Nommensen, "Stirling cycle engine," US Patent 6,195,992 B1 March 6, 2001.

[78] S. B. Horn, R. A. Wright, and M. S. Asher, "Means for producing an optimized cooler expander waveform," US Patent 4,417,448 November 29, 1983.

[79] N. M. Dehelean, "The Analysis of a Dwell Mechanism for Alpha - Stirling Engine," ed Dordrecht: Springer Netherlands, 2009, pp. 511-519.

[80] M. Nasser Seraj and S. Pascal, "Simulation of a Martini Displacer Free Piston Stirling Engine for Electric Power Generation," *International Journal of Thermodynamics,* vol. 3, pp. 27-34, 2000.

[81] C. C. Lloyd, "A low temperature differential stirling engine for power generation : a thesis submitted in partial fulfilment of the requirements for the degree of Master of Engineering in the University of Canterbury," Dissertation/Thesis, 2009.

[82] P. T. Gaynor, R. Y. Webb, and C. C. Lloyd, "Low temperature differential stirling engine based power generation," in *Sustainable Energy Technologies, 2008. ICSET 2008. IEEE International Conference on*, 2008, pp. 492-495.

[83] J. M. Olbermann and W. M. Anderson, "Hermetically sealed Ringbom-Stirling engine/generator," in *Energy Conversion Engineering Conference, 1989. IECEC-89., Proceedings of the 24th Intersociety*, 1989, pp. 2881-2884 vol.6.

[84] J. R. Senft, *Ringbom Stirling engines*: Oxford university press, 1993.

[85] X. Chen, Y. N. Wu, H. Zhang, and N. Chen, "Study on the phase shift characteristic of the pneumatic Stirling cryocooler," *CRYOGENICS,* vol. 49, pp. 120-132, 2008.

[86] T. Finkelstein, "A new isothermal theory for Stirling machine analysis and a volume optimization using the concept of 'ancillary' and 'tidal' domains," *Proceedings of the institution of mechanical engineers part C-Journal of mechanical engineering science,* vol. 212, pp. 225-236, 1998.

[87] R. Sier. (20th February). *Stirling and hot air engine home page*. Available: http://stirlingengines.org.uk/simulation/simulat.html

[88] S. K. Anderson, "Numerical Simulation of Cyclic Thermodynamic Processes," Ph.D, Department of Mechanical Engineering, Technical university of Denmark, Denmark, 2006.

[89] D. B. Israeli Urieli, *Stirling engine cycle analysis*, 1984.

[90] G. Chen, West, "Linear Harmonic Analysis of Stirling Engine Thermodynamics," *ORNL/CON-155,* 1984.

[91] D. Gedeon, *SAGE User's Guide*: Gedeon Associates, 1994.

[92] K. Mahkamov and D. B. Ingham, "Theoretical investigations on the Stirling engine working process," in *Energy Conversion*

Engineering Conference and Exhibit, 2000. (IECEC) 35th Intersociety, 2000, pp. 101-110 vol.1.

[93] K. Mahkamov, "Design Improvements to a Biomass Stirling Engine Using Mathematical Analysis and 3D CFD Modeling," *Journal of Energy Resources Technology,* vol. 128, pp. 203-215, 2006.

[94] V. K. Gopal, R. Duke, and D. Clucas, "Design and development of a test rig to validate the concept of an Active Stirling Engine," in *Universities Power Engineering Conference (AUPEC), 2010 20th Australasian*, 2010, pp. 1-6.

[95] P. Dean, "Wobble yoke and Stirling engine are key to reliable, green CHP system," *Eureka,* vol. 24, p. 10, 2004.

[96] F. Karen Auguston and M. Darius, "Linear motors 101," *Design News,* vol. 55, p. 61, 2000.

[97] S. Lin, C. Bi, and Q. Jiang, "An effective method to obtain commutation positions in BLDC drive mode," *Microsystem Technologies,* vol. 17, pp. 347-350, 2011.

[98] (2011, Two Servo Drives with Sinusoidal Commutation. *(Journal, Electronic)*.

[99] A. Thess, "Specific Applications," in *The Entropy Principle*, ed: Springer Berlin Heidelberg, 2011, pp. 87-145.

[100] . *Pressure sensor datasheet*. Available: http://www.gemssensors.com/~/media/GemsNA/CatalogPages/2200-and-2600-series-cat.ashx

[101] . *Omega K Type thermocouple datasheet*. Available: http://www.omega.com/prodinfo/thermocouples.html

[102] . *Flow sensor datasheet*. Available: http://www.gemssensors.com/Products/Flow/Electronic-Flow-Sensors/Turbo-Flow/FT-210-Series-Flow-Sensor

[103] P. T. Gaynor, R. Y. Webb, and C. C. Lloyd, "Low enthalpy heat stirling engine based electric power generation: A research design," in *Clean Electrical Power, 2009 International Conference on*, 2009, pp. 615-618.

[104] D. M. Clucas, "Reciprocating piston machine with oscillating balancing rotors," NZ Patent 549050, Aug 9, 2007.

18. Appendix 1. Test rig drawing and pictures

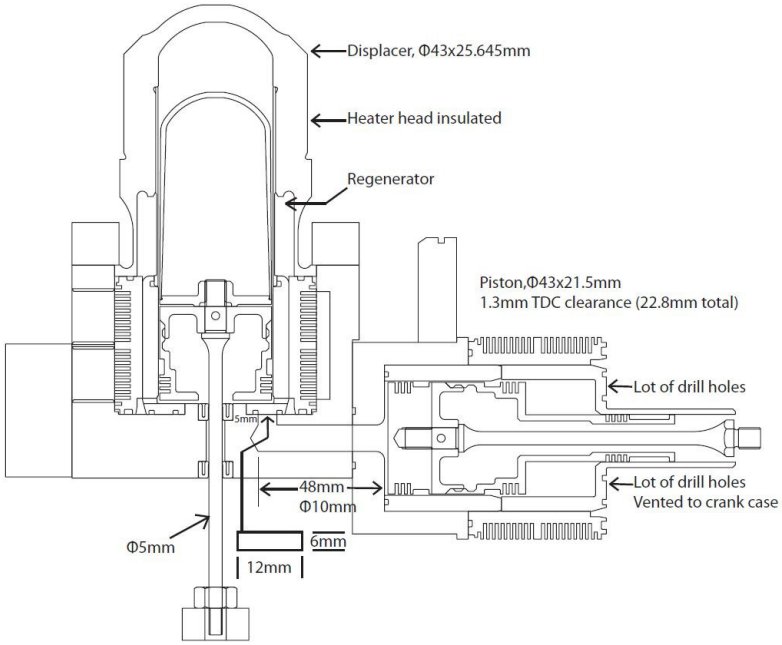

Figure 18-1. Drawing of the engine part of ASE test rig

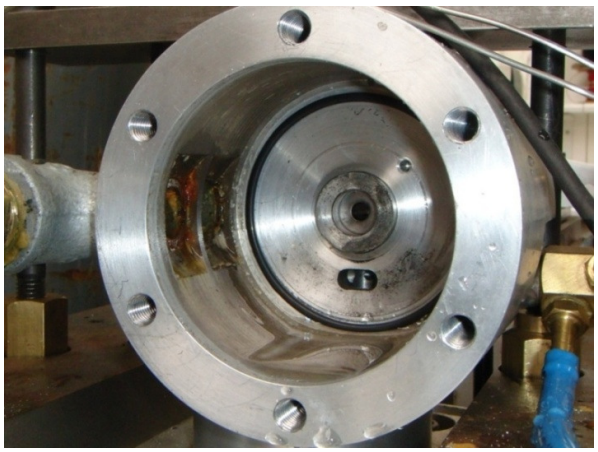

Figure 18-2. Cold end of the engine.

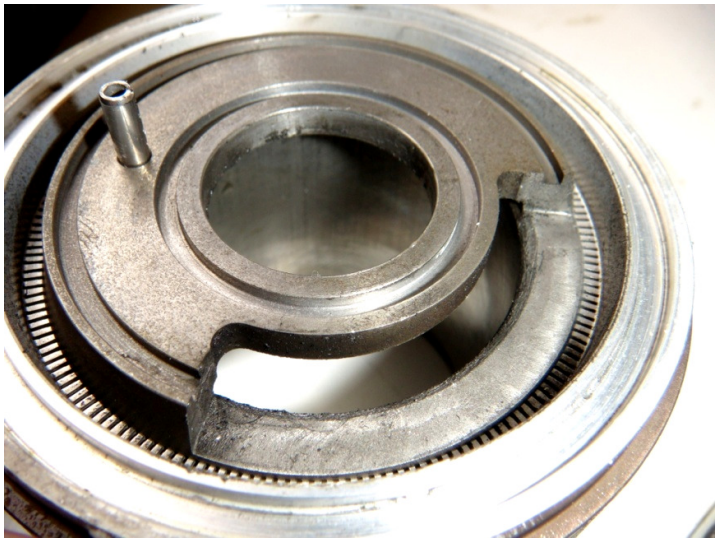

Figure 18-3. Cold end of ASE showing the fins

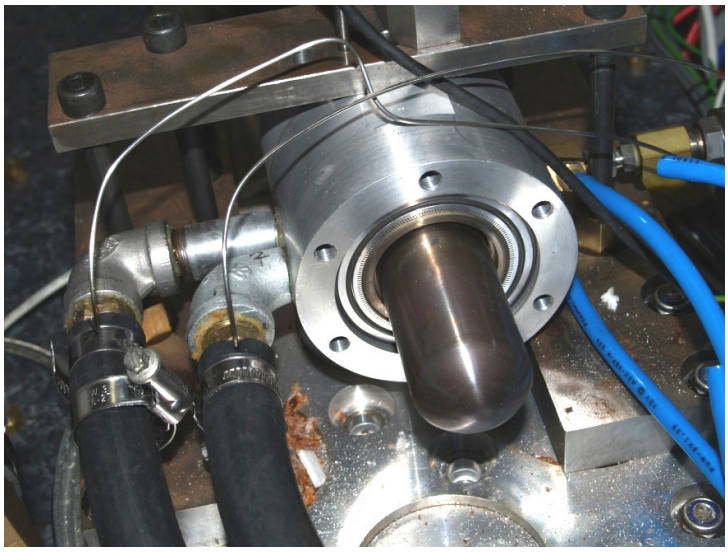

Figure 18-4. Displacer inserted into the cold end. The other end of the displacer comes out through a seal and is connected to the linear motor

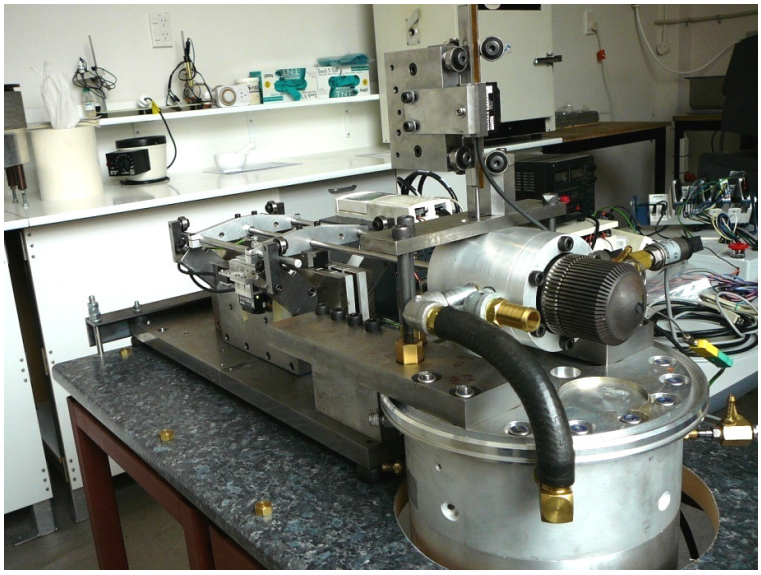

Figure 18-5. Heater head connected to the engine block

Figure 18-6. Frost developed on heater head when operating as refrigerator

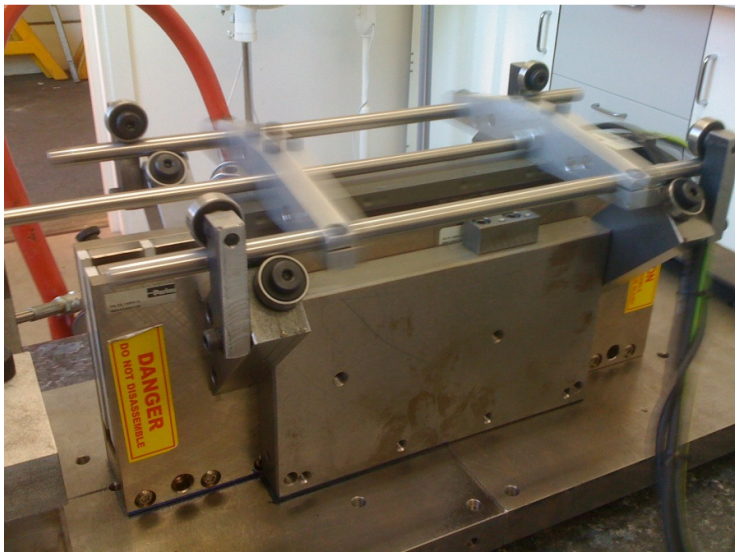

Figure 18-7. Photographed when the linear machine is working at 750RPM

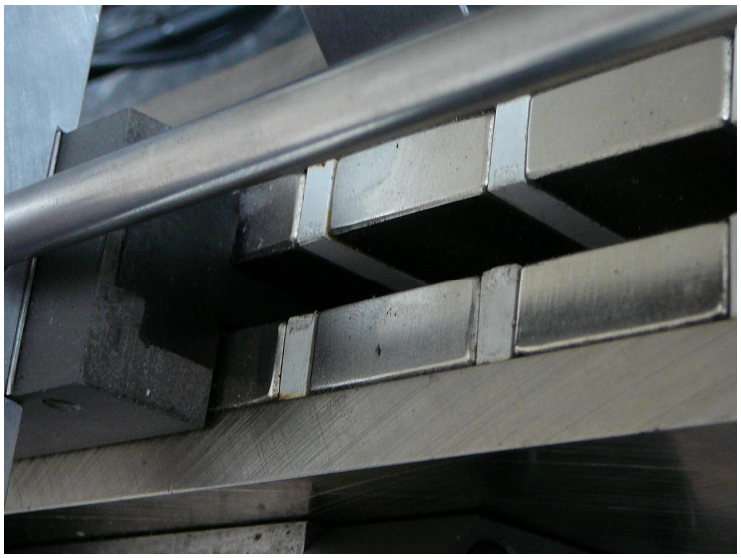

Figure 18-8. Linear machine track and magnets

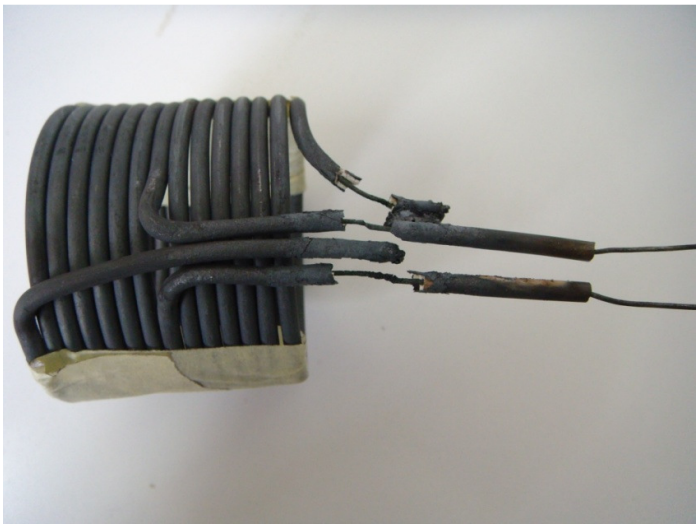

Figure 18-9. Burned heater head coil during an inadvertent short circuit

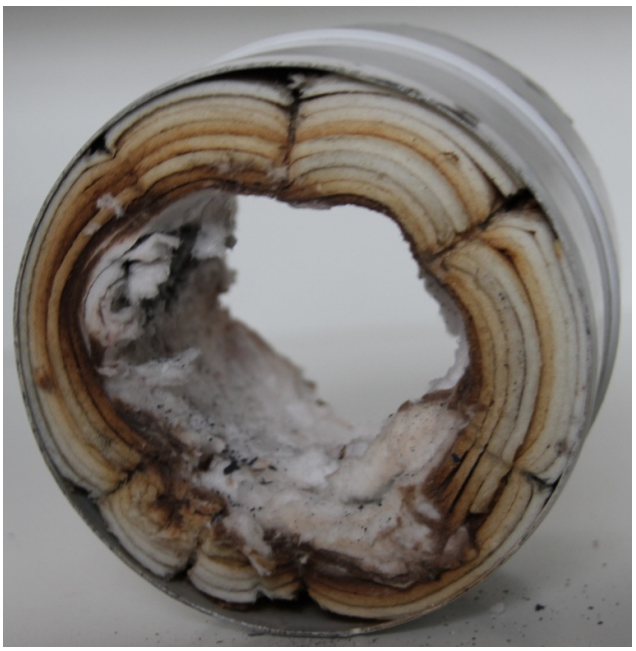

Figure 18-10. Insulator used on the heater head after six months use

Figure 18-11. Coolant bypass valve and the flow sensor

19. Appendix 2. Oscillomotor

Initially the plan was to design and make the displacer machine and control electronics for the ASE, inhouse. A purely linear machine for the displacer will have dynamic balancing issues when used in a product unless two of them are used in a dual opposed configuration. A rotary machine will need a transmission and makes the system complicated. A new oscillating machine was designed and developed which was neither rotary or linear. It had two counter rotating rotors which oscillate through a limited angle.

The counter rotating rotors were connected through a conrod to the displacer. The system is so simple, as it uses only two bushes and one bearing. The counter rotating rotors cancelled the moment and the system was properly balanced. The first prototype was built and it worked at high speed with almost no vibrations.

A more detailed prototype was built which is shown in Figure 19-1through 19-3. Power and control electronics was developed and the system was operated from a TMS320F2812 DSP. As the project proceeded, it was found that optimising this new oscillating machine and its drive and control system was beyond the scope of this thesis.

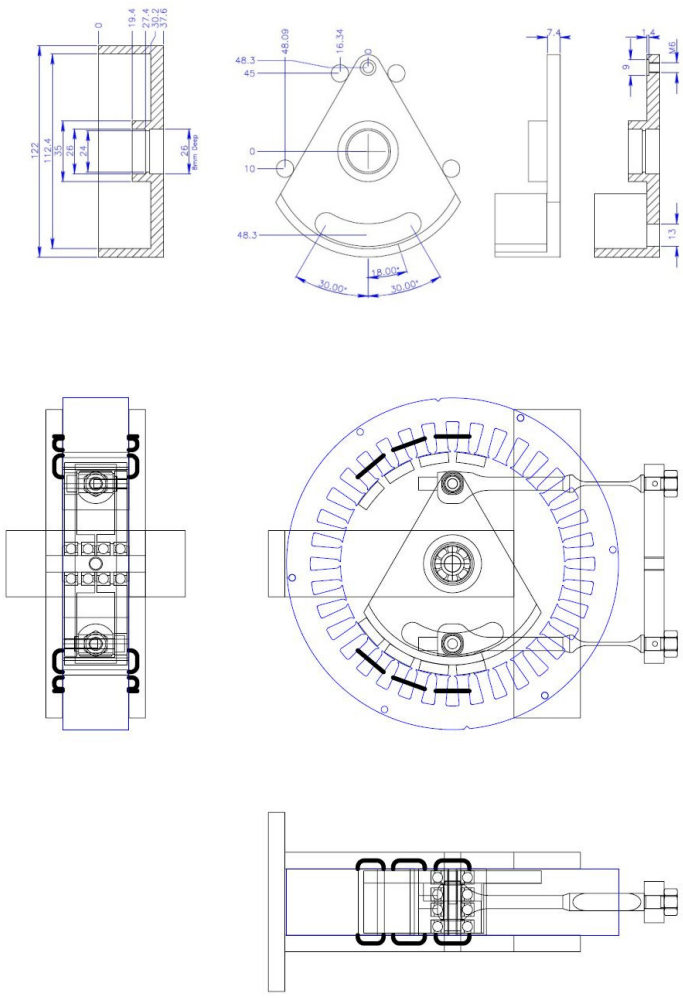

Figure 19-1. Drawings of the oscillomotor with counter rotating rotors

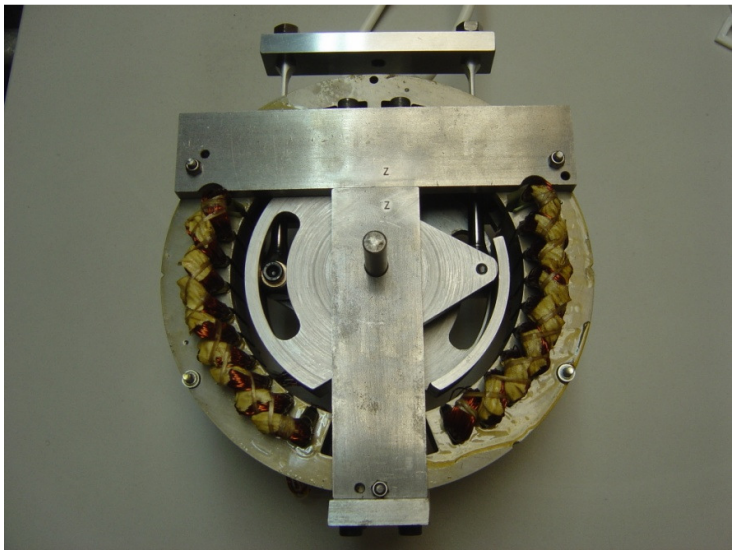

Figure 19-2. Oscillomotor with counter rotating rotors before pasting the high power Nd-Fe magnets

Figure 19-3. Photograph of the assembled oscillomotor

After spending almost a year and a half on the Oscillomotor; a linear motor, its drive and servo was purchased to continue with the development of the test rig.

20. Appendix 3. Pressure sensor response test

A test was designed to obtain the step response of the pressure sensor. The two sensors with different length connecting tubes were connected to a box with a diaphragm designed to explode.

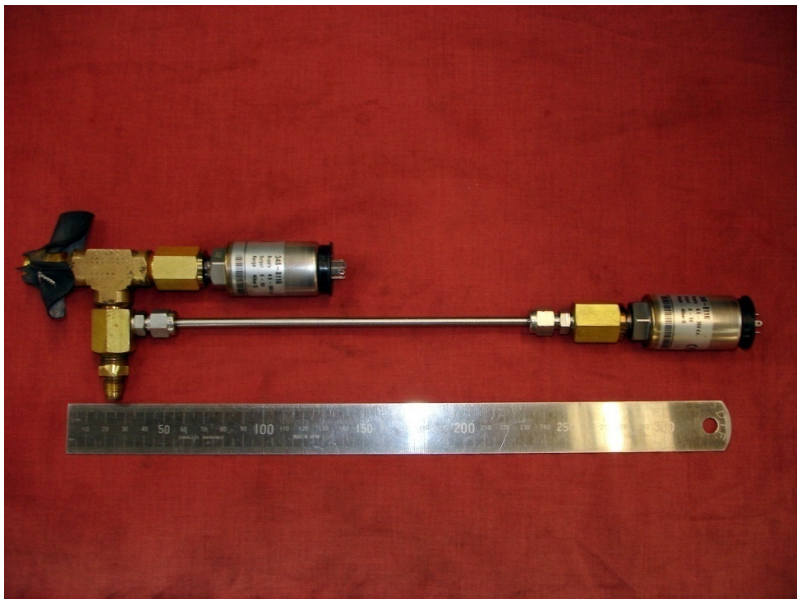

Figure 20-1Pressure sensors in preparation for a test to measure step response

The box was pressurized and the DA system switched on before the diaphragms ruptured. The sensor with the longer tube has a sluggish response and the one with the shorter tube was fast enough for the application. In the actual application, coolant was circulated to keep the temperature of the pressure sensor within specification and the temperature

of all pressure sensors were maintained within a degree to ensure that all of them remain cross calibrated. Also the length of the connecting tube was kept short and uniform to achieve similar and fast responses.

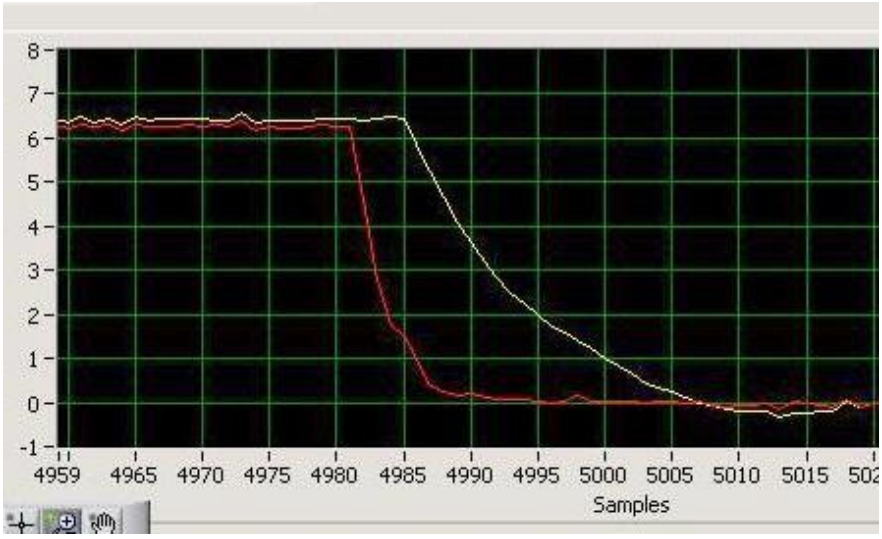

Figure 20-2 Response of the two pressure sensors. Sampling rate is 5kHz and the Y axis shows pressure in Bars

21. Appendix 4. ACROBASIC software code for displacer control

```
REM – This part is the Configuration Program
REM -- Configuration Originally Generated based on part number: ACR9000/P1/U2/M1
REM -- Primary System Settings for ACR Device
SYS
HALT ALL
NEW ALL
CLEAR
CLEAR STREAM1
CLEAR STREAM2
CLEAR STREAM3
CLEAR STREAM4
CLEAR STREAM5
CLEAR COM1
CLEAR COM2
DETACH ALL
 REM-----Allocate system memory-----
DIM PROG0(300000)
DIM PROG1(100)
DIM PROG2(300000)
DIM PROG15(114688)
REM Some Global Memory is used by Wizard Generated Code
 DIM P(4096)
DIM DEF(20)
DIM STREAM1(256)
DIM STREAM2(256)
DIM STREAM3(256)
DIM STREAM4(256)
DIM STREAM5(256)
DIM COM1(256)
DIM COM2(256)
 REM -- Hardware Configuration
 ADC0 FLT0
ADC1 FLT0
ADC2 FLT0
ADC3 FLT0
ADC4 FLT0
ADC5 FLT0
```

```
ADC6 FLT0
ADC7 FLT0
REM CANopen Settings
P32768=5
P32769=125
P32772=50
P32770=0
ATTACH AXIS0 ENC0 DAC0 ENC0
DAC0 GAIN 3276.8
AXIS0 PPU 200.000000
AXIS0 EXC (1,-1)
SET BIT8469
REM ACR Extended IO Settings
SET BIT8468
CLR BIT8464
CLR BIT8470
SET BIT8469
CLR BIT8453
CLR BIT8471
ENC0 SRC 0
ENC0 MULT 4
REM Axis Gains values
AXIS0 PGAIN 0.002441
AXIS0 IGAIN 0
AXIS0 ILIMIT 0
AXIS0 IDELAY 0
AXIS0 DGAIN 1e-005
AXIS0 DWIDTH 0
AXIS0 FFVEL 0
AXIS0 FFACC 0
AXIS0 TLM 10
AXIS0 FBVEL 0
REM Axis Limits
AXIS0 HLBIT 0
AXIS0 HLDEC 500
SET BIT16144
SET BIT16145
SET BIT16146
SET BIT16148
SET BIT16149
AXIS0 SLM (12,-12)
AXIS0 SLDEC 500
SET BIT16150
```

```
SET BIT16151
AXIS0 ON
 REM Turn off any unused Axes
 REM Program Level setup for the ACR Card
 PROG0
DETACH
ATTACH MASTER0
ATTACH SLAVE0 AXIS0 "X"
 REM the desired master acceleration
ACC 5000
REM the desired master deceleration ramp
DEC 5000
REM the desired master stop ramp (deceleration at end of move)
STP 5000
REM the desired master velocity
VEL 5000
REM the desired acceleration versus time profile.
JRK 0

REM – This part is the main program for motion control

PROGRAM
'Program 0
CLEAR
CAM CLEAR
' Allow line numbers to be shown with the list command
SET 5651
DIM $V(1,15)
DIM SV(10)
DIM SA(6)
DIM LV(1)
#DEFINE TIME SV0
#DEFINE FREQUENCY SV1
' Number is used for the squared wave form.
#DEFINE NUMBER SV2
#DEFINE AMPLITUDE SV3
#DEFINE DWELL SV4
#DEFINE PHASE SV5
#DEFINE HALFNUMBER SV6
#DEFINE HALFTABLE SV7
#DEFINE SCALER SV8
#DEFINE QUATERTABLE SV9
COUNTER = 0
```

```
DIM SA0(2) : REM Array for 5mm move gains
DIM SA1(2) : REM Array for 10mm move gains
DIM SA2(2) : REM Array for 15mm move gains
DIM SA3(2) : REM Array for 20mm move gains
DIM SA4(2) : REM Array for 25mm move gains

SA0(0) = 0.016 : REM P_Gain for 5mm move
SA0(1) = 0.000059 : REM D_Gain for 5mm move

SA1(0) = 0.014 : REM P_Gain for 10mm move
SA1(1) = 0.00006 : REM D_Gain for 10mm move

SA2(0) = 0.012 : REM P_Gain for 15mm move
SA2(1) = 0.000057 : REM D_Gain for 15mm move

SA3(0) = 0.011 : REM P_Gain for 20mm move
SA3(1) = 0.000057 : REM D_Gain for 20mm move

SA4(0) = 0.01 : REM P_Gain for 25mm move
SA4(1) = 0.000056 : REM D_Gain for 25mm move

OPEN "COM1:9600,N,8,1" AS #1

' Default gains
PGAIN X(SA0(0))
DGAIN X(SA0(1))
IGAIN X0.00005
TLM X4.4

'Setup ENC8
ENC8 LIMIT 10
ENC8 WIDTH 10
ENC8 DST 0
ENC8 SRC 3
ENC8 CLOCK 1
ENC8 MULT -4
ENC8 RES

'Disable software end of travel limits
SLIM X0

DRIVE ON X
RES X
```

```
DWL 0.2
EXC X0.5

' Find home so that motor is centralised.
TMOV OFF
JOG ACC X10
JOG DEC X10
JOG JRK X0
JOG VEL X5
bit16152 = 1
bit16154 = 0
bit16153 = 0
JOG HOMVF X1
INPUT; #1, "Home positive or negative (+/-) ", $V0
   PRINT #1, $V0
IF ($V0 = "-")
   JOG HOME X-1
ELSE IF ($V0 = "+")
   JOG HOME X1
ENDIF
INH 16134
IF (BIT 16134)
   PRINT #1, "Home Found"
   ENC0 RES
ELSE
   Halt all
ENDIF

'Setup software end of travel limits.
SLM X(12,-12)
SLIM X3

' Motion profile used for tracking.
ACC 1
DEC 1
STP 1
VEL 0.5

' Setup CAM table
dim LA(3)
dim LA0(361)
'dim LA1(17)
dim LA2(21)
```

```
' Sine CAM table
LA0(0) = 0
LA0(1) = 2
LA0(2) = 3
LA0(3) = 5
LA0(4) = 7
LA0(5) = 9
LA0(6) = 10
LA0(7) = 12
LA0(8) = 14
LA0(9) = 16
LA0(10) = 17
LA0(11) = 19
LA0(12) = 21
LA0(13) = 22
LA0(14) = 24
LA0(15) = 26
LA0(16) = 28
LA0(17) = 29
LA0(18) = 31
LA0(19) = 33
LA0(20) = 34
LA0(21) = 36
LA0(22) = 37
LA0(23) = 39
LA0(24) = 41
LA0(25) = 42
LA0(26) = 44
LA0(27) = 45
LA0(28) = 47
LA0(29) = 48
LA0(30) = 50
LA0(31) = 52
LA0(32) = 53
LA0(33) = 54
LA0(34) = 56
LA0(35) = 57
LA0(36) = 59
LA0(37) = 60
LA0(38) = 62
LA0(39) = 63
LA0(40) = 64
LA0(41) = 66
```

LA0(42) = 67
LA0(43) = 68
LA0(44) = 69
LA0(45) = 71
LA0(46) = 72
LA0(47) = 73
LA0(48) = 74
LA0(49) = 75
LA0(50) = 77
LA0(51) = 78
LA0(52) = 79
LA0(53) = 80
LA0(54) = 81
LA0(55) = 82
LA0(56) = 83
LA0(57) = 84
LA0(58) = 85
LA0(59) = 86
LA0(60) = 87
LA0(61) = 87
LA0(62) = 88
LA0(63) = 89
LA0(64) = 90
LA0(65) = 91
LA0(66) = 91
LA0(67) = 92
LA0(68) = 93
LA0(69) = 93
LA0(70) = 94
LA0(71) = 95
LA0(72) = 95
LA0(73) = 96
LA0(74) = 96
LA0(75) = 97
LA0(76) = 97
LA0(77) = 97
LA0(78) = 98
LA0(79) = 98
LA0(80) = 98
LA0(81) = 99
LA0(82) = 99
LA0(83) = 99
LA0(84) = 99

LA0(85) = 100
LA0(86) = 100
LA0(87) = 100
LA0(88) = 100
LA0(89) = 100
LA0(90) = 100
LA0(91) = 100
LA0(92) = 100
LA0(93) = 100
LA0(94) = 100
LA0(95) = 100
LA0(96) = 99
LA0(97) = 99
LA0(98) = 99
LA0(99) = 99
LA0(100) = 98
LA0(101) = 98
LA0(102) = 98
LA0(103) = 97
LA0(104) = 97
LA0(105) = 97
LA0(106) = 96
LA0(107) = 96
LA0(108) = 95
LA0(109) = 95
LA0(110) = 94
LA0(111) = 93
LA0(112) = 93
LA0(113) = 92
LA0(114) = 91
LA0(115) = 91
LA0(116) = 90
LA0(117) = 89
LA0(118) = 88
LA0(119) = 87
LA0(120) = 87
LA0(121) = 86
LA0(122) = 85
LA0(123) = 84
LA0(124) = 83
LA0(125) = 82
LA0(126) = 81
LA0(127) = 80

LA0(128) = 79
LA0(129) = 78
LA0(130) = 77
LA0(131) = 75
LA0(132) = 74
LA0(133) = 73
LA0(134) = 72
LA0(135) = 71
LA0(136) = 69
LA0(137) = 68
LA0(138) = 67
LA0(139) = 66
LA0(140) = 64
LA0(141) = 63
LA0(142) = 62
LA0(143) = 60
LA0(144) = 59
LA0(145) = 57
LA0(146) = 56
LA0(147) = 54
LA0(148) = 53
LA0(149) = 52
LA0(150) = 50
LA0(151) = 48
LA0(152) = 47
LA0(153) = 45
LA0(154) = 44
LA0(155) = 42
LA0(156) = 41
LA0(157) = 39
LA0(158) = 37
LA0(159) = 36
LA0(160) = 34
LA0(161) = 33
LA0(162) = 31
LA0(163) = 29
LA0(164) = 28
LA0(165) = 26
LA0(166) = 24
LA0(167) = 22
LA0(168) = 21
LA0(169) = 19
LA0(170) = 17

LA0(171) = 16
LA0(172) = 14
LA0(173) = 12
LA0(174) = 10
LA0(175) = 9
LA0(176) = 7
LA0(177) = 5
LA0(178) = 3
LA0(179) = 2
LA0(180) = 0
LA0(181) = -2
LA0(182) = -3
LA0(183) = -5
LA0(184) = -7
LA0(185) = -9
LA0(186) = -10
LA0(187) = -12
LA0(188) = -14
LA0(189) = -16
LA0(190) = -17
LA0(191) = -19
LA0(192) = -21
LA0(193) = -22
LA0(194) = -24
LA0(195) = -26
LA0(196) = -28
LA0(197) = -29
LA0(198) = -31
LA0(199) = -33
LA0(200) = -34
LA0(201) = -36
LA0(202) = -37
LA0(203) = -39
LA0(204) = -41
LA0(205) = -42
LA0(206) = -44
LA0(207) = -45
LA0(208) = -47
LA0(209) = -48
LA0(210) = -50
LA0(211) = -52
LA0(212) = -53
LA0(213) = -54

LA0(214) = -56
LA0(215) = -57
LA0(216) = -59
LA0(217) = -60
LA0(218) = -62
LA0(219) = -63
LA0(220) = -64
LA0(221) = -66
LA0(222) = -67
LA0(223) = -68
LA0(224) = -69
LA0(225) = -71
LA0(226) = -72
LA0(227) = -73
LA0(228) = -74
LA0(229) = -75
LA0(230) = -77
LA0(231) = -78
LA0(232) = -79
LA0(233) = -80
LA0(234) = -81
LA0(235) = -82
LA0(236) = -83
LA0(237) = -84
LA0(238) = -85
LA0(239) = -86
LA0(240) = -87
LA0(241) = -87
LA0(242) = -88
LA0(243) = -89
LA0(244) = -90
LA0(245) = -91
LA0(246) = -91
LA0(247) = -92
LA0(248) = -93
LA0(249) = -93
LA0(250) = -94
LA0(251) = -95
LA0(252) = -95
LA0(253) = -96
LA0(254) = -96
LA0(255) = -97
LA0(256) = -97

LA0(257) = -97
LA0(258) = -98
LA0(259) = -98
LA0(260) = -98
LA0(261) = -99
LA0(262) = -99
LA0(263) = -99
LA0(264) = -99
LA0(265) = -100
LA0(266) = -100
LA0(267) = -100
LA0(268) = -100
LA0(269) = -100
LA0(270) = -100
LA0(271) = -100
LA0(272) = -100
LA0(273) = -100
LA0(274) = -100
LA0(275) = -100
LA0(276) = -99
LA0(277) = -99
LA0(278) = -99
LA0(279) = -99
LA0(280) = -98
LA0(281) = -98
LA0(282) = -98
LA0(283) = -97
LA0(284) = -97
LA0(285) = -97
LA0(286) = -96
LA0(287) = -96
LA0(288) = -95
LA0(289) = -95
LA0(290) = -94
LA0(291) = -93
LA0(292) = -93
LA0(293) = -92
LA0(294) = -91
LA0(295) = -91
LA0(296) = -90
LA0(297) = -89
LA0(298) = -88
LA0(299) = -87

LA0(300) = -87
LA0(301) = -86
LA0(302) = -85
LA0(303) = -84
LA0(304) = -83
LA0(305) = -82
LA0(306) = -81
LA0(307) = -80
LA0(308) = -79
LA0(309) = -78
LA0(310) = -77
LA0(311) = -75
LA0(312) = -74
LA0(313) = -73
LA0(314) = -72
LA0(315) = -71
LA0(316) = -69
LA0(317) = -68
LA0(318) = -67
LA0(319) = -66
LA0(320) = -64
LA0(321) = -63
LA0(322) = -62
LA0(323) = -60
LA0(324) = -59
LA0(325) = -57
LA0(326) = -56
LA0(327) = -54
LA0(328) = -53
LA0(329) = -52
LA0(330) = -50
LA0(331) = -48
LA0(332) = -47
LA0(333) = -45
LA0(334) = -44
LA0(335) = -42
LA0(336) = -41
LA0(337) = -39
LA0(338) = -37
LA0(339) = -36
LA0(340) = -34
LA0(341) = -33
LA0(342) = -31

```
LA0(343) = -29
LA0(344) = -28
LA0(345) = -26
LA0(346) = -24
LA0(347) = -22
LA0(348) = -21
LA0(349) = -19
LA0(350) = -17
LA0(351) = -16
LA0(352) = -14
LA0(353) = -12
LA0(354) = -10
LA0(355) = -9
LA0(356) = -7
LA0(357) = -5
LA0(358) = -3
LA0(359) = -2
LA0(360) = 0

cam dim x1

' Loop through here asking for an input until a valid input is received.
WHILE (NOT BIT 32)
   INPUT; #1, "Input ", $V0
   $V0 = UCASE$($V0)
   PRINT #1, $V0

   IF ($V0 = "SIN")
      GOSUB SIN

   ELSE IF ($V0 = "SQUARE")
      GOSUB SQUARE

   ELSE IF ($V0 = "SMALLDWELL")
      GOSUB SMALLDWELL

   ELSE IF ($V0 = "EXIT")
      SET 32
      DRIVE OFF X
   ENDIF
WEND
CLR 32
WHILE (NOT BIT 32)
```

```
   ' If the input was "exit" then get out of this loop and stop the code.
   IF ($V0 = "EXIT")
      SET 32
      ' This break should break from the above while but the code starts
again is the closest "wend".
      BREAK
   ENDIF
   ' Toggle bit 33, output 2, every time the rotary encoder is 256 and 768.
   while (SIN((P6272) * 360 / 1024) < 0.99)
      clr 32
   wend
      IF (BIT 33)
      CLR 33
   ELSE IF (NOT BIT 33)
      SET 33
   ENDIF
      ' Because code starts again at above "wend" another break statement is
requried.
   IF ($V0 = "EXIT")
      ' Setting 32 causes the main while to be exited.
      SET 32
      BREAK
   ENDIF

   while (SIN((P6272) * 360 / 1024) > -0.99)
      'PRINT 1
      clr 32
   wend
   IF (BIT 33)
      CLR 33
   ELSE IF (NOT BIT 33)
      SET 33
   ENDIF
WEND
CLR 32
CLOSE #1
END

_SIN
   INPUT; #1, "Amplitude (mm), max amplitude 11mm ", $V0
   IF ($V0 = "EXIT")
      SET 32
      DRIVE OFF X
```

```
      RETURN
   ENDIF
   AMPLITUDE = VAL($V0)
   PRINT #1, AMPLITUDE
   ' If the amplitude asked for is greater than 11mm then loop back to the
start of this subroutine.
   IF (AMPLITUDE > 11)
      PRINT #1, "Amplitude must be 11mm or less."
      GOTO SIN
      ENDIF
   ' This number is multiplied with the cam table.  It scales the cam table to
the desired amplitude of travel.
   SCALER = AMPLITUDE / 100
   PRINT #1, SCALER
   ' Tell the cam function to use long array zero, and to use that array for
one whole revolution.
   cam seg x(0, 1024, LA0)
   cam scale x(SCALER)
   INPUT; #1, "Phase (degrees), 0 to 360 ", $V0
   IF ($V0 = "EXIT")
      SET 32
      DRIVE OFF X
      RETURN
   ENDIF
   PHASE = VAL($V0)
   PRINT #1, PHASE
   ' Set CAM source to encoder 8.
   cam src x8
   ' This will start the cam cycle at the rotary encoder position that
corresponds to the requested phase.
   cam on x ihpos (1024 + ((181 - (PHASE)) / 360 * 1024))
   SET 32
RETURN
_SQUARE
   INPUT; #1, "Amplitude (mm), max amplitude 11mm ", $V0
   IF ($V0 = "EXIT")
      SET 32
      DRIVE OFF X
      RETURN
   ENDIF
   AMPLITUDE = VAL($V0)
   PRINT #1, AMPLITUDE
   IF (AMPLITUDE > 11)
```

```
      PRINT #1, "Amplitude must be 11mm or less."
      GOTO SQUARE
      ENDIF
   ' This number is multiplied with the cam table.  It scales the cam table to
the desired amplitude of travel.
   SCALER = AMPLITUDE / 100
   PRINT #1, SCALER
_DWELL
   INPUT; #1, "Dwell (%), must be greater than 33% ", $V0
   IF ($V0 = "EXIT")
      SET 32
      DRIVE OFF X
      RETURN
   ENDIF
   DWELL = VAL($V0)
   PRINT #1, DWELL
   ' Check that the dwell is greater than 33%.
   IF (DWELL < 33)
      PRINT #1, "Dwell must be 33% or greater."
      GOTO DWELL
      ENDIF
   DWELL = DWELL / 100
   ' Calculate the number of "amplitude" values required in CAM table.
   NUMBER = ((-2 * DWELL - 2) / (DWELL - 1))
   PRINT #1, NUMBER
   ' Make sure that this is a whole number.
   NUMBER = CEIL(NUMBER)
   ' If the number isn't even then this dwell is unachievable.
   IF ((NUMBER MOD 2) > 0)
      PRINT #1, "Dwell requested is unachievable, try slightly higher or
lower dwell."
      GOTO DWELL
      ENDIF
   ' Calculate the dwell achieved with the rounded whole number.
   DWELL = (100 * ((NUMBER - 2) / (NUMBER + 2)))
   PRINT #1, "Dwell achieved = ", DWELL
   DIM LA1(NUMBER + 3)
   HALFNUMBER = (NUMBER / 2)
   ' Generate square CAM table.
   LA1(0) = 0
   FOR LV0 = 1 TO (NUMBER + 2) STEP 1
      IF (LV0 = (HALFNUMBER + 1))
         LA1(LV0) = 0
```

```
      ELSE IF (LV0 = (NUMBER + 2))
         LA1(LV0) = 0
      ELSE IF (LV0 > (HALFNUMBER + 1))
         LA1(LV0) = -100
      ELSE IF (LV0 < (HALFNUMBER + 1))
         LA1(LV0) = 100
      ENDIF
      NEXT
   cam seg x(0, 1024, LA1)
   cam scale x(SCALER)
   INPUT; #1, "Phase (degrees), 0 to 360 ", $V0
   IF ($V0 = "EXIT")
      SET 32
      DRIVE OFF X
      RETURN
   ENDIF
   PHASE = VAL($V0)
   PRINT #1, PHASE
   ' Set CAM source to encoder 8.
   cam src x8
   cam on x ihpos (1024 + ((181 - (PHASE)) / 360 * 1024))
   SET 32
RETURN
_SMALLDWELL
   INPUT; #1, "Amplitude (mm), max amplitude 11mm ", $V0
   IF ($V0 = "EXIT")
      SET 32
      DRIVE OFF X
      RETURN
   ENDIF
   AMPLITUDE = VAL($V0)
   PRINT #1, AMPLITUDE
   IF (AMPLITUDE > 11)
      PRINT #1, "Amplitude must be 11mm or less."
      GOTO SMALLDWELL
      ENDIF
   ' This number is multiplied with the cam table.  It scales the cam table to
the desired amplitude of travel.
   SCALER = AMPLITUDE / 100
   PRINT #1, SCALER
_DWELL2
   INPUT; #1, "Dwell (%), must be less than 33% ", $V0
   IF ($V0 = "EXIT")
```

```
      SET 32
      DRIVE OFF X
      RETURN
   ENDIF
   DWELL = VAL($V0)
   PRINT #1, DWELL
   ' Check that the dwell is less than 33%.
   IF (DWELL > 32)
      PRINT #1, "Dwell must be less than 33%, if more dwell required then
use square wave."
      GOTO DWELL2
      ENDIF
   DWELL = DWELL / 100
   ' Calculate the number of values required in CAM table.
   NUMBER = (2 / DWELL + 1)
   PRINT #1, NUMBER
   ' Make sure that this is a whole number.
   NUMBER = CEIL(NUMBER)
   HALFTABLE = ((NUMBER - 1) / 2)
   QUATERTABLE = (HALFTABLE / 2)
   QUATERTABLE = FLOOR(QUATERTABLE)
   ' If the number isn't odd then this dwell is unachievable.
   IF ((NUMBER MOD 2) = 0)
      PRINT #1, "Dwell requested is unachievable, try slightly higher or
lower dwell."
      GOTO DWELL2
      ENDIF
   ' If HALFTABLE isn't odd then this dwell is unachievable.
   IF ((HALFTABLE MOD 2) = 0)
      PRINT #1, "Dwell requested is unachievable, try slightly higher or
lower dwell."
      GOTO DWELL2
      ENDIF
   ' Calculate the dwell achieved with the rounded whole number.
   DWELL = (100 * (2 / (NUMBER - 1)))
   PRINT #1, "Dwell achieved = ", DWELL
   DIM LA1(NUMBER)

   ' Generate square CAM table.
   LA1(0) = 0
   LA1(QUATERTABLE) = 100
   LA1(QUATERTABLE + 1) = 100
   LA1(QUATERTABLE + HALFTABLE) = -100
```

```
   LA1(QUATERTABLE + HALFTABLE + 1) = -100
   LA1(NUMBER - 1) = 0
   FOR LV0 = 1 TO (HALFTABLE + QUATERTABLE - 1) STEP 1
      IF (LV0 = (HALFTABLE))
         LA1(LV0) = 0
      ELSE IF (LV0 > (HALFTABLE))
         LA1(LV0) = ((-100 / QUATERTABLE) * (LV0 - HALFTABLE))
         LA1((NUMBER - 1) - (LV0 - HALFTABLE)) = ((-100 /
QUATERTABLE) * (LV0 - HALFTABLE))
      ELSE IF (LV0 < (QUATERTABLE))
         LA1(LV0) = ((100 / QUATERTABLE) * LV0)
         LA1(HALFTABLE - LV0) = ((100 / QUATERTABLE) * LV0)
      ENDIF
      NEXT
   cam seg x(0, 1024, LA1)
   cam scale x(SCALER)
   INPUT; #1, "Phase (degrees), 0 to 360 ", $V0
   IF ($V0 = "EXIT")
      SET 32
      DRIVE OFF X
      RETURN
   ENDIF
   PHASE = VAL($V0)
   PRINT #1, PHASE
   ' Set CAM source to encoder 8.
   cam src x8
   cam on x ihpos (1024 + ((181 - (PHASE)) / 360 * 1024))
   SET 32
RETURN

ENDP
```